MICROZONATION WITH RESPECT TO RAINFALL – INDUCED LANDSLIDES

by

Okan İlhan

B.S., Civil Engineering, Dokuz Eylül University, 2010

Submitted to Kandilli Observatory and Earthquake Research Institute
in partial fulfillment of the requirements for the degree of
Master of Science

Graduate Program in Earthquake Engineering
Boğaziçi University
2015

MICROZONATION WITH RESPECT TO RAINFALL – INDUCED LANDSLIDES

APPROVED BY:

Prof. Dr. Erdal Şafak .....
(Thesis Supervisor, Boğaziçi University)

Prof. Dr. Atilla Ansal .....
(Thesis Co - Supervisor, Özyeğin University)

Assoc. Prof. Ayşe Edinçliler .....
(Boğaziçi University)

Assoc. Prof. Özer Çinicioğlu .....
(Boğaziçi University)

Assist. Prof. Gökçe Tönük .....
(Mef University)

DATE OF APPROVAL: 14.01.2015

ACKNOWLEDGEMENTS

In the process of this study, I owe thanks to a great many people, who facilitates the way of constructing this thesis. I would like to express my appreciation to Prof. Dr. Atilla Ansal for his guidance in rainfall – induced landslide hazard concept and also encouragement for my future career. This proposed methodology cannot be improved without his great mentor.

I also would like to thank and express my appreciation to Prof. Dr. Erdal Şafak to accept me for concluding my thesis after retirement of Prof. Dr. Atilla Ansal and also for all his patience and helps.

I would like to thank to Assist. Prof. Gökçe Tönük for her patience and helps to recommend this methodology and also extend my thanks in order for her kind responses in each time I consult her about my thesis. Also, I would like to express my gratitude and thanks to Dr. Hadi Khanbabazadeh for analysing the mentioned methodology, for proposing enlightening ideas to further develop it and for all his patience.

Finally, I would like to thank my family, Hüseyin İlhan and Günay İlhan, to support and appreciate my works in the course of my thesis and also to adapt their lives to aid me to conclude my studies during five years.

This study was conducted with the support from SciNetNatHazPrev: A Scientific Network for Earthquake, Landslide and Flood Hazard Prevention project numbered as TR11C1.01-02_309 granted by European Union Black Sea Basin Cross Border Cooperation Programme.

To my family

ABSTRACT

MICROZONATION WITH RESPECT TO RAINFALL – INDUCED LANDSLIDES

Expansion of scientific methodologies to quantify the rainfall – induced hazard paves the way for constructing proper investigation of potential landslide in interested areas. In this context, a simple, concise but sufficiently detailed to incorporate all the phenomena in itself microzonation methodology is proposed which merges two different approaches (1) Iverson (2000), which bears on the exact solution of Richards' Equation and (2) uniform seepage condition, dependent on topographical features rather than solution to water movement equation in soil continuum. Such a straightforward concept enables utilizers to perform factor of safety calculations not exhaustive but elaborative on GIS system. In this study, hypothetical topography is at first produced to portray the efficacy of recommended algorithm with an intention that different soil conditions and fluctuations in rainfall intensities on soil mass are able to be evaluated. In addition to this, Tekirdağ City Center is selected to examine the pros and cons of proposed routine but all the required parameters for the analysis are specified by means of plenty of empirical correlations, which may lead to unexpected results. Thus, two additional methodology, Montgomery and Dietrich (1994), Mora and Vahrson (1994) are also, employed for the justification of below – stated method since the former one operates on similar parameters and the latter one sketches the potential hazardous locations in relevant area. The outcome of comparison between these three algorithms is able to be interpreted that suggested technique can fairly be presumed as one simulating the pore – pressure acumulations and corresponding factor of safety degradations properly.

ÖZET

YAĞMUR KAYNAKLI YAMAÇ KAYMALARI İÇİN MİKROBÖLGELEME

Yağmur suyu kaynaklı yamaç göçmeleri üzerine bu zamana kadar geliştirilen yöntemler, şev kaymalarına karşı doğru biçimde korunma planları üretmeye imkan sağlamıştır. Bu bağlamda, kısa ve öz fakat mevcut tüm etkileri kapsayacak biçimde bir mikrobölgeleme yöntemi geliştirilmeye çalışılmıştır. Bu metot, (1) Iverson (2000) tarafından önerilen Richards Denkleminin kesin çözümüne dayanan algoritma ile (2) salt topografyaya bağlı üniform sızma konseptini birleştirmiştir. Yöntemin avantajlı taraflarından biri de, CBS ortamına rahatça uygulanabilir olmasıdır. Bu çalışma kapsamında öncelikle, farklı zemin koşullarını içeren ve değişken yağmur şiddetlerine maruz kalan kuramsal bir topografya üretilerek metot üzerinde fayda/zarar analizi yürütülmüştür. Daha sonra, Tekirdağ şehir merkezi bir örnek arazi olarak seçilerek, benzer analizler tekrarlanmıştır. İlgili tüm parametreler, ampirik bağıntılar elde edilerek bulunduğu için ve çalışmanın doğrulanması gerektiği düşünüldüğünden iki farklı, (1) Montgomery ve Dietrich (1994) (2) Mora ve Vahrson (1994) prosedür de benimsenmiştir. Bunlardan ilki, önerilen yöntem ile benzer parametrelere dayandığından ötürü çalışmaya dahil edilmiş, ikincisi ise arazi üzerindeki muhtemel tehlikeli alanları işaret etmesi sebebiyle seçilmiştir.

Karşılaştırmalar sonucunda görülmüştür ki bu çalışmada sunulan metodoloji, yağmur esnasında meydana gelen zamana bağlı boşluk suyu basınçlarının birikimini ve ona paralel hesaplanan güvenlik katsayısı azalımlarını kabul edilebilir ölçüde modelleyebilmektedir.

TABLE OF CONTENTS

LIST OF FIGURES

LIST OF TABLES

LIST OF SYMBOLS/ABBREVIATIONS

[D]	Stifffness matrix
[E]	Capacitance matrix
[F]	Flux vector reflecting the boundary conditions
A	Partial catchment area
a	Parameter primarily controlling location of maximum probability in three – parameter inverse – gamma probability distribution
A_L	Area of landslide
A_t	Total catchment area
b	Lower bound to each element in interested catchment area
C	Hillslope capacity
c	Soil cohesion
D	Hydraulic diffusivity
D_0	Maximum characteristic diffusivity governing transmission of pressure head
D_r	Relative density
d_z	Groundwater table depth
e	Void ratio
FoS	Factor of safety
GWT	Ground water table
GWL	Ground water level
h	Groundwater height
H_i	Hazard index
I_p	Plasticity index
I_z	Rain water infiltration rate
K	Hydraulic conductivity
LL	Liquid limit
L_*	Depth to water table
M	Slope angle
N_{70}	SPT – N value at energy rate of 70
N_L	Number of landslide
P_0	Atmospheric pressure
P_a	Atmospheric pressure

PL	Plastic limit
PWP	Pore – water pressure
q	Water flux
Q_0	Water efflux
q_A^*	Initial flux at the soil surface which, along with ψ0, determines the initial pressure distribution in the soil
q_B^*	Prescribed flux at the soil surface (rainfall amount)
s	Parameter primarily controlling exponential rollover for small values in three – parameter invers – gamma probablity distribution
S_0	Specific surface
S_h	Value of index of influence of natural humidity of the soil
S_l	Value of lithologic susceptibility
S_r	Value of relative relief index
T	Rainfall duration
$\overline{T}$	Mean transmissivity of catchment.
T_p	Value of influence of rainfall precipitation intensity
T_s	Value of influence of rainfall precipitation intensity
$t^*_{Short-Term}$	Minimum time required for strong slope – normal pore pressure transmission from the ground surface to depth.
$t^*_{Long-Term}$,	Minimum time required for strong slope – normal pore pressure transmission from the area, A to the point (x, y, H)
u_a	Pore – air pressure
u_w	Pore – water pressure
USCS	Unified Soil Classification System
USDA	United States Department of Agriculture
W	Wetness state
w_r	Water content at residual state
γ_{sat}	Unit weight at saturated condition
γ_w	Unit weight of water
θ	Slope angle
λ_{bc}	Pore – size distribution index
μ_g,	Fitting parameter which is a function of air – entry value of the soil

n_g,	Fitting parameter which is a function of rate of water extraction from soil once air – entry value of soil has been exceeded
ρ	Parameter primarily controlling power – law decay for medium and large values in three – parameter inverse – gamma probability distribution
σ_{v0}'	Overburden pressure
φ	Internal friction angle
ψ	Pressure head
ψ_{aev}	Pressure head at air – entry value
ω	Water content

1. INTRODUCTION

It is widely known that saturation due to heavy rainfall on hillslope poses great threat on slope stability since water seepage causes shear strength capacity to decrease to an extent which driving forces overcome resisting forces. Researchers have attempted to develop plenty of methods in order to cope with such possible devastating effects of this hazard that each methodology makes its unique assumptions and imposes certain boundary conditions depending on the type of problem. Such endeavours result in the diversification of approaches and conceptions in the research of percolating rain water influence on hillslope mass.

In this study, a microzonation methodology is proposed by an intention of covering all the possible phenomena constituting the aforementioned hazard in site provided that this logic places significance on deriving a succinct, comprehensible but fairly elaborative algorithm. The justification of such idea is performed by two different methodologies; (1) Montgomery and Dietrich (1994) (2) Mora and Vahrson (1993) in that the former one bears on two simple calculations and be capable of producing factor of safety value but the latter one can be explained as an both earthquake and rainfall hazard determination of site by visual inspection of related parameters.

In the following paragraphs, readers can find the literature review on rainfall – instigated slope stability approaches and be able to execute a comparison on under which side the recommended methodology falls. Theoretical background presented in third Chapter is supplied in this document to shed light on to which conditions it can respond and what are the limitations of this methodology in different circumstances.

In the final chapters, Case Study of Tekirdağ City Center and Application on Hypothetical Topography are submitted in order that pros and cons of three different methods are illustrated to display the adequateness of them to possible utilizers. What is yielded after the implementation of these algorithms is plugged into the Conclusion Chapter, which outlines the key points and advantages/disadvantages of developed one over another procedures.

2. LITERATURE REVIEW ON RAINFALL – INDUCED SLOPE STABILITY METHODS

In this document, slope stability methods considering rainfall and water seepage effects are compiled in order to be able to select the most suitable way of quantifying related hazard. Classification is performed to give detail on the content of possible methods as;

1. Topographical Methods
2. Statistical Methods
3. Analytical Methods
4. Numerical Methods

Each method is elaborated to provide insight into the its procedure adopted for the evaluation of defined hazard and to clarify the process of how the proposed methodology is selected among them and furher improved to be employed for risk mitigation.

2.1. Topographical Methods

In these methods, it is proposed that a criterion can be derived for ascertaining the saturated zones after heavy rainfall in that whether encountered soil layer(s) have capacity to transmit the incoming water flow or not. As known, tranmissivity of soil is quantified by conductivity characteristic of corresponding site which can be obtained with the help of lithological classification or based onlab measurements performed on undisturbed samples. This allows to estimate the drainage feature of investigated site indicating that how the subsurface flow occurring after rainfall is transmitted to the downstream in that soil transmissivity, hillslope gradient and wetness state, characterized by the base flow discharge from catchment determine this process. Therefore, these quantities pertaining to corresponding hillslope are employed to assess the hydrological response of soil layers during rainfall.

The starting point is to develop a criterion so that the topographic features of hillslope under consideration and drainage characteristic of corresponding soil layer(s) can be lumped into dimensionless parameters. It will be seen that there is a nonlinear relationship between this parameter and saturated areas where chances are available that saturated catchment area can be determined. This is because this routine is called as preliminary analysis allowing one to focus on saturated areas or those exposed to surface runoff which should be elaborated by means of more detailed slope stability analysis.

In addition, there is possibility to establish threshold levels in the context of this method by estimating expansion of saturated areas with respect to different rainfall magnitudes that can be mapped. This means that required improvement on corresponding waterlogged site would provide the transmission of percolating rain water.

In conclusion, topographical methodologies pave the way for predicting such vulnerable areas which might have lower factor of safety that may require reevaluation of all zones whose wetness state are computed as greater than declared threshold levels.

2.1.1. Method Proposed by O'Loughlin (1981) and (1986)

The first step in this routine is to quantify the width of saturated zone which leads to the establishment of a criterion depending on both related soil and topographical properties. What is meant by the width of saturated zone (x_s) is illustrated in Figure 2.1.

x_s is again defined as the intersection point of groundwater table and hillslope profile which can be estimated by means of Darcy's Law including the Dupuit Assumption. Initial presumption is made on the fact that interested site has homogeneous soil characteristic with saturated conductivity K in that that slope – parallel groundwater flow occurs after the percolation of rain water on surface.

In the first place, the streamflow prior to a storm event with the presumption of Dupuit – Forchheimer hydrostatic pressure which represents the total flow from this seepage zone for a stream of unit length and may be regarded as the baseflow before the storm can be computed with the help of Darcy's Law as;

$$q = Kh\left(\frac{dh}{dx}\right) \tag{2.1}$$

where h is the height of the water table above the impermeable layer at a distance x from the stream; and the discharge is defined as positive when directed in the negative direction.

Then, the groundwater shape can be computed as;

$$\frac{h}{h_0} = \sqrt{1 + \frac{2qx}{Kh_0^2}} \tag{2.2}$$

If the hillside has a slope of M, its surface elevation at a distance x from the stream is;

$$z = h_0 + Mx \tag{2.3}$$

If the Eq. (2.2) and Eq. (2.3) are solved simulateously, it yields;

$$x_s = \frac{2(q - KMh_0)}{KM^2} \tag{2.4}$$

In order to provide the condition that x_s in Figure 2.1 should be greater than zero;

$$q > KMh_0 \tag{2.5}$$

Surface run – off will take place right from the onset of a subsequent storm over a width of hillside given by Eq. (2.4). The width and the run – off contributing area will be large if;

1. K is low (Great impermeability)
2. M is low (Flat topography)
3. q is high (Wet catchment)

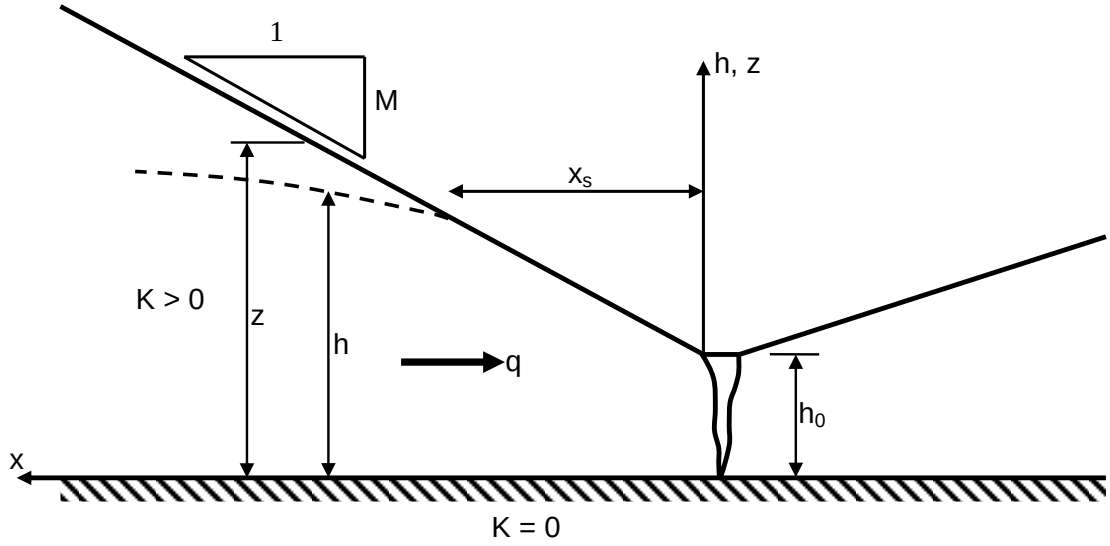

Figure 2.1. Saturated groundwater flow in plane hillslopes: horizontal impermeable layer.

Until this point, it is set forth that soil are homogeneous, slope shapes are plane, etc but these are not the conditions encountered in nature, thus resulting in the modification of Darcy's Law such as (Figure 2.2);

$$dq = K(z)\frac{\partial h}{\partial s}dz \tag{2.6}$$

The water flux towards downstream is computed as;

$$q = \int_0^l dq = \int_0^l K(z)\frac{\partial h}{\partial s}dz \tag{2.7}$$

where the limit of integration l is the depth at which K(z) approaches zero, h is the sum of pressure and elevation heads.

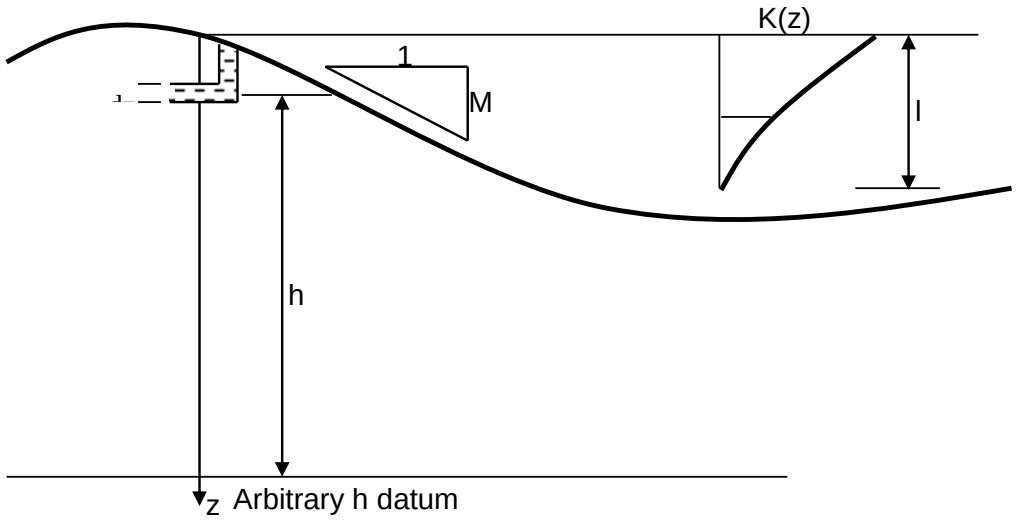

Figure 2.2. Definition sketch for flow in a real hillslope.

As done in Eq. (2.1), Dupuit – Forchheimer Assumption is embraced so that the second term at the right – hand side of Eq. (2.7) can be taken as equal to the hillslope gradient, M. This means that the maximum water – table gradient cannot exceed the value of M, thus concluding that the maximum subsurface flux which can occur parallel to the hillslope is;

$$C = M\int_0^I K(z)dz = MT \tag{2.8}$$

where C is called as hillslope capacity, T, is the transmissivity of the soil profile.

In general, catchment topography can be decomposed into several areas or strips in that boundaries of those elements are usually thought to be parallel to the subsurface flow resulting from the percolation of water in slope. Figure 2.3 enables one to propose such an argument that if the width of a strip is b(x), and if it is assumed that the subsurface discharge passing any cross – section of the strip is proportional to the strip area upslope from that section, A, then the discharge per unit width in the strip is;

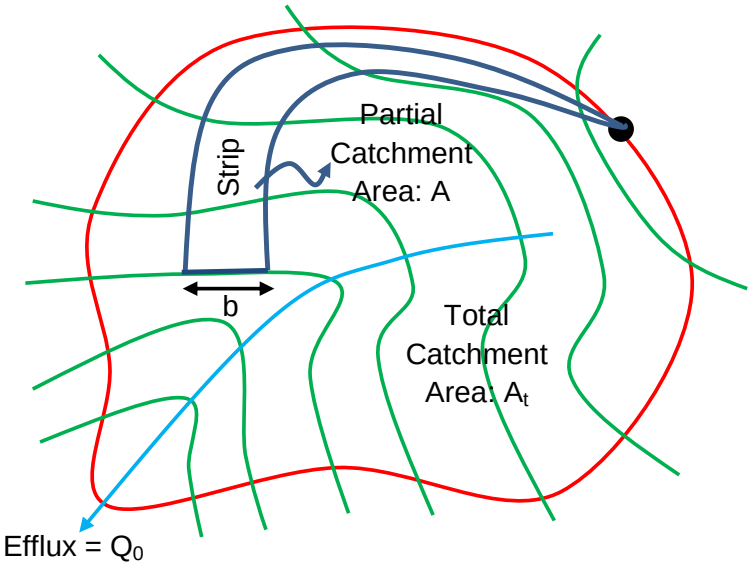

Figure 2.3. Catchment topography.

$$q(x) = \frac{AQ}{b} \tag{2.9}$$

O'Loughlin (1986) states that soil heterogenity imposes the condition of varying water discharge through soil layers such that it is better to define the Q value in integral with respect to catchment area, A in many situations. However, measuring water flux on site is quite troublesome process due to the fact that both quantification of soil conductivities within the different part of interested region and losses because of interception and evapotransporation prevent one to perform reliable measurements. This is because Q is related to water efflux which makes it possible for adopting a constant Q value for corresponding catchment

$$\int_{A_t} qdA = Q_0 \tag{2.10}$$

At this point, the criterion derived in Eq. (2.5) is applied as by comparing hillslope capacity with actual hillslope drainage flux, thus yielding,

$$\frac{1}{bd}\int q(x,y)dA > \frac{TM}{d} \tag{2.11}$$

where d is the hillslope length and adopted for normalizing Eq. (2.11).

What we obtain in the case of including mean drainage flux and transmissivity conditions is;

$$W = \frac{1}{Mbd}\left(\frac{\overline{T}}{T}\right)\int\left(\frac{q}{\overline{q}}\right)dA \geq \frac{\overline{T}A_t}{Q_0 d} \tag{2.12}$$

where, $\overline{T}$, is the mean transmissivity of catchment, W, is the wetness state of related catchment.

Eq. (2.12) is attained by the fact that Eq. (2.11) is normalized with respect to both Eq. (2.10) and mean catchment transmissivity, $\overline{T}$. As stated above, w(x,y) is the wetness state of corresponding catchment area compared with the right – hand side of Eq. (2.12).

Also, Eq. (2.9) reveals that a saturated zone occurs where this criterion is satisfied. This condition could arise through separately identifiable effects associated with;

Topography

Soil transmissivity, T

The wetness state of the hillslope which determines the discharge, Q.

Application of Eq. (2.12) requires the evaluation of w(x,y) in that $\overline{T}/T$ and M are quantified at every grid of interested catchment, thus resulting in delineation of detailed topographic map.

2.1.2. Method Proposed by Montgomery and Dietrich (1994)

Method Proposed by Montgomery and Dietrich (1994) attempts to develop a method, bearing on the logic proposed by Method Proposed by O'Loughlin (1981) and (1986), which is built on the assumption that topography creates the most detrimental effect on slope stability. It is stated that since interested areas exhibit themselves as convergent or divergent topographical structures, it requires to introduce a methodology considering local surface topograhy as primary parameter, and that the water transmission capacity of soil

should be determined to assess whether it is cabaple of conducting infiltrated rain water or not.

As a matter of fact, this routine is dependent on the combination of Darcy's Law and infinite – slope stability concept in that elevated groundwater causes related soil mass to be exposed to failure under rainfall percolation. Therefore, it would be possible to generate hazard maps, detecting potential collapse locations, with the help of both rapid and simpler analysis. To that end, quantitative thresholds are established to take soil/topographical properties and meteorological conditions of related site into consideration in order that stability of different types of landshapes can be evaluated.

As stated, topographical effect combined with rainfall infiltration hazard on related site is extracted from catchment area which is partitioned into topographic elements consisting of contour lines and flow tubes perpendicular to these contours. Such an application enables one to derive a parameter, called wetness, which can be given as;

$$W = \frac{I_z A}{bT\sin\theta} \tag{2.13}$$

where I_z (or q in Figure 2.4) is the net rainfall rate (≈ rainfall rate), A and b is presented in Figure 2.3, T is the soil transmissivity at saturation $(K_h * z * \cos\theta)$, θ is the slope angle.

Eq. (2.13) is achieved by the logic in Method Proposed by O'Loughlin (1981) and (1986) but what is imposed upon by Method Proposed by Montgomery and Dietrich (1994) is to associate this with the location of groundwater table. Since wetness parameter is defined as the ratio of local flux at a given steady state rainfall to that at soil profile saturation, this Eq. (2.13) is able to be rearranged as (Figure 2.4);

$$W = \frac{K_x \sin\theta h \cos\theta}{K_x \sin\theta z \cos\theta} = \frac{h}{z} \tag{2.14}$$

where K_h is the saturated horizontal hydraulic conductivity of soil, h is the thickness of the saturated soil, z is the total soil thickness.

This model proceeds with the infinite – slope stability assumption, in which the limiting state can be redefined as including the wetness parameter;

$$W = \left(\frac{\gamma_{sat}}{\gamma_w}\right)\left[1 - \left(\frac{\tan\theta}{\tan\varphi}\right)\right] \tag{2.15}$$

where γ_{sat} is the saturated unit weight of soil, γ_w is the unit weight of water, φ is the internal friction angle of soil.

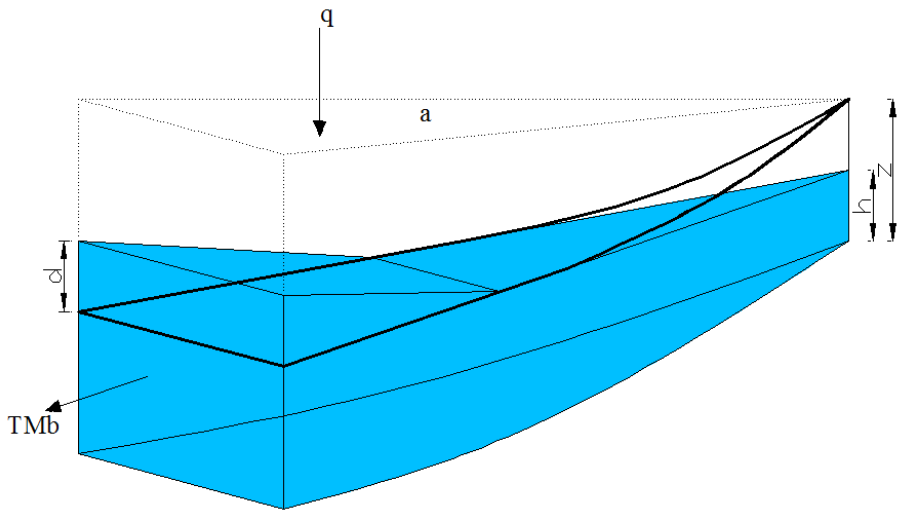

Figure 2.4. The cross – section of area draining across the contour length.

As can be seen, wetness is able to be computed from Eq. (2.13) to be substituted into Eq. (2.15) provided that if W is obtained as greater than 1, it should be equated to 1, as the remaining water runs off as overland flow. Hence, the topographic elements are estimated as unstable if;

$$\frac{A}{b} \geq \left(\frac{T}{I_z}\right)\sin\theta\left(\frac{\gamma_{sat}}{\gamma_w}\right)\left[1 - \left(\frac{\tan\theta}{\tan\varphi}\right)\right] \tag{2.16}$$

Eq. (2.16) reveals that T/I_z , defined as infiltration rate , primarily specifies the wetness state of encountered topographic element, thus resulting in the fact that W is a function of rainfall intensity (I_z). ncrease in W is essentially dependent on Iz such an extent that if a certain treshold of Iz is exceeded, relevant element is exposed to instability. Thus, it is more feasible to express Eq. (2.16) as;

$$(I_z)_{cr} \geq \left(\frac{Tb}{A}\right) \sin\theta \left(\frac{\gamma_{sat}}{\gamma_w}\right) \left[1 - \left(\frac{\tan\theta}{\tan\varphi}\right)\right] \quad (2.17)$$

2.1.3. Method Proposed by Mora and Vahrson (1994)

Method Proposed by Mora and Vahrson (1994) developed a landslide stability evaluation model by depending on visual inspection of site in that certain values for topographical features of interested region and triggering factors are extracted from given tables. A degree of slope failure hazard is introduced as;

$$H_l = |S_r * S_l * S_h| * |T_s + T_p| \quad (2.18)$$

where H_l is the landslide hazard index, S_r, is the value of relative relief index, S_l, is the value of lithologic susceptibility, S_h, is the value of index of influence of natural humidity of the soil, T_s, is the value of influence of seismic intensity, T_p, is the value of influence of rainfall precipitation intensity.

The values for determining the susceptibility of site to triggering effects can be obtained from tables below;

Table 2.1. Relative relief values (R_r) values and their classes of influence in landslide susceptibility.

Relative Relief	**Susceptibility**	**Parameter, S_r**
0 – 75m/km^2	Very Low	0
76 – 175	Low	1
176 – 300	Moderate	2
301 – 500	Medium	3
501 – 800	High	4
> 800	Very High	5

Table 2.2. Classification of lithologic influence, according to general conditions, representative for Central America.

Lithology	**Susceptibility**	**Value, S_l**
Permeable limestone, slightly fissured intrusions, basalt, andesites, granites, ignimbrite, gneiss, hornfels; low degree of weathering, low water table, clean – rugose fractures, high shear strength rocks	Low	1
High degree of weathering of above mentioned lithologies and of hard massive clastic sedimentary rocks; low shear strength; shearable structures	Moderate	2
Considerably weathered sedimentary, intrusive, metamorphic, volcanic rocks, compacted sandy regolithic soils, considerable fracturing, fluctuating water tables, compacted colluvium and alluvium	Medium	3
Considerably weathered, hydrothermally altered rocks of any kind, strongly fractures and fissured, clay filled; poorly compacted pyroclastic and fluvio – lacustrine soils, shallow water tables	High	4
Extremely altered rocks, low shear resistance alluvial, colluvial and residual soils, shallow water tables	Very high	5

Table 2.3. Weighting for annual precipitation.

Summation of Precipitation Averages	**Susceptibility**	**Value, S_h**
0 – 4	Very low	1
5 – 9	Low	2
10 – 14	Medium	3
15 – 19	High	4
20 – 24	Very high	5

Table 2.4. Classes of average monthly precipitation.

Average Monthly Precipitation (mm/month)	**Assigned Value**
< 125	0
125 - 250	1
250 <	2

Table 2.5. Influence of seismic intensity (Modified Mercalli Scale) as a triggering factor for landslide generation.

Intensities (MM) T_r = 100 years	**Susceptibility**	**Value, T_s**
III	Slight	1
IV	Very low	2
V	Low	3
VI	Moderate	4
VII	Medium	5
VIII	Considerable	6
IX	Important	7
X	Strong	8
XI	Very Strong	9
XII	Extremely Strong	10

Table 2.6. Influence of rainfall precipitation intensity as a triggering factor for landslides.

Maximum Rainfall n > 10 years: T_r = 100 years	**Rainfall n<10 years; Average**	**Susceptibility**	**Value, T_p**
< 100 mm	< 50 mm	Very low	1
101 – 200	51 – 90	Low	2
201 – 300	91 – 130	Medium	3
301 – 400	131 – 175	High	4
> 400	> 175	Very High	5

Table 2.7. Classes of the potential landslide hazards, as derived from Eq. (2.18).

Value from Eq. (2.18)	**Class**	**Susceptibility of Hazard**
0 – 6	I	Negligible
7 – 32	II	Low
33 – 162	III	Moderate
163 – 512	IV	Medium
513 – 1250	V	High
> 1250	VI	Very High

Then, an example of landslide hazard map Costa Rica is shown in Figure 2.5.

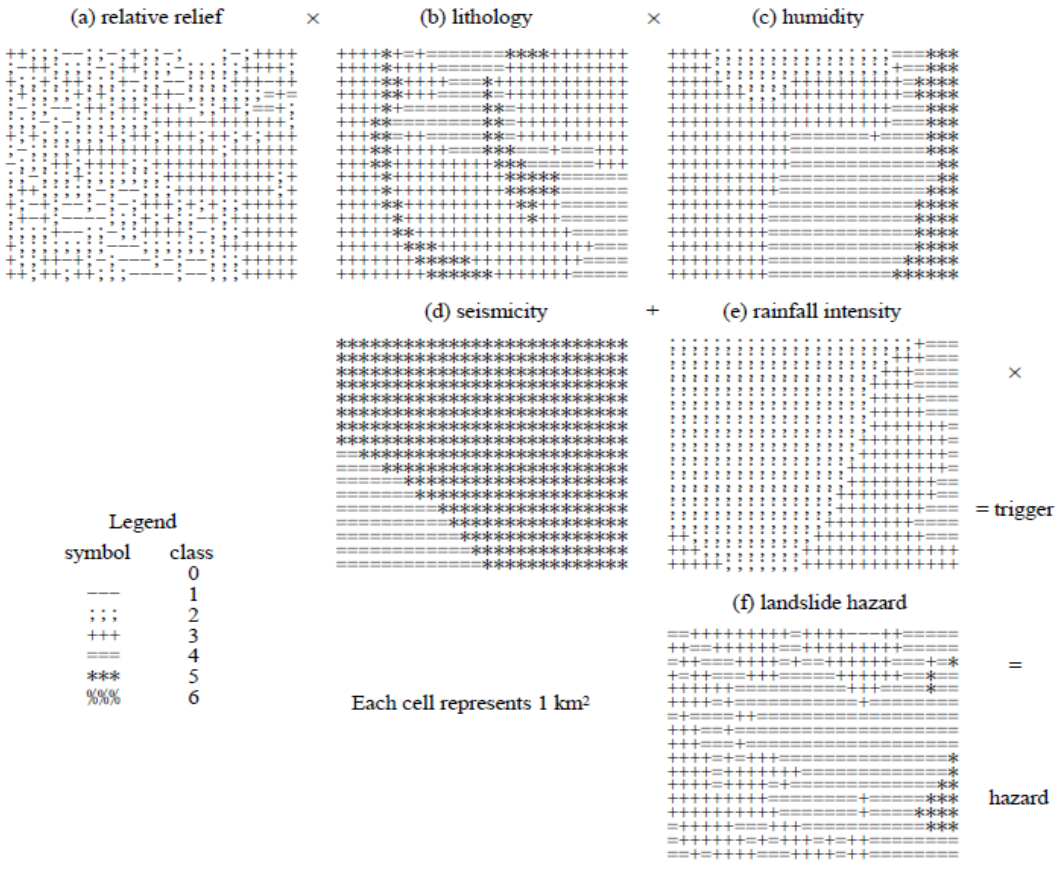

Figure 2.5. Hazard map for landslide at Tapanti in Costa Rica.

2.2. Statistical Methods

In landslide evaluation techniques, the most troublesome process is to suggest reasonable soil and topographical properties for carrying out factor of safety computations, thus concluding in that researchers should allocate time for obtaining qualified data as much as that spent for selecting or deriving appropriate methodologies. As partly done in Method Proposed by Papa, Medina, Ciervo and Bateman (2013), stochastic nature of such parameters is able to be simulated by adoptation of different routines or certain probability distributions are assessed as whether *goodness of fit* between data and chosen function is fulfilled or not.

On the other hand, probabilistic approaches properly serve the purpose of landslide failure estimation within the context of collecting event inventory rather than dealing with soil and topographical features of intetested site. Even if topography is able to be extracted from GIS programs, soil characteristics consisting of permeability, internal friction angle shear strength angle, cohesion, etc. compel researches to conduct lab tests or site investigations, which are generally undesired situations for them. In other words, being supplied with a chance to gain landslide inventory implicates that one is granted for grasping both hazard created by different effects such as rainfall and/or earthquake and vulnerability of relevant hillslopes.

All of the routines incorporated into this methodology approximately consult on same procedure that collection of landslide inventory is followed by the adoptation of convenient probability distribution function. Here is presented a methodology referred quite a few times in literatüre.

2.2.1. Method Proposed by Malamud, Turcotte, Guzetti and Reichenbach (2004)

This methodology is launched by the emphasis on the significance of producing reliable and complete landslide inventory in order that selected and/or generated probability distribution function are expected to present more reasonable results. It states that four important points should be looked out for the techniques employed to prepare inventory maps;

1. The cause of landslide inventory map generation
2. The extent of the study area
3. The map scale
4. The resources available to conduct the mapping process.

What should be performed in this procedure is to focus on historical information on individual landslide events and aerial photographs revealing the landslide scars on interested site. The former is embraced for constructing a landslide archive in which the location of each event is able to be observed and the latter portrays the distribution of slide deposits, also called as geomorphological maps. These maps usually consist of (1) *a landslide – event inventory*, including all of the slope failures related to earthquake, rainfall or snowmelts, or (2) *a historical landslide inventory*, occurred in past.

On the other hand, this article gives places to the limitations that might be encountered during the preparation of landslide inventory maps such as the projection of landslide's location onto paper and/or being unable to identify the presence of drainage lines, vegetation covers and man – made constructions, which is also quite imporant in terms of sliding evaluation. In addition to this, the determination of landslide geometry might sometimes be such distressfull operations that deep – seated events cannot be identified easily from aerial photographs. However, it is stated that the development of GIS Program, in which coding through vector – based GIS system is expected to be simple, annihilates the drawbacks arising within the context of this process.

After that point, Method Proposed by Malamud, Turcotte, Guzetti and Reichenbach (2004) proceeds with the declaring of probability density function, which can be proposed as;

$$p(A_L) = \frac{1}{N_{LT}} \frac{\delta N_L}{\delta A_L} \tag{2.19}$$

where, $\delta N_L / \delta A_L$, is the number of landslide with areas between A_L and $A_L + \delta A_L$, N_{LT}, is the total number of landslides.

In this article, three – parameter inverse gamma distribution is adopted such as;

$$p(A_L;\rho,a,s)=\frac{1}{a\Gamma(\rho)}\left[\frac{a}{A_L-s}\right]^{\rho+1}e^{\left[-\frac{a}{A_L-s}\right]} \tag{2.20}$$

where ρ is the parameter primarily controlling power – law decay for medium and large values in three – parameter inverse – gamma probability distribution, a is the parameter primarily controlling location of maximum probability in three – parameter inverse – gamma probability distribution, s is the parameter primarily controlling exponential rollover for small values in three – parameter invers – gamma probablity distribution, A_L is the area of landslide, Γ(ρ), is the gamma function of ρ.

Also, Eq. (2.20) is able to be normalized to 1 so that simplification of results can be provided, that is, the cumulative distrubution for inverse – gamma function is attained as;

$$\int_s^{\infty}\frac{1}{a\Gamma(\rho)}\left[\frac{a}{A_L-s}\right]^{\rho+1}e^{\left[-\frac{a}{A_L-s}\right]}=1 \tag{2.21}$$

Then, the ultimate equation can be concluded by mathematical manupulations such as;

$$1-\frac{\Gamma(\rho,-a/s)}{\Gamma(\rho)} \tag{2.22}$$

where,

$$\Gamma\left(\rho,-\frac{a}{s}\right)=\left(-\frac{a}{s}\right)^{\rho-1}e^{\frac{a}{s}} \tag{2.23}$$

What is obtained after the probabilistic approach proposed by Method Proposed by Malamud, Turcotte, Guzetti and Reichenbach (2004) is presented in Figure 2.6. As stated, landslide area is able to be estimated for a given probability degree.

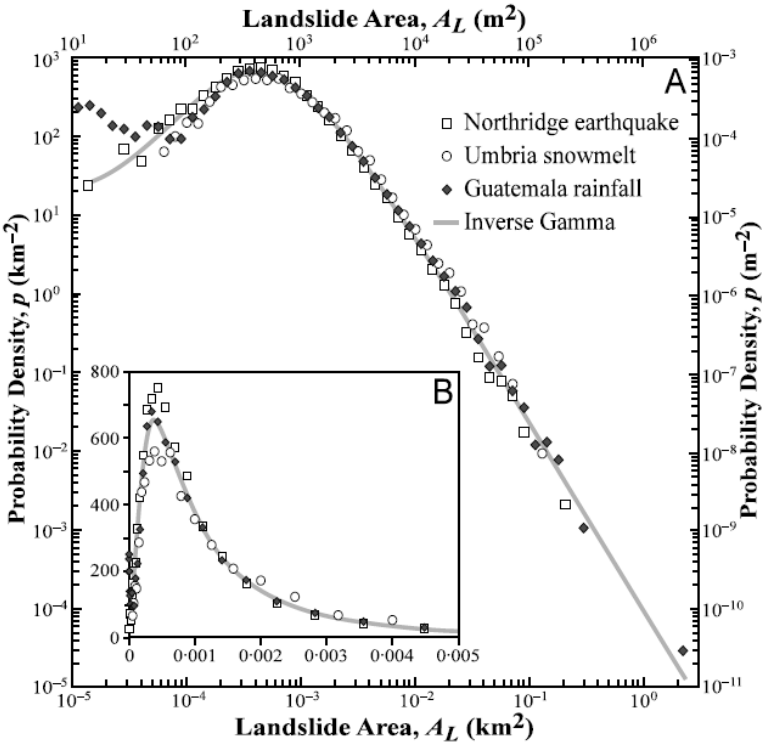

Figure 2.6. Dependence of landslide probability densities p on landslide area A_L, for three landslide inventories.

2.3. Analytical Methods

The most important issue in rainfall – triggered landslide is to ascertain the pore water pressure generation with regard to rain water percolation through soil in that the quantification of this phenomenon results in the derivation of Richards' Equation. This equation can be recasted in 2 – D or 3 – D conditions in which do not allow one to apply analytical solution in order to obtain water seepage profile during rainfall if certain assumptions are able to be accounted for parameters included in relevant equation. The method presented below begins with the construction of 3 – D Richards' Equation by appealing such an presumption that it is possible to reduce 3 – D equation into 1- D form which can be treated with the help of analytical approaches. After that, the generated solution for quantifying pore pressure development is combined with the traditional infinite – slope stability model to monitor the change in factor of safety with respect to time.

2.3.1. Method Proposed by Iverson (2000)

In general, most of the approaches are devised with the help of this statement that "*If water goes in, and does not come out, then it is still here*". This is called as conservation of mass and the same route is adopted in this report so that an analytical model will be able to be generated to compute the pore pressure redistribution in response to heavy rainfall effect. Also, since it is known that physical processes influencing the groundwater pressures operate on disparate timescales , the definition of long – term and short – term timescales are included in the analysis to analyze both the effect of topography, geology, and climate on slope failure potential and hillslope response to individual rainstorms or groups of storms, respectively. Furthermore, these timescales paves the way for linearizing the nonlinear Richards' Equation so that it can be treated easier than available methods for solving nonlinear partial differential equations.

The last part is reserved for incorparating this pore water pressure into the limit equilibrium analysis of infinite slope model in that the pressure head component of equation is modified to insert the increase / decrease in pressure with respect to rainfall duration. This means that short time scale is used as a way of computing the transient rainfall effect on hillslope stability whereas, the long time scale corresponds to one required for reaching the steady state groundwater flow conditions.

In the first step, consider Darcy' s Law;

$$\mathrm{q} = -\mathrm{K}\frac{\partial \mathrm{h}}{\partial \mathrm{z}} \tag{2.24}$$

where q is the water dischage, K is the hydraulic conductivity of the soil, $\partial \mathrm{h}/\partial \mathrm{z}$ is the hydraulic gradient.

As stated previously, the insertion of water into soil cause to increase in moisture content formulized as (conservation of mass for inflow and outflow water);

$$\frac{\partial \omega}{\partial t} + \frac{\partial q}{\partial z} = 0 \tag{2.25}$$

where ω, is the moisture content of the soil.

Also, this eq can be recasted such that;

$$\frac{\partial \omega}{\partial t} = \frac{\partial}{\partial z}\left(K\frac{\partial h}{\partial z}\right) \tag{2.26}$$

where h is the total head.

The total head is composed of two components; pressure head and elevation head in that the former is dependent on the suction of capillary action in unsaturated part of soil and the latter corresponds to the height of overlying water from a horizontal datum. Thus, h can be defined as;

$$h = \psi + z \tag{2.27}$$

Then,

$$\frac{\partial \omega}{\partial t} = \frac{\partial}{\partial z}\left(K\frac{\partial(\psi + z)}{\partial z}\right) \tag{2.28}$$

or,

$$\frac{\partial \omega}{\partial t} = \frac{\partial}{\partial z}\left(K\frac{\partial \psi}{\partial \theta}\frac{\partial \omega}{\partial z} + K\right) \tag{2.29}$$

Where $K\,{}^{\partial\psi}/_{\partial\omega}$, is called as diffusivity (D). Then,

$$\frac{\partial \omega}{\partial t} = \frac{\partial}{\partial z}\left(D\frac{\partial \omega}{\partial z} + K\right) \tag{2.30}$$

This is the conventional Ricahards' Equation derived for one – dimensional water infiltration but we should further develop it to incorparate the three – dimensionality of the problem as;

$$\frac{d\alpha}{d\Psi}\frac{\partial\Psi}{\partial t} = \frac{\partial}{\partial x}\left[K_L(\Psi)\left(\frac{\partial\Psi}{\partial x} - \sin\theta\right)\right] + \frac{\partial}{\partial y}\left[K_L(\Psi)\left(\frac{\partial\Psi}{\partial y}\right)\right] + \frac{\partial}{\partial z}\left[K_z(\Psi)\left(\frac{\partial\Psi}{\partial z} - \cos\theta\right)\right] \quad (2.31)$$

where Ψ, is the pressure – head, $K_z(\Psi)$ and $K_L(\Psi)$ are vertical and horizontal hydraulic conductivity, respectively.

At this stage, Method Proposed by Iverson (2000) is exploited to decouple Eq. (2.34) into its components in that it is possible to evaluate both time – dependent pressure head values and seepage forces arising due to the water movement through different regions in site by embracing appropriate time scales;

$$t^*_{Short-Term} = \frac{tD_0}{H^2} \quad (2.32)$$

$$t^*_{Long-Term} = \frac{tD_0}{A} \quad (2.33)$$

where $t^*_{Short-Term}$ represents the minimum time required for strong slope – normal pore pressure transmission from the ground surface to depth, H, $t^*_{Long-Term}$ represents the minimum time required for strong slope – normal pore pressure transmission from the area, A to the point (x, y, H), D_0, is the maximum characteristic diffusivity governing transmission of pressure head, and it thereby provides a convenient reference diffusivity.

- **Normalization Process:**

Iverson (2000) attempts to perform a normalization process for each parameters included in Eq. (2.24) in order that assessment of pore pressure at interested depth, H, and areal position, (x, y), can be feasible. The former one is embraced to make it possible for constructing an appropriate reference for the pressure head ψ that develops at certain depth

in response to rainfall effect. The latter one allows one to establish a criteria for lateral groundwater flow which commences after a long time of vertical seepage. For those purposes, H and $\sqrt{A}$ parameters are employed in the application of normalization to the Eq. (2.24), respectively;

$$\psi^* = \frac{\psi}{H}, z^* = \frac{z}{H}, x^* = \frac{x}{\sqrt{A}}, y^* = \frac{y}{\sqrt{A}} \tag{2.34}$$

$$K_L^* = \frac{K_L(\psi)}{K_{sat}}, K_z^* = \frac{K_z(\psi)}{K_{sat}} \tag{2.35}$$

$$D_L = \frac{K_L(\psi)}{C(\psi)}, D_z = \frac{K_z(\psi)}{C(\psi)}, D_0 = \frac{K_{sat}}{C_0} \tag{2.36}$$

- **Short - Term Response**

As mentioned above, both normalization parameters in from Eq. (2.36) to Eq. (2.34) and timescale adopted for short – term response, Eq. (2.32), are substituted into Eq. (2.31) such as;

$$\frac{C(\psi)}{C_0}\frac{\partial \Psi^*}{\partial t^*} = \varepsilon^2 \frac{\partial}{\partial x^*}\left[K_L^*\left(\frac{\partial \Psi^*}{\partial x^*} - \frac{1}{\varepsilon}\sin\alpha\right)\right] + \varepsilon^2 \frac{\partial}{\partial y^*}\left[K_L^*\left(\frac{\partial \Psi^*}{\partial y^*}\right)\right] + \frac{\partial}{\partial z^*}\left[K_z^*\left(\frac{\partial \Psi^*}{\partial z^*} - \cos\alpha\right)\right] \tag{2.37}$$

where,

$$\varepsilon = \sqrt{\frac{H^2/D_0}{A/D_0}} = \frac{H}{\sqrt{A}} \tag{2.38}$$

If catchment area is selected as making $\varepsilon \ll 1$, Eq. (2.37) is reduced into;

$$\frac{C(\psi)}{C_0}\frac{\partial \Psi^*}{\partial t^*} = \frac{\partial}{\partial z^*}\left[K_z^*\left(\frac{\partial \Psi^*}{\partial z^*} - \cos\alpha\right)\right] \tag{2.39}$$

At this point, vertical coordinate definition can be intoduced to modulate the Eq. (2.39) as;

$$\frac{C(\psi)}{C_0}\frac{\partial \Psi^*}{\partial t^*} = \cos^2\alpha \frac{\partial}{\partial Z^*}\left[K_z^*\left(\frac{\partial \Psi^*}{\partial Z^*} - 1\right)\right] \tag{2.40}$$

where The elevation head, $Z = x\sin\alpha + z\cos\alpha$ is measured vertically downward from a horizontal reference plane that passes through the origin on the ground surface.

Also, Eq. (2.40) is employed to monitor the pore pressure change during rainfall infiltration in that it should be recasted as containing rain water flux. In literature, there exists a great variety of methods to model the rainfall effect as function of a chosen parameter, such as time, those depending on rainfall characteristics of relevant area, and so on. Iverson (1990) alternatively devises that rain water flux can be grasped within the boundaries of Darcy's Law, $I_Z = -K_Z(\partial h/\partial Z)$, provided that one should be brace enough to overestimate pressure head values with regard to true condition. Then, Eq. (2.40) takes its form as;

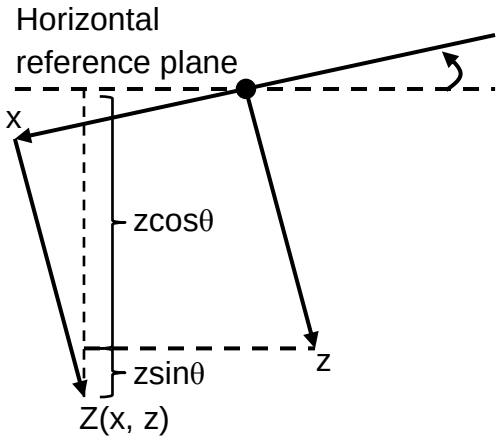

Figure 2.7. Definition of the vertical coordinate.

$$\frac{C(\psi)}{C_0}\frac{\partial \Psi^*}{\partial t^*} = \cos^2\alpha \left[K_z^*\frac{\partial^2 \Psi^*}{\partial Z^{*2}} - \frac{I_Z}{K_Z}\frac{\partial K_z^*}{\partial Z^*}\right] \tag{2.41}$$

However, this equation still disallows one to conclude in exact solution due to its nonlinearity but Eagleson (1970) states that if soil medium is initially wet, the 2_{nd} term in

square bracket at RHS of Eq. (2.41) can be omitted because of the fact that $K_z \rightarrow K_{sat}$, $C(\psi) \rightarrow C_0$ and gravity – driven term become negligible. Thus, it yields;

$$\frac{\partial \Psi^*}{\partial t^*} = \frac{C_0 K_z^* \cos^2\alpha}{C(\psi)} \frac{\partial^2 \Psi^*}{\partial Z^{*2}} \tag{2.42}$$

This is 2_{nd} order linear partial differential equation, which resembles heat equation in terms of its form, and can be solved by means of "*similarity solution*". To that end, two boundary and one initial conditions are defined as;

$$\psi(Z, 0) = (Z - d_Z)\beta \tag{2.43}$$

$$\frac{\partial \psi}{\partial Z}(\infty, t) = \beta \tag{2.44}$$

$$\frac{\partial \psi}{\partial Z}(0, t) = \begin{cases} -I_Z/K_z + \beta & t \leq T \\ \beta & t > T \end{cases} \tag{2.45}$$

where,

$$\beta = \cos^2\theta - (I_Z/K_Z)_{Steady} \tag{2.46}$$

$$(I_Z/K_Z)_{Steady} = (I_Z/K_Z) * \cos^2\theta \tag{2.47}$$

As a matter of fact, Eq. (2.44) and Eq. (2.43) overlap with each other within the context of similarity solution but we give place to both of them in order to emphasize the physical significance of pore pressure development. Eq. (2.43) remarks that hydrostatic groundwater level governs the initial condition, and there is no rainfall effect at greater depths as dictated by Eq. (2.44). Also, Eq. (2.45) reveals the Darcy's Law presumption for water flux arising as a result of rainfall percolation. Finally, it is possible to come up with a solution given as;

$$\frac{\psi}{Z}(Z, t \leq T) = \beta\left(1 - \frac{d_Z}{Z}\right) + \frac{I_Z}{K_Z}[R(t^*)] \tag{2.48}$$

$$\frac{\psi}{Z}(Z, t > T) = \beta\left(1 - \frac{d_Z}{Z}\right) + \frac{I_Z}{K_Z}[R(t^*) - R(t^* - T^*)] \tag{2.49}$$

where d_Z is the groundwater table depth, T is the rainfall duration.

$$\widehat{D} = 4D_0\cos^2\alpha \tag{2.50}$$

$$t^* = \frac{t}{Z^2/\widehat{D}} \tag{2.51}$$

$$T^* = \frac{T}{Z^2/\widehat{D}} \tag{2.52}$$

are normalized times,

$$R(t^*) = \sqrt{t^*/\pi}\, e^{-1/t^*} - \mathrm{Erfc}\left[1/\sqrt{t^*}\right] \tag{2.53}$$

is a pressure head response function, which depends only on normalized time.

Up to this point, only hydrological response of the soil is quantified but the critical issue is to evaluate whether there occurs any failure at any depth of soil continuum or not. It is widely known that the force equilibrium is able to be provided for infinite – slope as;

$$FoS(Z, t) = \frac{c' + (Z\gamma_{sat} - h\gamma_w)\cos^2\theta\tan\varphi'}{Z\gamma_{sat}\cos\theta\sin\theta} \tag{2.54}$$

If $h\cos^2\theta$ term in square bracket at the nominator of Eq. (2.54) is replaced with time – dependent pressure head in short – term response, we are supplied with a chance to rewrite Eq. (2.54) as;

$$FoS(Z, t) = \frac{\tan\varphi'}{\tan\theta} - \frac{\psi(Z, t)\gamma_w\tan\varphi'}{\gamma_{sat}Z\sin\theta\cos\theta} + \frac{c'}{\gamma_{sat}Z\sin\theta\cos\theta} \tag{2.55}$$

where φ’ is the shear strength angle, c’ is the cohesion intercept, γ_{sat} is the saturated unit weight.

- **Long – Term Response:**

As implied in the definition of the timescales, seepage drag occurs within the soil continuum due to the elevated groundwater table in that this stage is followed by the emergence of steady – state condition which it is actually quantified in Montgomery and Dietrich (1994) Method. However, Iverson (2000) puts forward another approach and strives for combining the differential solution of Richards' Equation and that proposed by Montgomery and Dietrich (1994) but reaches contradictory results. Normalization parameters in Eq. from (2.34) to (2.36) and timescale identified for steady – state condition, Eq. (2.33), are incorporated into Eq. (2.31) as;

$$\varepsilon^2 \frac{C(\psi)}{C_0}\frac{\partial \Psi^*}{\partial t^*} = \varepsilon^2 \frac{\partial}{\partial x^*}\left[K_L^*\left(\frac{\partial \Psi^*}{\partial x^*} - \frac{1}{\varepsilon}\sin\alpha\right)\right] + \varepsilon^2 \frac{\partial}{\partial y^*}\left[K_L^*\left(\frac{\partial \Psi^*}{\partial y^*}\right)\right] + \frac{\partial}{\partial z^*}\left[K_z^*\left(\frac{\partial \Psi^*}{\partial z^*} - \cos\alpha\right)\right] \tag{2.56}$$

As similar to short – term response, if appropriate selection can be made for H and $\sqrt{A}$, $\varepsilon \ll 1$. Then, Eq. (2.56) becomes,

$$\frac{\partial}{\partial z^*}\left[K_z^*\left(\frac{\partial \Psi^*}{\partial z^*} - \cos\theta\right)\right] = 0 \tag{2.57}$$

Eq. (2.57) is able to be solved by direct integration, which creates the expression in dimensional form;

$$\Psi = z[\cos\theta + f(x,y)(K_{sat}/K_z)] + c \tag{2.58}$$

where,

c, is a constant of integration that depends on water table depth

f, is a function that depends on the rate and spatial distribution of long – term rain infiltration.

At this point, Iverson (2000) consults on constant flux boundary condition for rainfall infiltration as similar to performed in short – term response, where flux is specified as I_z, and the fact that pressure head is zero at GWL yields,

$$\Psi = (z - d_Z)[\cos\theta - (I_z/K_z)] \tag{2.59}$$

$$h = -x\sin\theta - d_Z\cos\theta - (z - d_Z)(I_z/K_z) \tag{2.60}$$

where h is used to denote total head variation in soil mass.

2_{nd} in square bracket at RHS of Eq. (2.59) can be omitted in the case that rainfall infiltration is known to be quite slow, thus resulting in the justification of the presumption above;

$$\Psi = (z - d_Z)\cos\theta \tag{2.61}$$

$$h = -x\sin\theta - d_Z\cos\theta \tag{2.62}$$

As can be observed in Eq. (2.62), water movement only occurs in x direction since hydraulic gradient exists such as, $\partial h/\partial x = \sin\theta$.

At that point, if a reference depth, δ, is selected to quantify the water flow in x – direction, the water discharge can be written as;

$$Q_x = b(\delta - d_Z)K_x\sin\theta \tag{2.63}$$

Iverson (2000) attempts to compound Eq. (2.63) and Eq. (2.13), which yields;

$$\psi = (z - \delta)\cos\theta + \frac{I_z A\cot\theta}{bK_x} \tag{2.64}$$

However, Eq. (2.64) seems to generate a conflicting pressure head vealues in that $I_z/K_z \to 0$, adopted in the derivation of Eq. (2.61) and Eq. (2.62), requires the presumption

of $K_z \gg K_x$, (which yields ${I_z}/{K_z} \gg {I_z}/{K_x}$), which is not usually encountered in natural slopes. Therefore, (Iverson, 2000) only employs the Eq. (2.61) for the identification of steady – state condition.

2.3.2. Method Proposed by Papa, Medina, Ciervo and Bateman (2013)

The core of this methodology is dependent on the routine developed in Method Proposed by Iverson (2000) but the current one is separated from the former by difference that it is aware of stochastic nature of governing soil parameters in interested site. In other words, it states that there exists a possibility of inserting uncertainty of related paramters into the analysis by means of statistical approaches, Monte Carlo Simulation.

This model starts with the performance of a sensitivity analysis on failure percentage, which is defined as the ratio of the number of unstable cells to the total number of basin cells. This permits one not to take the whole region into consideration for slope stability calculations, which is quite time – consuming. Also, the input parameters are sorted out into two main categories as, static and dynamic, in which the former is composed of morphological features (A/b, Z_T, θ) and soil parameters (c, φ, γs, K_x, K_Z, D_0) the latter consists of the rainfall related variables ($(I_z)_{steady}$, I_Z, T).

At the last part of the methodology, critical rainfall threshols, plotted for certain failure percentages with respect to rainfall intensity and rainfall duration, are generated to construct an eartly warning system for debris flow occurrence under the possible heavy rainfall conditions. Even if the nucleus of this methodology stands on the one improved by Method Proposed by Iverson (2000), it examines the boundaries of the former in the name of generating appropriate simulations for interested rainfall duration ranges. In other words, the Eq. (2.48) can be derived with respect to time T, where I_z is given as H/T and H is the accumulated rainfall during T. This yields;

$$\mathrm{Erfc}\left[1/\sqrt{T^*}\right] - 0.5\sqrt{T^*/\pi}\, e^{-1/T^*} \tag{2.65}$$

which reveals that the function, Ψ/Z, increases with rainfall duration when;

$$T^* < 5.33 \tag{2.66}$$

If the Eq. (2.66) is substituted into the Eq. (2.52), T_{crit} can be obtained as;

$$T_{crit} = 1.4 \frac{Z^2}{D_0 \cos(\beta)} \tag{2.67}$$

This T_{crit} tallies with the definition presented in Method Proposed by Iverson (2000), which states that the time required for strong normal pore pressure transmission from ground surface to the depth, H, is H^2/D_0 . This means that rainfall duration should be greater than T_{crit} value in order to simulate rain water percolation to the relevant destination in soil medium properly. In order to perform rainfall – induced landslide stability analysis, The Sambuca Basin is selected which is a steep coastal watershed of Amalfi Peninsula, southern Italy (Figure 2.8). It covers an area of about 6.4 km^2. The mean slope is 320 and the elevations spread from 1000 m, with a mean elevation of 422 m. In this study, topographical features (A/b, α) are extracted from GIS program.

In this area, 21 homogeneous districts in Figure 2.9 are detected and are all assigned to the variables as given in Table 2.8. By assigning T_{crit} values which are computed with respect to different values of soil depth and permeability in the 21 soil districts and those given in Table 2.8, three pair of simulations for FP = 1% and 3% are performed such that the first and second simulations base on the deterministic soil properties wheres the sim03 adopts a probabilistic distribution for these features. Results are presented in Figure 2.10. It can be seen that deterministic curves usualy lies on the probabilistic one, thus revealing that deterministic approach underestimates the hazard It can be concluded that stochastic way of selecting soil parameters may yield to more reliable results.

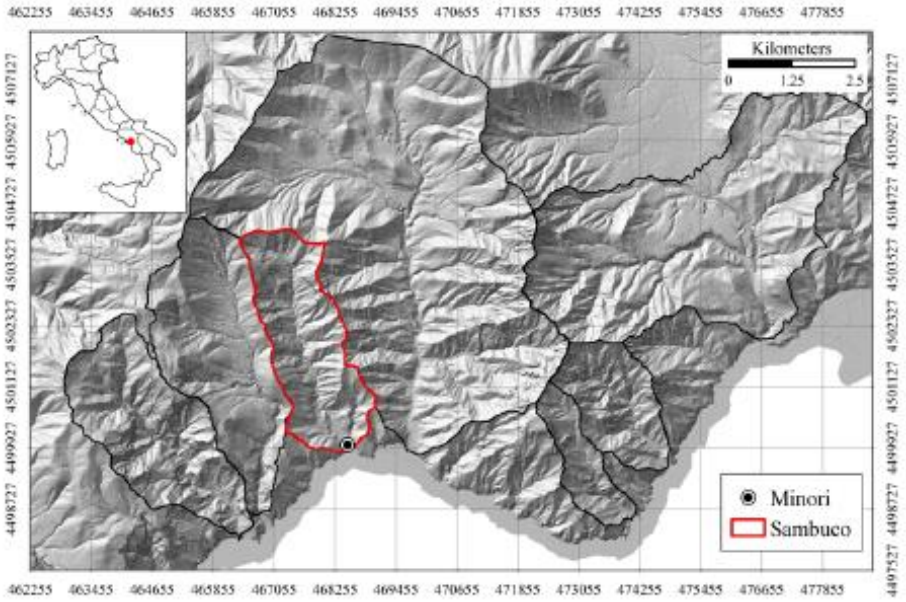

Figure 2.8. Geographical context of the study area (WGS, 1984, UTM Zone 330 N).

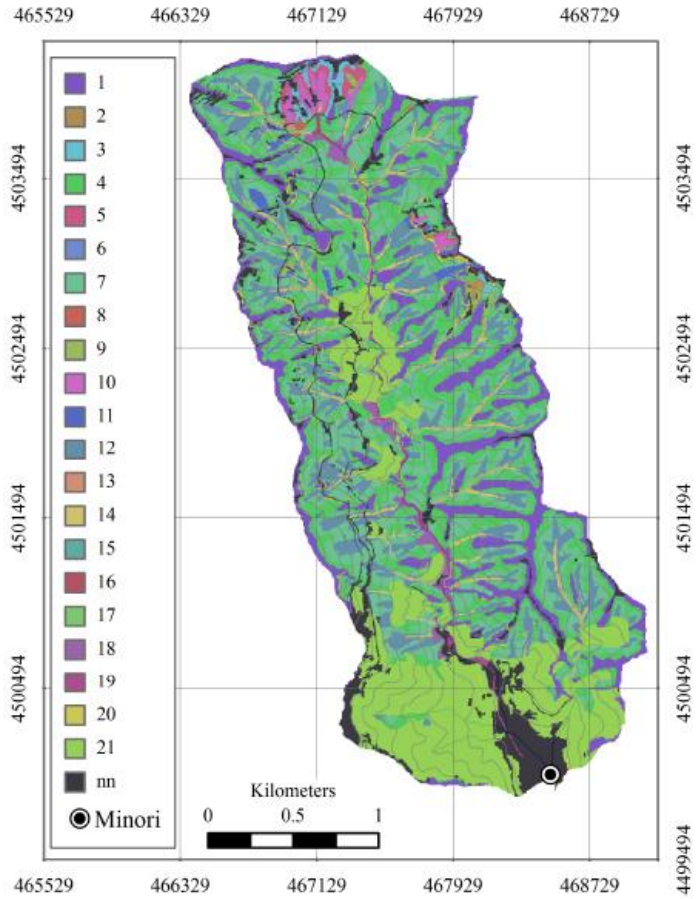

Figure 2.9. Map of the geomorphological homogeneous districts.

Table 2.8. Values of the static variables for the 21 homogeneous districts of Sambuca Basin.

Districts [-]	Z_T [m]	γ_s (kg/m^3)	Φ^0	c [kPa]	K_x [mm/sec]	K_z [mm/sec]
1	0.5	1500	32	10	0.96	0.96
2	0.5	1400	35	5	0.36	0.06
3	0.5	1400	35	5	0.36	0.06
4	1	1400	35	5	0.36	0.06
5	1.5	1400	35	5	0.36	0.06
6	1	1400	35	5	0.36	0.06
7	1.5	1400	35	5	0.36	0.06
8	2	1400	35	5	0.36	0.06
9	5	1400	35	5	0.36	0.06
10	1	1500	32	10	0.22	0.11
11	1.5	1500	32	10	0.22	0.11
12	2	1500	32	10	0.22	0.11
13	3.5	1500	32	10	0.22	0.11
14	5	1500	32	10	0.22	0.11
15	1	1800	35	0	0.68	0.68
16	1.5	1800	35	0	0.68	0.68
17	3.5	1800	35	0	0.68	0.68
18	5	1800	35	0	0.68	0.68
19	4.5	1500	32	10	0.18	0.10
20	5	1800	35	0	0.68	0.68
21	4	1500	32	10	0.09	0.09

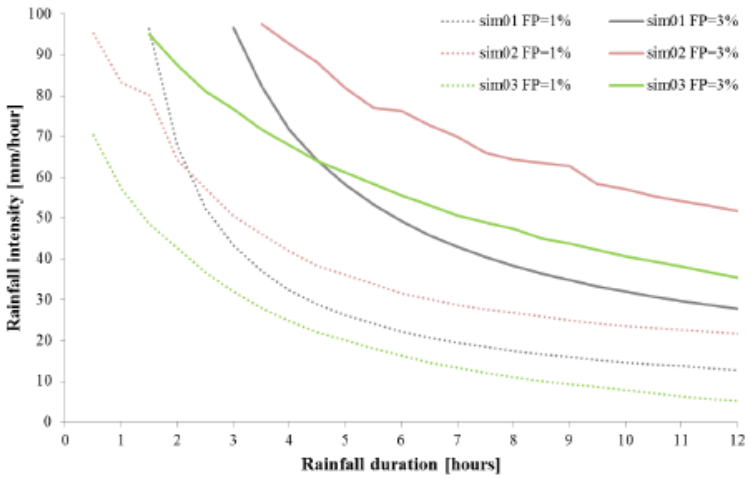

Figure 2.10. Simulated and generated crt curves.

2.3.3. Method Proposed by Srivastava and Yeh (1991)

What is achieved by Srivastava and Yeh (1991) with respect to Method Proposed by Iverson (2000) is to give place to the unsaturated part of soil mass rather than omitting it by assuming that hydraulic conductivity in unsaturated portion of hillslope converges to saturationed one (Figure 2.11). However, as stated previously, it is impossible to perform exact analytical solutions to governing Richards' Equation but Srivastava and Yeh (1991) intoduced some functions for hydraulic conductivity and volumetric water content in that the remedy for getting rid of using numerical methodolgies is created.

This routine begins with the definiton of one – dimensional vertical water flow in soil continuum such as;

$$\frac{\partial \omega}{\partial t_*} = \frac{\partial}{\partial z_*}\left[K_*(\psi)\frac{\partial(\psi + z_*)}{\partial z_*}\right] \tag{2.68}$$

where z_*, is the vertical coordinate, positive upward, K_* is the unsaturated hydraulic conductivity, which is a function of pressure head, ψ (negative for unsaturated flow), ω is the moisture content, t_* denoted the time.

Gardner (1958b) declares that functions for hydraulc conductivity and volumetric water content can be proposed as

$$K_*(\psi) = K_s e^{\alpha\psi} \tag{2.69}$$

$$\omega = \omega_r + (\omega_s - \omega_r)e^{\alpha\psi} \tag{2.70}$$

where K_s is the saturated hydraulic conductivity, ω_s is the saturated volumetric water content, ω_r is the residual volumetric water content, α is the soil pore – size distribution parameter representing the rate of reduction in hydraulic conductivity or moisture content as ψ becomes more negative.

Then, the relevant constituive equation depending on Eq. (2.68), Eq (2.69) and Eq. (2.70) simultaneously can be obtained as;

$$\frac{\partial^2 K_*}{\partial z_*^2} + \alpha \frac{\partial K_*}{\partial z_*} = \frac{\alpha(\omega_s - \omega_r)}{K_s} \frac{\partial K_*}{\partial t_*} \tag{2.71}$$

As can be seen, the Eq. (2.71) is the 2_{nd} order linear partial differential equation, which can be solved analytically by means of certain normalization process. To illustrate the process, consider one – dimensional vertical rain water infiltration through homogeneous soil layer. At that point, Srivastava and Yeh (1991) appeals to dimensionless parameters arising from the normalization of those included in Eq. (2.71);

$$z = \alpha z_* \text{ so that } L = \alpha L_* \tag{2.72}$$

$$K = \frac{K_*}{K_s} \tag{2.73}$$

$$q_A = \frac{q_A^*}{K_s}, \qquad q_B = \frac{q_B^*}{K_s} \tag{2.74}$$

$$t = \frac{\alpha K_s t_*}{\omega_s - \omega_r} \tag{2.75}$$

where L_*, is the depth to water table, ψ_0 is the prescribed pressure at the water table, q_A^* is the initial flux at the soil surface which, along with ψ_0, determines the initial pressure distribution in the soil, q_B^* is the prescribed flux at the soil surface (rainfall amount)

Then, Eq. (2.71) becomes,

$$\frac{\partial^2 K}{\partial z^2} + \frac{\partial K}{\partial z} = \frac{\partial K}{\partial t} \tag{2.76}$$

The appropriate initial and boundary conditions for coming up with the result is able to be presented as;

$$K(z, 0) = q_A - \left(q_A - e^{\alpha \psi_0}\right) e^{-z} = K_0(z) \tag{2.77}$$

$$K(0,t) = e^{\alpha\psi_0} \tag{2.78}$$

$$\left(\frac{\partial K}{\partial z} + K\right)_{z=L} = q_B \tag{2.79}$$

The prefered equation is derived in the form of K with the help of Laplace Transform;

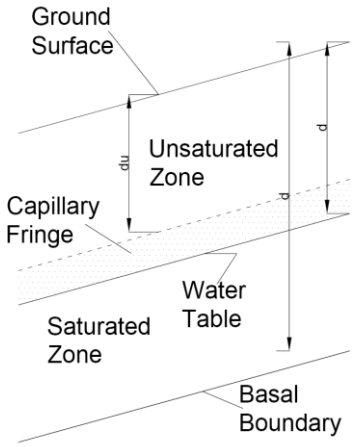

Figure 2.11. Ground – water condition in a related slope.

$$\overline{K} = \frac{K_0(z)}{s} + (q_B - q_A)e^{(L-z)/2}F(s) \tag{2.80}$$

where,

$$F(s) = \frac{1}{s}\frac{\sinh\left[z\left(s+\frac{1}{4}\right)^{1/2}\right]}{\frac{1}{2}\sinh\left[z\left(s+\frac{1}{4}\right)^{1/2}\right] + \left(s+\frac{1}{4}\right)^{1/2}\cosh\left[z\left(s+\frac{1}{4}\right)^{1/2}\right]} \tag{2.81}$$

After conducting inverse Laplace Transformation, the ultimate form is able to be presented as;

$$K = q_B - \left(q_B - e^{\alpha\psi_0}\right)e^{-z} - 4(q_B - q_A)e^{(L-z)/2}e^{-t/4}\sum_{n=1}^{\infty}\frac{\sin(\lambda_n L)e^{-\lambda_n^2 t}}{1 + (L/2) + 2\lambda_n^2 L} \tag{2.82}$$

Also, developing pore pressures are able to be attained as;

$$\psi = \frac{\ln K}{\alpha} \tag{2.83}$$

where λ_n is the positive roots of the characteristic equation;

$$\tan(\lambda L) + 2\lambda = 0 \tag{2.84}$$

What is the aberration in this methodology is that lower boundary is set forth as water table, whose pore pressure is 0, thus resulting in the lack of computing the actual location of ground – water table. Thus, one intending to determine the ground water table position after vertical rainfall infiltration, which is in essence required for the calculation of seepage drag, is deprived of incorporating horizontal water movement in hilslope mass into his analysis.

2.4. Numerical Methods

All the methods that have been explained until this point refer to the certain presumptions in order to avoid nonlinearity in Richards' Equation, which is the quantification of percolating rain water through soil medium. The fact that researchers are forced to derive methodologies not quite elaborative but produce reasonable results restricts them not to deal with numerical solutions because mass conservation during analysis and time constraints are the most imporant issue in their use. In these methods, the soil layers are discretized into small areas consisting of nodes and boundaries in order that Richards's Equation is numerically solved step by step for each nodes to have pore pressure profile through soil. To that end, certain numerical scheme is adopted to get solutions provided that numerical errors should be smaller than a prescribed value and mass conservation (water mass in our case) also should be satisfied throughout the analysis.

2.4.1. Method Proposed by Freeze and Witherspoon (1966)

This methodology is initiated by such an intent of modeling the steady – state groundwater flow in soil mass that theoretical flow patterns are able to be delineated both in two and three dimensional cases. The logic bears on the comparison of analytical and numerical methods and their efficiencies in different conditions but the numerical treatments asserting throughout the article is presented here to display its significance in process.

Freeze and Witherspoon (1966) begins with the certain presumptions as;

1. Permeable soil layer is underlied by impervious one in that the former is able to be quantified by the selection of reasonable hydraulic conductivity value.
2. The water table is devised as the upper bound of saturated part of the soil continuum, where the pore pressure is set equal to 0.
3. As adopted in Montgomery and Dietrich (1994) Methodology, the steady – state condition governs the hydrological response of soil mass, which means that the height of water table does not fluctuate with time. This phenomenon is called as "steady – rainfall" case in soil science literatüre.

Numerical solution implies the removal of the limitations in analytical ones with a simplification that continuum characteristics of soil medium is replaced by the condition consisting of plenty of nodes at different locations. Then, the differential equation produced for imitating the water flow is recasted as a finite system of simultaneous linear equations for mesh points by means of well – known Taylor's Expansion (Figure 2.12). This process is called as *discretization* and pore water pressure value at each node is calculated by the solution of the system of n smultaneous linear finite – difference equations.

At the first case, Richads' Equation should be declared to illustrate the mathematical approach improved for steady – state water flow through soil continuum;

$$\frac{\partial}{\partial \mathrm{x}}\left[\mathrm{K}(\mathrm{x},\mathrm{y},\mathrm{z})\frac{\partial \psi}{\partial \mathrm{x}}\right]+\frac{\partial}{\partial \mathrm{y}}\left[\mathrm{K}(\mathrm{x},\mathrm{y},\mathrm{z})\frac{\partial \psi}{\partial \mathrm{y}}\right]+\frac{\partial}{\partial \mathrm{z}}\left[\mathrm{K}(\mathrm{x},\mathrm{y},\mathrm{z})\frac{\partial \psi}{\partial \mathrm{z}}\right]=0 \qquad (2.85)$$

$$\frac{\partial\psi(I-1/2\,,J)}{\partial x}=\frac{[\psi(I,J)-\psi(I-1,J)]}{J} \tag{2.86}$$

$$\frac{\partial\psi(I+1/2\,,J)}{\partial x}=\frac{[\psi(I+1,J)-\psi(I,J)]}{J} \tag{2.87}$$

As a result of intrusion of varying permeability value with respect to x direction, pore pressure put forward for the point of (I, J) in Figure 2.12 (b) can be recasted as;

$$\left\{\frac{K_H(I-1,J)[\psi(I,J)-\psi(I-1,J)]}{h^2}-\frac{K_H(I,J)[\psi(I+1,J)-\psi(I,J)]}{h^2}\right\} \tag{2.88}$$

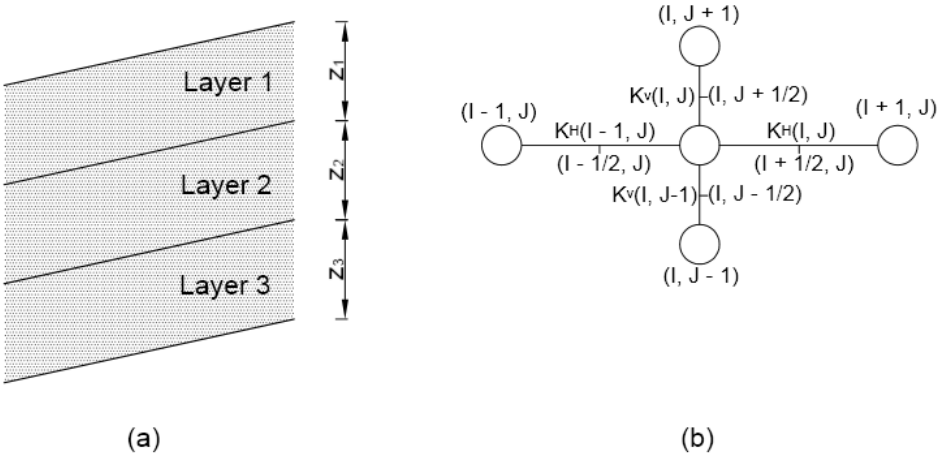

Figure 2.12. (a) Continuum model of analytical method, (b) Stencil for finite – difference scheme.

Also, the identical procedure can be carried out for z direction, which yields;

$$\left\{\frac{K_V(I,J-1)[\psi(I,J)-\psi(I,J-1)]}{l^2}-\frac{K_V(I,J)[\psi(I,J+1)-\psi(I,J)]}{l^2}\right\} \tag{2.89}$$

where K_H is the permability value in x direction, K_V is the permeability value in z direction, h is the point spacing in x direction, l is the point spacing in z direction.

Finally, the pore pressure value at the point of (I, J) can be attained as;

$$\psi(I,J)=\frac{\{K_H(I-1,J)\psi(I-1,J)+K_H(I,J)\psi(I+1,J)\}}{K_H(I-1,J)+K_H(I,J)+\alpha K_V(I,J-1)+\alpha K_V(I,J)}+\frac{\{\alpha K_V(I,J-1)\psi(I,J-1)+\alpha K_V(I,J)\psi(I,J+1)\}}{K_H(I-1,J)+K_H(I,J)+\alpha K_V(I,J-1)+\alpha K_V(I,J)} \quad (2.90)$$

Where,

$$\alpha=\frac{h^2}{l^2} \quad (2.91)$$

What Eq. (2.90) reveals that pore pressure at discrete points can be computed throughout soil mass provided that convergence criterion required for generating stable results should be pursued. Factor of safety calculations also are able to be conducted along with those of pore pressure with the help of appropriate selection of soil and topographical properties.

2.4.2. Method Proposed by Lam, Fredlund and Barbour (1987)

In this method, the complete soil system is envisaged as continuum encompassing flow in both saturated and unsaturated zones. The stress – state variables and the constituve relationships for an unsaturated soil are employed in the process. The finite element solution to the governing differential equation is based on the Galerkin weighted – residual method in that nonlinearity of the equation is solved by iterative procedures. What differs this logic from others is that "saturated only" approach is dispensed with, which states that groundwater table is located at ground surface, so that unsaturated part having negative pressure head can be incorporated into analysis.

In the context of this model, 2 – D Richards' Equation is derived as;

$$\Delta q=\frac{\partial\theta_w}{\partial t}=-\frac{\partial}{\partial x}\left(k_x\frac{\partial\Psi}{\partial x}\right)-\frac{\partial}{\partial z}\left(k_z\frac{\partial\Psi}{\partial z}\right) \quad (2.92)$$

At this point, this routine appeal to a definition of volumetric water content, which is casted as a function of stress (Figure 2.13);

$$d\theta_w = m_1^w d(\sigma - u_a) + m_2^w (u_a - u_w) \tag{2.93}$$

where m_1^w, is the slope of $(\sigma - u_a)$ versus θ_w plot when $d(u_a - u_w)$ is zero, m_2^w is the slope of $(u_a - u_w)$ versus θ_w plot when $d(u_a - u_w)$ is zero, σ is the total stress in x – and (or) y – direction, u_a is the pore – air pressure, u_w is the pore water pressure.

If anisotropic soil conditions where the direction of the major coefficient of permeability is inclined at an arbitrary angle to the x – axis is incorporated into the analysis and is employed to rearrange the Eq. (2.92), it becomes,

$$\frac{\partial}{\partial x}\left(k_{xx}\frac{\partial \Psi}{\partial x} + k_{xz}\frac{\partial \Psi}{\partial z}\right) + \frac{\partial}{\partial z}\left(k_{zx}\frac{\partial \Psi}{\partial x} + k_{zz}\frac{\partial \Psi}{\partial z}\right) = \rho_w g m_2^w \frac{h}{\partial t} \tag{2.94}$$

Where,

$$k_{xx} = k_1 \cos^2\alpha + k_2 \sin^2\alpha \tag{2.95}$$

$$k_{yy} = k_1 \sin^2\alpha + k_2 \cos^2\alpha \tag{2.96}$$

$$k_{xy} = k_{yx} = (k_1 - k_2)\sin\alpha\cos\alpha \tag{2.97}$$

k_1 is the major coefficient of permeability, k_2 is the minot coefficient of permeability, α is inclined angle between k_1 and the x – axis.

As discussed above, Eq. (2.94) is solved by means of Galerkin Solution in that the finite difference method which gives the nodal heads of an element in two successive time steps can be obtained as;

$$\left([D] + \frac{2[E]}{\Delta t}\right)[h^n]_{t+\Delta t} = \left(\frac{2[E]}{\Delta t} - [D]\right)[h^n]_t - 2[F] \tag{2.98}$$

$$\left([D] + \frac{[E]}{\Delta t}\right)[h^n]_t = \frac{2[E]}{\Delta t}[h^n]_t - [F] \tag{2.99}$$

where,

$$[D] = [B]^T[K][B]A \tag{2.100}$$

is the stifffness matrix

$$[E] = \frac{\lambda A}{12}\begin{bmatrix}2 & 1 & 1\\ 1 & 2 & 1\\ 1 & 1 & 2\end{bmatrix} \tag{2.101}$$

is the capacitance matrix

$$[F] = \frac{ql}{2}\begin{bmatrix}1\\ 1\\ 0\end{bmatrix} \text{ or } \frac{ql}{2}\begin{bmatrix}1\\ 0\\ 1\end{bmatrix} \text{ or } \frac{ql}{2}\begin{bmatrix}0\\ 1\\ 1\end{bmatrix} \tag{2.102}$$

is the flux vector reflecting the boundary conditions, $\left[\dot{h}^n\right]$ is the time derivative of nodal total head.

Eq. (2.98) is derived using the central difference approximation, whereas Eq. (2.99) is established on the backward difference theory. The whole procedure is diagrammatized in Figure 2.14.

After convergence criterion is fulfilled, seepage equation is solved for one time in order to pore – water pressure, gradients, velocities, and flux quantities can be attained.

The equation for nodal pore – water pressure can be presented as;

$$[u_w]_t = ([h^n]_t - [z^n])\rho_w g \tag{2.103}$$

where $[z^n]$ is elevation at nodes of the elements.

Then, the equation for element velocity is given as;

$$\begin{bmatrix}i_x\\ i_y\end{bmatrix} = [B][h^n]_t \tag{2.104}$$

The equation for flux,

$$\left[q_{ij}\right]_t = [K]_t[B][h^n]_t \tag{2.105}$$

where $\left[q_{ij}\right]_t$ is flux quantity to node i contributed from node j.

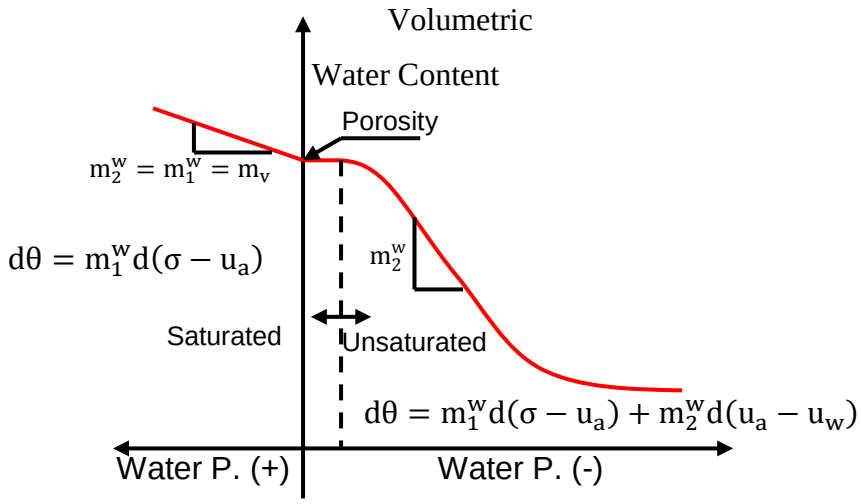

Figure 2.13. Moisture retention curve and m_2^w for saturated – unsaturated soil.

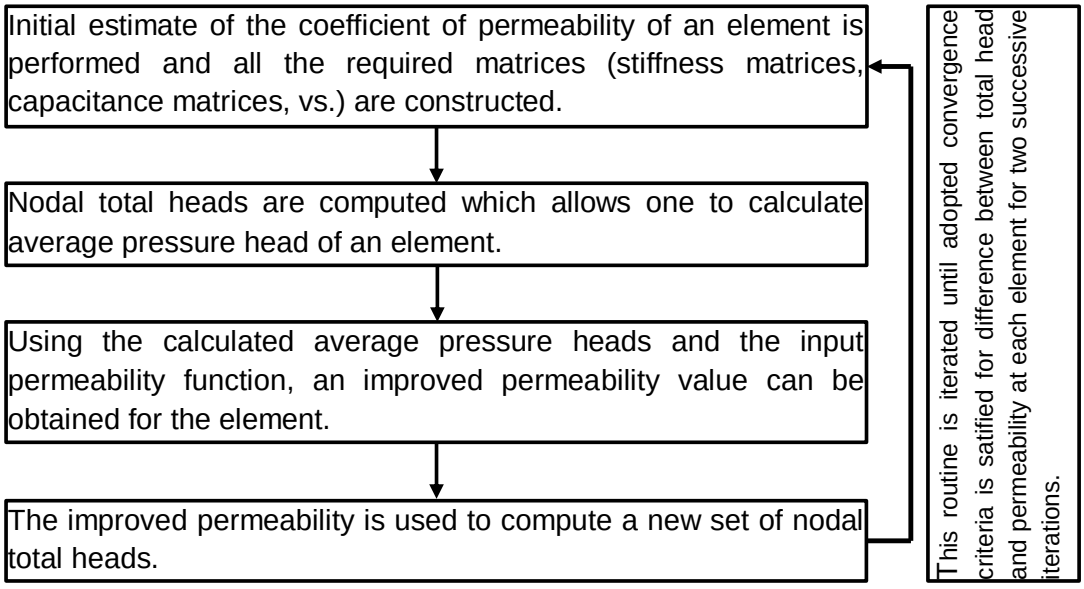

Figure 2.14. Outline of the methodology.

3. THEORETICAL BACKGROUND OF DEVELOPED METHODOLOGY

This algorithm is devised in an intent to quantify the transient rainfall effects on interested site, which previously be in hydrostatic condition in that vertical infiltration of rain water (slope – parallel equipotentials) dominates the hydrological response of soil continuum during and immediate after rainfall. After it ceases, elevated groundwater starts to flow different regions in site, thus resulting in the occurrence of seepage forces. Infinite – slope assumption, which does not require to consider moment equilibrium, is adopted for the sake of simplicity throughout the calculations and both time – dependent pressure heads and following seepage forces are incorporated into force equilibrium equation written for slope – stability.

3.1. Short – Term Response

Short – term response is totally quantified by the approach of Iverson (2000) which is elaborated previously. To illustrate the effectiveness of this methodology, an example is presented in Figure 3.1;

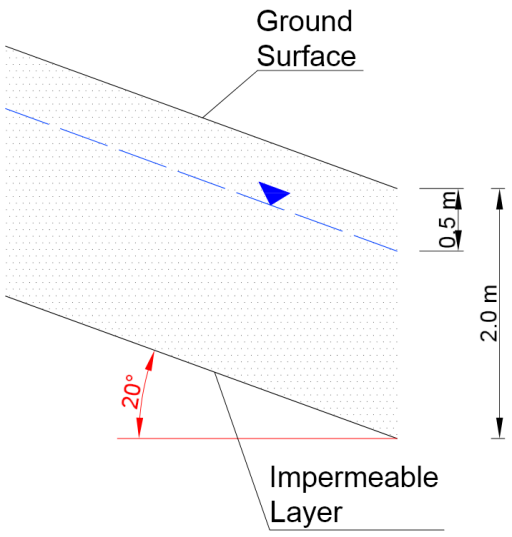

Figure 3.1. Sample slope geometry.

Then, related soil properties and rainfall characteristics are also provided in Table 3.1 below;

Table 3.1. Soil and rainfall characteristics of hillslope.

Friction angle, φ	30^0
Saturated unit weight, γ_{sat} (kN/m^3)	22
Groundwater depth, d_Z (m)	0.5
Slope height, H (m)	2.0
Cohesion, c (kPa)	0.4
Hydraulic conductivity, K_{sat} (m/sec)	10^{-4}
Hydraulic diffusivity, D_0 (m^2/sec)	10^{-3}
Rainfall Intensity, I_z (m/sec)	$5 * 10^{-5}$
Rainfall Duration, T (sec)	600

Compatible results can be attained by following the procedure as given in Figure 3.2.

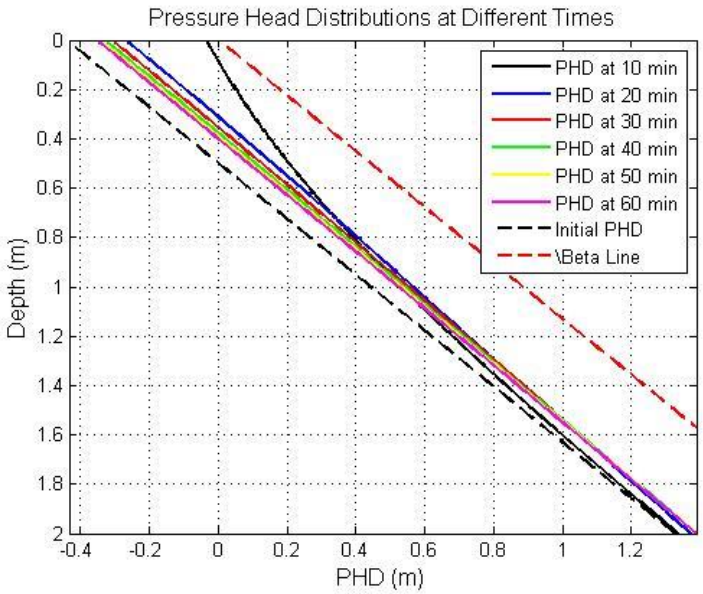

Figure 3.2. Pressure head distributions at different times.

As portrayed in Figure 3.2, pore pressure reaches its maximum at the end of rainfall and the groundwater level (GWL) is accumulated to the level of 0.4 m at the end of short – time response. Pore pressure variations should be bounded by the beta line, which indicates

the maximum capacity of soil continuum to hold water. In other words, beta line cannot be exceeded during the rain water infiltration but Iverson (2000) can predict pressure head values as greater than those corresponding to beta line. This is one of the issues in Iverson (2000) methodology resulting from the neglection of gravity – driven component in Eq. (2.41) and water flux modeled as totally emerging from rainfall percolation. Also, factor of safety values with respect to time are able to be computed as presented in Figure 3.3. Minimum factor of safety (FoS) value throughout the transient response is calculated as 1.0584.

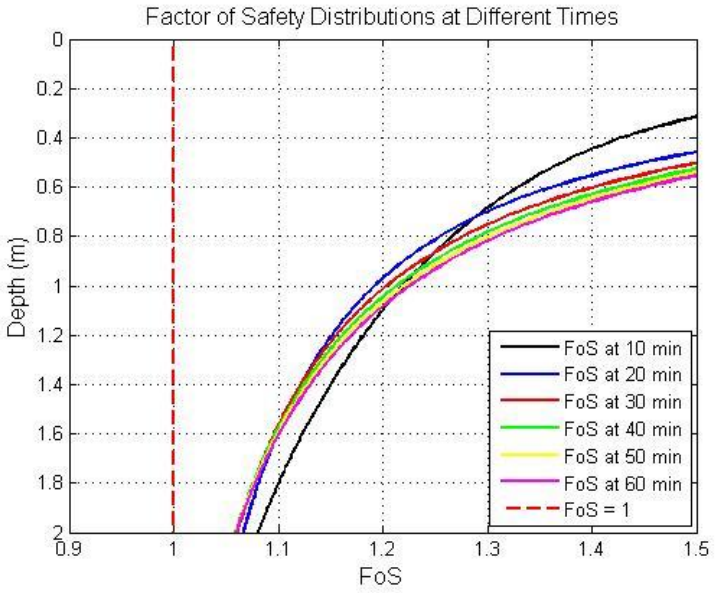

Figure 3.3. Factor of safety distributions at different times.

The fact that there does not exist any failure during transient pore pressure variations would ensue the horizontal groundwater movement, the occurrence of seepage forces in soil continuum, which overlaps at the timescale recommended for long – term response. This effect and how it is quantified in improved algorithm is explained in the following chapter.

3.2. Seepage Condition

After the dynamic effect of rainfall terminates, accrued groundwater commences to flow towards the regions whose total heads are lower than interested one, hence seepage

thrust to soil mass should be taken into consideration. Luckily, Bear (1972) states that seepage force can be thought as proportional to groundwater flow such as;

$$f = (q/K)\rho_w g = -\gamma_w \nabla h \tag{3.1}$$

The relevant seepage force in concordance with infinite – slope stability assumption can be calculated as (Figure 3.4);

$$F_w = ih\gamma_w b\cos\theta \tag{3.2}$$

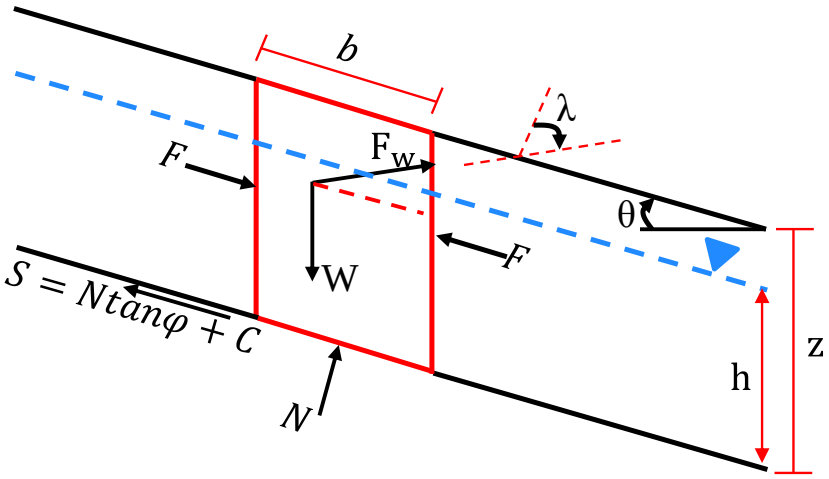

Figure 3.4. Uniform seepage in infinite – slope mass.

If Eq. (3.2) is inserted into the limit equilibrium eq. as identical to done in short – term response, the resultant eq.can be presented as;

$$FoS = \frac{S}{W\sin\theta + F_w\sin\lambda} = \frac{(W\cos\theta - F_w\cos\lambda)\tan\varphi' + c'b}{W\sin\theta + F_w\sin\lambda} \tag{3.3}$$

where h is the grondwater table height, λ is the seepage direction angle between seepage drag and slope – normal in the clockwise direction.

Eq. (3.3) displays how this seepage effect can be appended in force – equilibrium equation but what is of more significance is to verify the uniform seepage condition allowing one to extract hydraulic gradient with regeard to topographical attributes. As stated by Iverson (1990) and Ghiassian and Gareh (2008), the flow lines and corresponding

equipotentials constituting the flow net become straight lines under the presumption of homogeneous soil layer, which is in essence called as *uniform seepage*. Hence, hydraulic gradient value is able to be computed as compatible with topography (Figure 3.5);

$$h_B = h_C = h_{elev.} + h_{press.} \tag{3.4}$$

$$i_{AB} = \frac{h_B - h_A}{\overline{AB}} = \frac{\Delta h}{\overline{AB}} = \frac{\overline{AC}\sin(\theta)}{\overline{AC}\sin(\theta - \Psi)} = \frac{\sin(\theta)}{\sin(\theta - \Psi)} \tag{3.5}$$

$$\Psi = \theta + \lambda - 90 \tag{3.6}$$

$$i_{AB} = \frac{\sin(\theta)}{\sin(\lambda)} \tag{3.7}$$

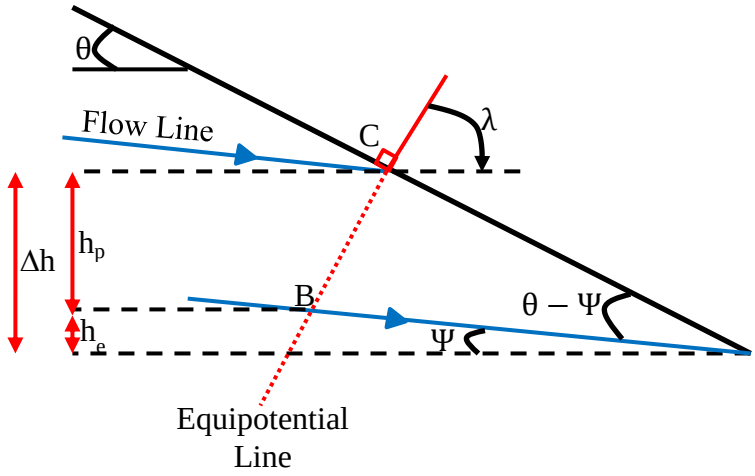

Figure 3.5. Deviation of exit seepage gradient in slopes with locally uniform flow.

To proceed with computations, we should be aware of appropriate seepage directions in hillslope medium since reasonable selections can be made within ascertained values. Iverson (1986) came up with a solution at the end of a parametrich study that seepage direction, $\lambda = 90^0 - \varphi$, eventuates in the most unfavourable condition. Thus, utiliser struggling for evaluating the most damaging conditions is provided with making such an assumption rather than proceeding with his calculation by slope – parallel seepage thrust. However, Ghiassian and Gareh (2008) states that if the hydraulic gradient in hillslope is not controlled by artesian seepage condition, flow direction is likely to be dominated by topographical features, that is, slope – parallel seepage condition.

Should the example given in Figure 3.1 be taken into consideration for seepage effect on hillslope, minimum FoS is obtained as 1.0487 by assuming that $\lambda = 90^0$. Table 3.2 can be constructed to summarize how FoS alter from hydrostatic condition to that of seepage drag;

Table 3.2. FoS variation with respect to different hydrological condition in site.

Hydrological Condition in Site	**FoS**
Hydrostatic Condition	1.0840
Short – Term Response	1.0584
Seepage Condition	1.0487

However, the most unfavourable seepage direction declared by Iverson (1986) results in the FoS value of 0.9298, which indicates the instability in hillslope medium. Thus, this sharp discrepancy ensuing from different seepage directions must be watched out for procuding reasonable results.

4. APPLICATION OF DEVELOPED METHODOLOGY ON HYPOTHETICAL TOPOGRAPHY

The purpose of begining with the analysis on hypothetical topography is to draw attention on the effectiveness and inaccuracy of the proposed methodology since selected parameters reveals the conditions where it fails or represents properly. Should this routine be capable of undertaking the effect of transient rainfall patterns on different soil and topographical features, one is ensured to consult on this algorithm in the case of dealing with true conditions.

On the other hand, the determination of topographical properties might not be effortless as anticipated and/or soil conditions prevent user from implementing this methodology. The fact that hypothetical topography removes such issues and grants time to be spent for specifying the required parameters to one enables researchers to capture the essence of the theory behind this routine.

4.1. The Generation of Hypothetical Topography

The first thing to do is to demarcate the boundary of hypothetical topography and to divide it by certain number of cells possessing prescribed dimensions. In this context, such a border encompassing the area of 361.5 km^2 and having the total perimeter of 82.71 km is partitioned into 1552 number of cells, whose dimensions are 500 X 500 m (Figure 4.1).

Table 4.1. Soil types in hypothetical site.

Soil Type	ϕ	γ_{sat} (kN/m^3)	K_{sat} (m/sec)	D_0 (m^2/sec)	Z (m)	d_z (m)
1	30	22	1.0E-06	2.0E-04	1	0.6
2	35	19	1.0E-05	2.0E-03	0.5	0.3
3	25	20	5.0E-06	1.0E-03	1.5	0.7
4	28	20	5.0E-06	1.0E-03	1.5	0.7
5	28	18	3.0E-05	6.0E-03	2	1

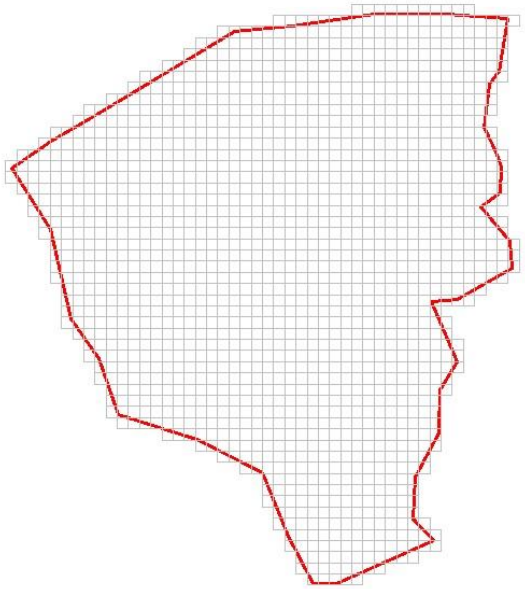

Figure 4.1. Hypothetical topography and representation by cells.

Then, the varying soil conditions in Table 4.1 are projected onto hypothetical map as illustrated in Figure 4.2.

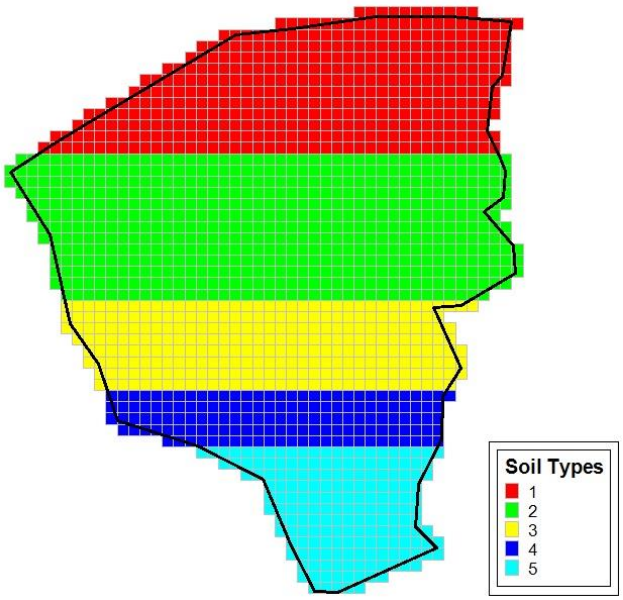

Figure 4.2. Soil types in hypothetical site.

The remaining part to be followed in improved methodology is to generate slope angle value in each cell to conduct transient and seepage analysis presented in from Eq. (2.48) to Eq. (2.55) and from Eq. (3.1) to Eq. (3.3), respectively. What is attained after the generation of random slope value is delineated in Figure 4.3.

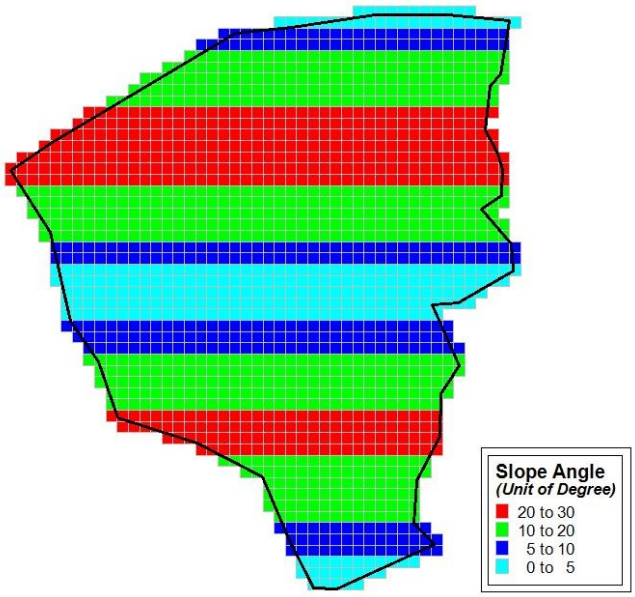

Figure 4.3. Slope angles in hypothetical site.

Also, rainfall patterns should be produced to model the rainfall – instigated landslide process and Iverson (2000) luckily supplies resarchers to employ the varying rainfall intensity values for factor of safety calculations. The adopted rainfall sequence is able to be plotted in Figure 4.4 in an attempt to display that the hypothetical site is firstly exposed to increasing amount of rainfall (from 3 mm to 5 mm) but its effect is slowly ceased at the end of 4.5 hours (2 mm).

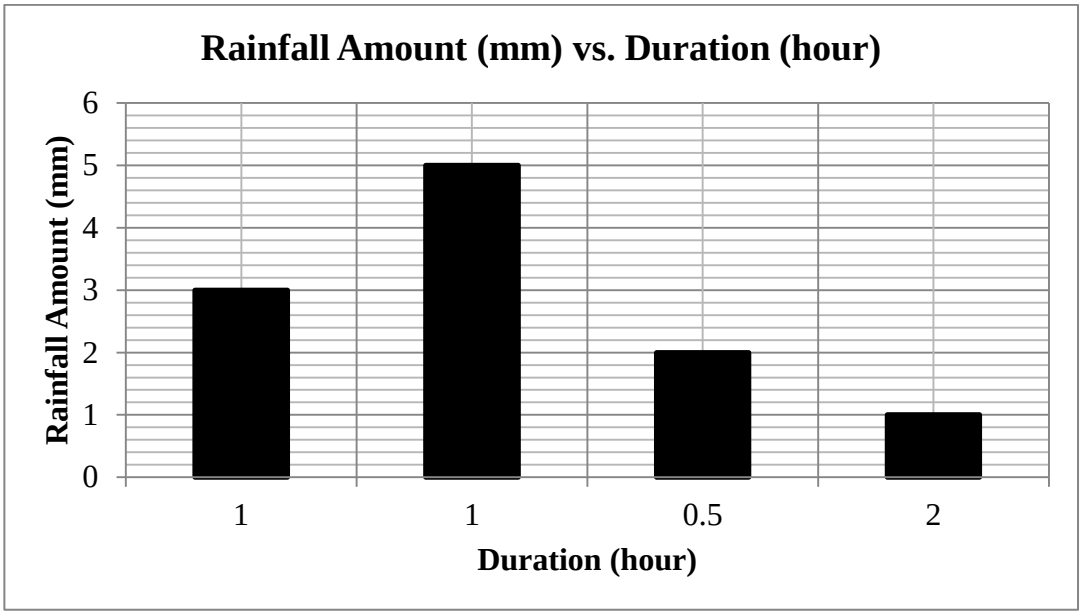

Figure 4.4. Rainfall amount (mm) vs. duration (hour).

4.2. Results

The transient rainfall analysis are carried out as compatible with Method Proposed by Iverson (2000) in that the rainfall amounts given in Figure 4.4 are applied to each cell, whose hydrological response is determined by Eq. (2.53), to monitor the change in pressure head values and to calculate the accrued level of groundwater table. The latter one is required for the calculation of seepage forces to go ahead with the second step in developed methodology. What is foreseen from the suggested methodology is to calculate reasonable factor of safety values throughout the transient rainfall effect, which is concluded by the seepage condition.

As can be deduced from the factor of safety (FoS) map plotted for hydrostatic condition (Figure 4.5), there does not occur any failure (0 to 1) in any cell but the cells quantified as "on the verge of failure" (1 to 1.5) at this stage are subjected to sliding at the end of 1_{st} hour (Figure 4.6) and these are the ones standing on greater slope values. The following step reveals the fact that the increase in rainfall amount is greeted with the expansion of failure zones and this trend proceeds with until the end of rainfall (From Figure 4.7 to Figure 4.9).

After Figure 4.9, as mentioned previously, seepage drag governs the driving forces in hillslope continuum after this stage in that seepage direction is assumed as $\lambda = 90^0 - \varphi$ to stay within the safe side. This effect also results in the enlargement of failure regions in hypothetical site (Figure 4.10).

Secondly, the groundwater table (GWT) level is elevated at ground surface in large portion of hypothetical topography but the cells lying within soil type 5 are not exposed to such a condition since the permeability, or hydraulic diffusivity, given for this type disallows vertical subsurface flux to become perched above static level of GWT (pore water pressure dissipation) and the accumulated level of incoming rain water is not sufficient for filling the portion presumed as initially wet at the hydrostatic condition (Figure 4.11).

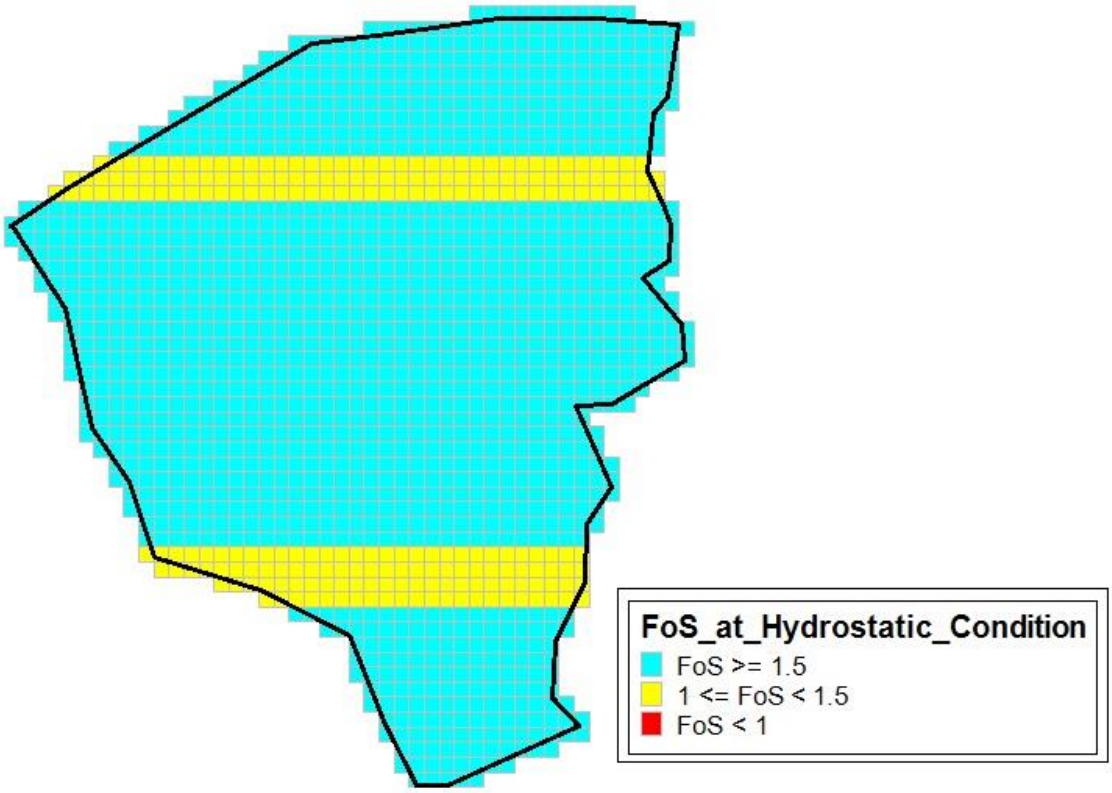

Figure 4.5. FoS at hydrostatic conditions.

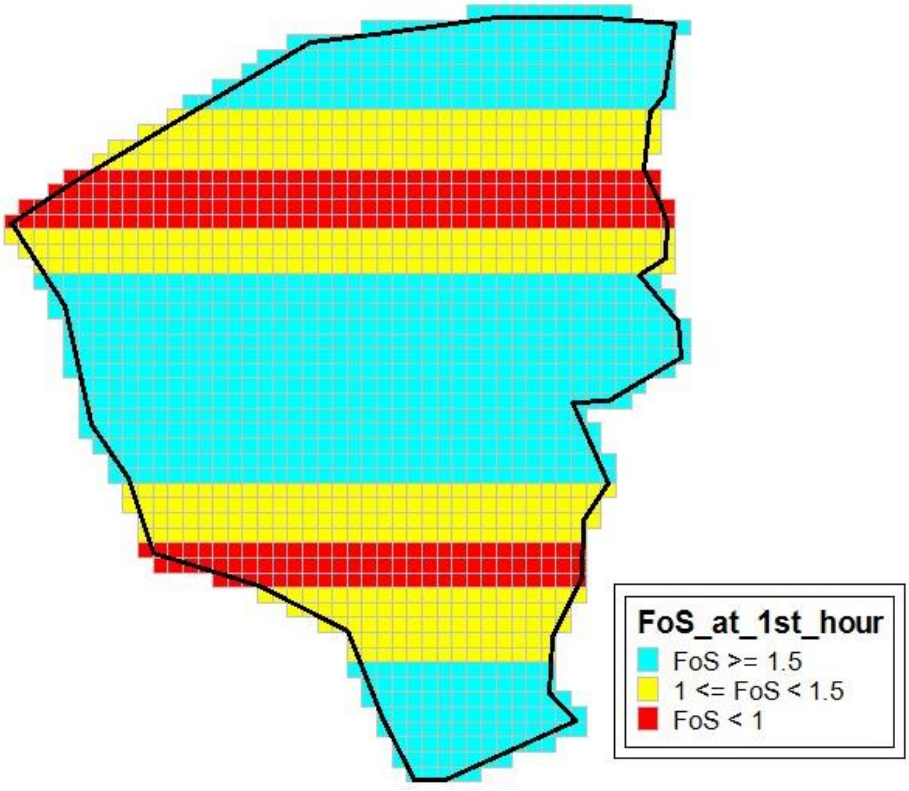

Figure 4.6. FoS at the end of 1_{st} hour.

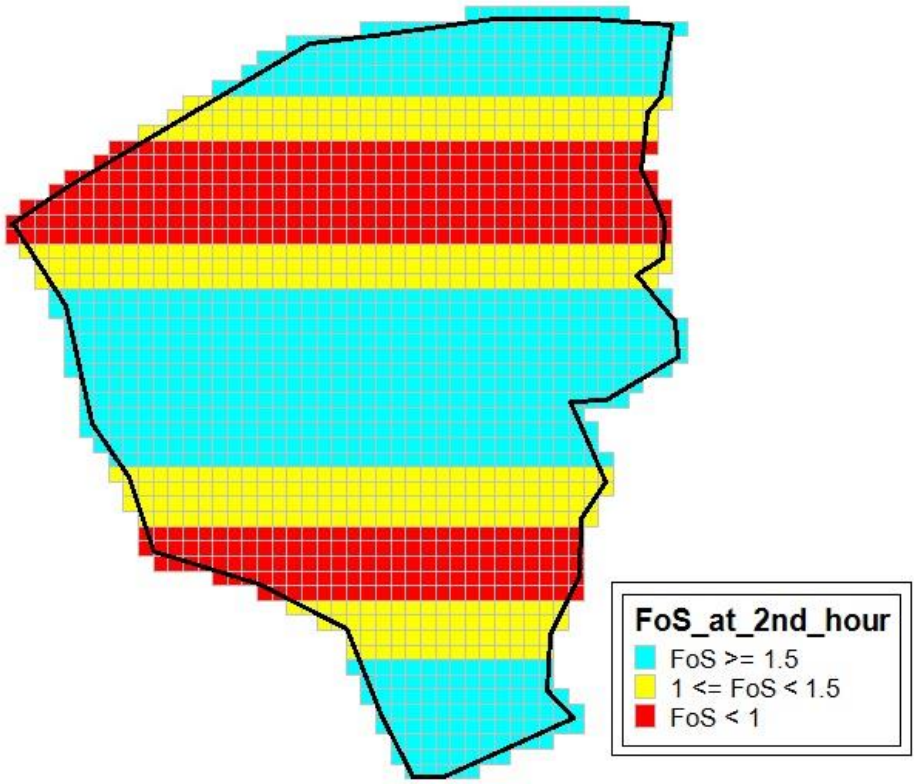

Figure 4.7. FoS at the end of 2_{nd} hour.

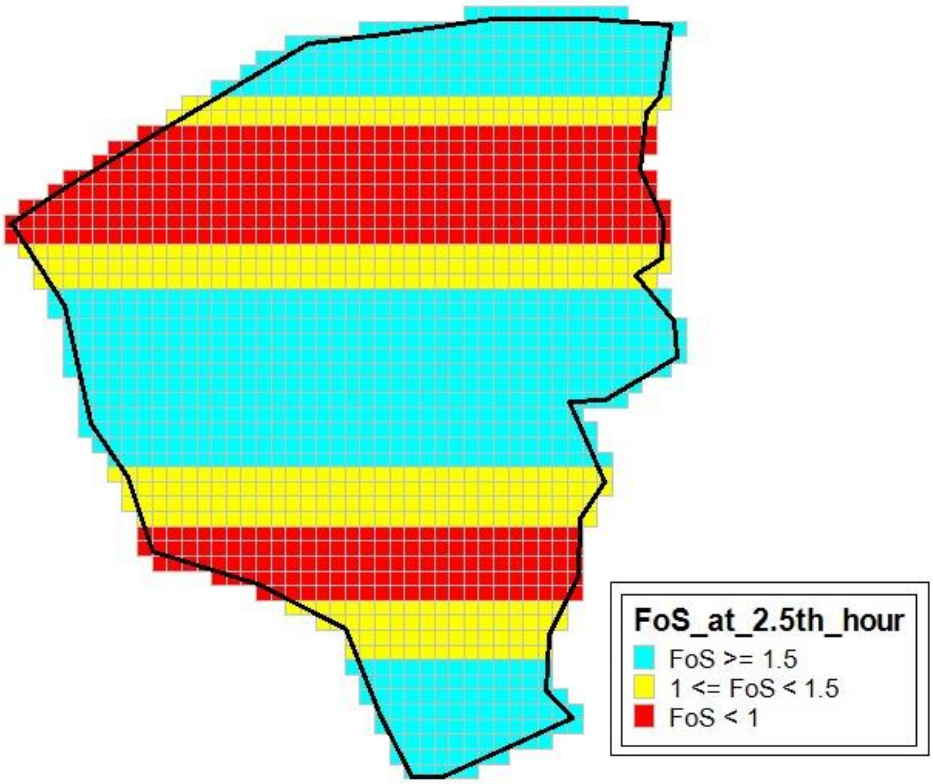

Figure 4.8. FoS at the end of 2.5_{th} hour.

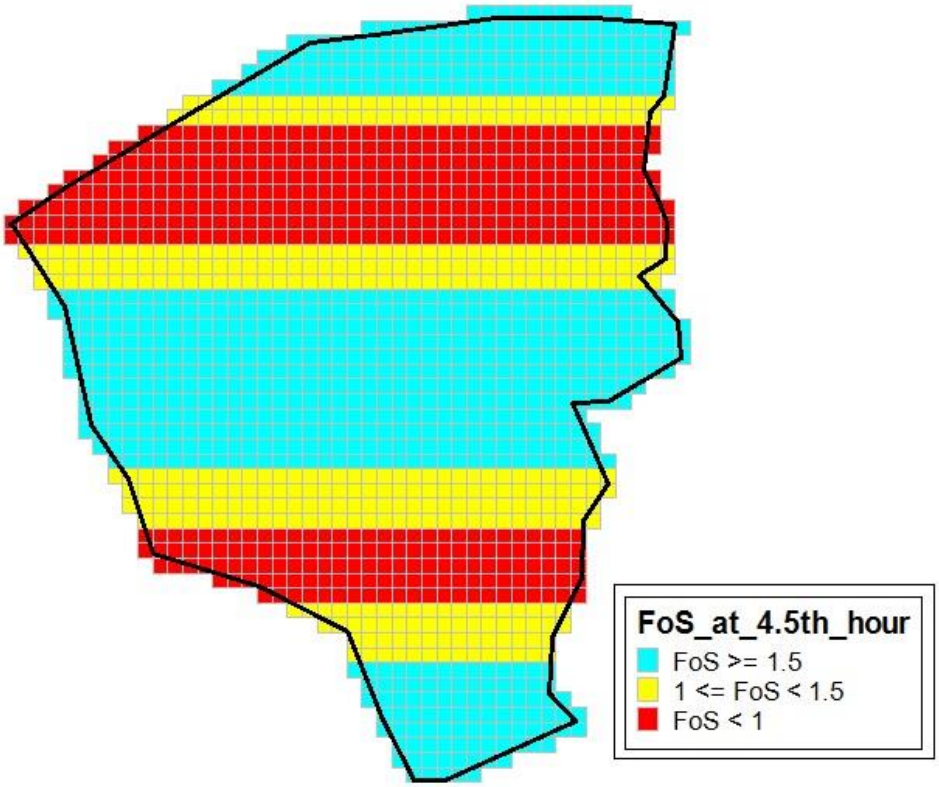

Figure 4.9. FoS at the end of 4.5_{th} hour.

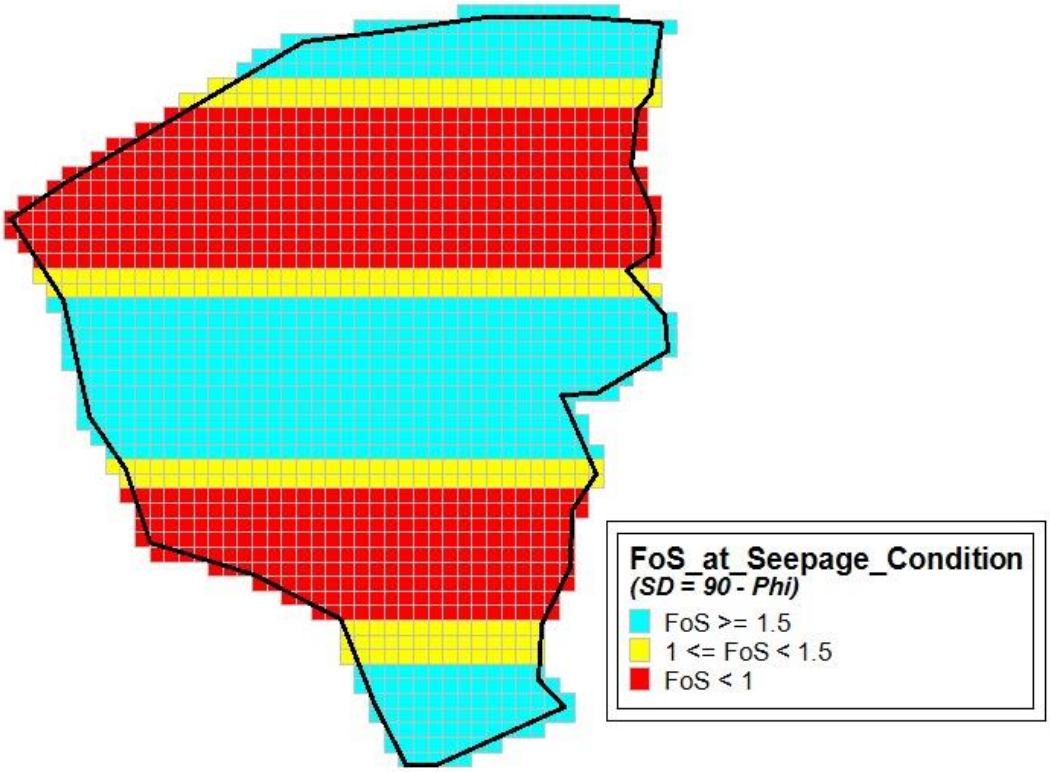

Figure 4.10. FoS at seepage condition.

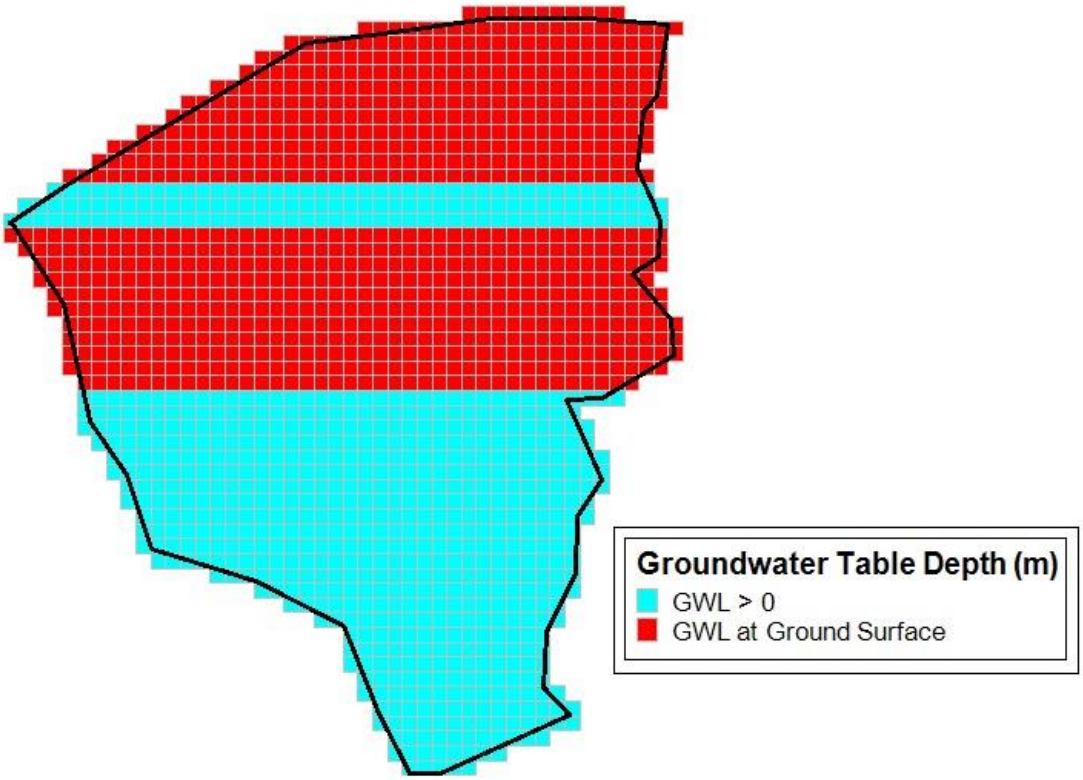

Figure 4.11. GWL at the end of short – term response.

All in all, what is able to be inferred from the application of proposed methodology to hypothetical topography can be declared that (1) the degree of rainfall intensity causes dramatic decrease in FoS and dominates the behaviour of hillslopes under transient rainfall effect (2) seepage condition may lead to undesirabele conditions if the seepage gradient in soil is controlled by any other sources instead of topographical features.

5. TEKİRDAĞ CASE STUDY

Case studies are perceived as such an examination of derived methodologies that their acceptence over researchers and/or validity is totally bound up with how hazard in relevant site is accurately modelled. To that end, Tekirdağ City Center is selected to evaluate the aforementioned methodology, which is also tested within the context of hypothetical topography, and also is exposed to Montgomery and Dietrich (1994) and Mora and Vahrson (1994) Methods to pick out whether each of then yields identical results or not.

5.1. Definition of Study Area

Tekirdağ City Center is situated onto 23.64 km^2 area with total perimeter of 64.15 km in that its map is divided into 173 number of cells, whose dimensions are 500 X 500 m (Figure 5.1). Each cell is also equipped with a boring log presenting the SPT test results conducted on site, groundwater level and also sieve analysis, moist density and water content tests are conducted on UD samples. All these data are exploited in order to quantify the parameters required for carrying out these methods by means of empirical correlations provided that if absurd values are calculated for any soil property, it is excluded from the analysis and reasonable selection is performed through the specification given in the literature (Table 5.1).

5.2. The Calculation of Soil and Topographical Properties for Tekirdağ Region

One who intents to adopt this method for rainfall – induced slope – stability analysis has to compute A, b, z, K_h, γ_{sat}, θ, φ, D_0, I_z. The last parameter, I_z, can be extracted from the meteorological measurements but the others depending on topographical characteristics and governing soil properties of site should be determined from GIS programs and emprical correlations, respectively. The quantification of soil properties is firstly initiated.

.

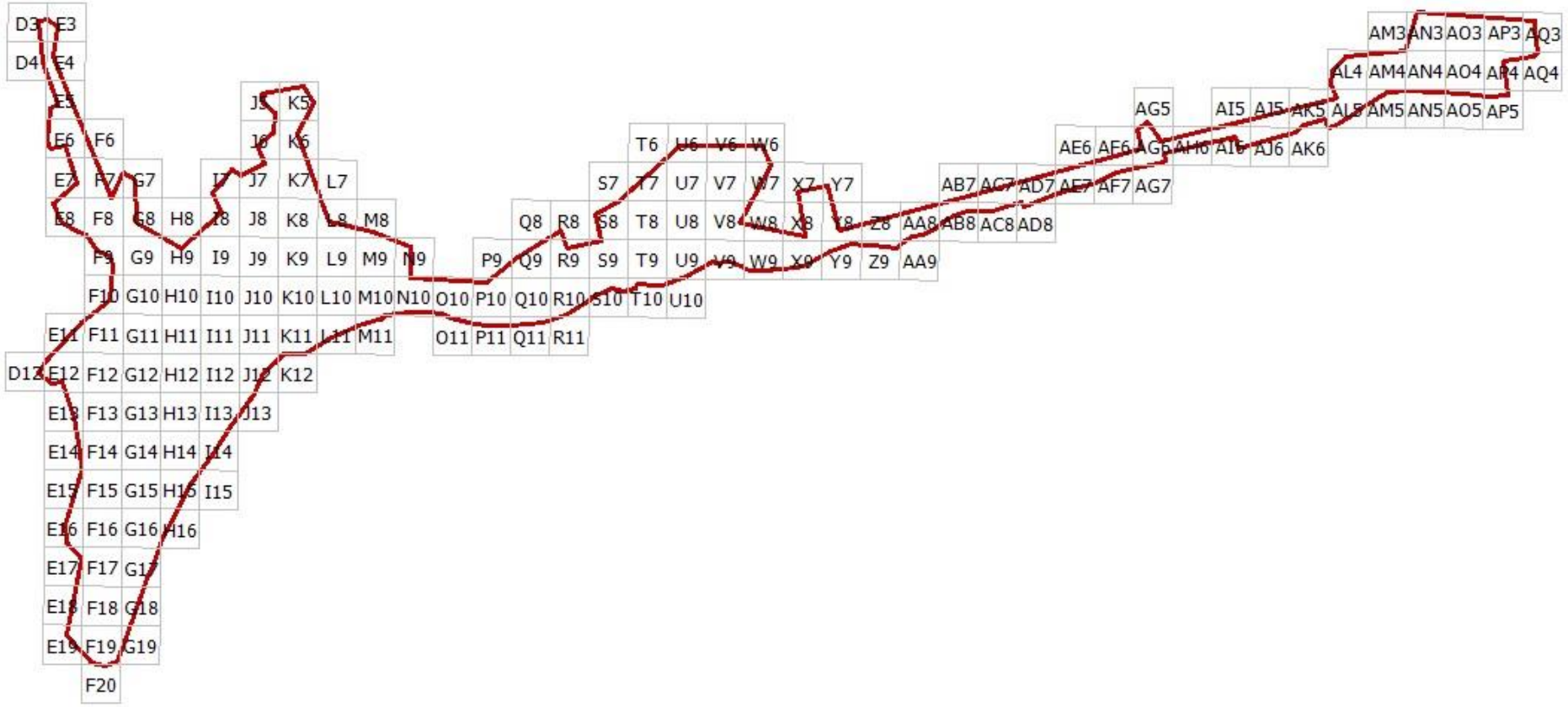

Figure 5.1. Tekirdağ City Center.

5.2.1. The Determination of Hydraulic Conductivity

Hydraulic conductivity is in essence able to be measured both in lab (falling – head or constant – head methods) or in site (Augerhole method) but if researchers are not provided with such data, there exists empirical correlations based on gradation of soil for granular soils and Atterberg Limits of cohesive soils.

- **Hazen's Formula**

Hazen (1892, 1911) improved a formula to compute the hydraulic conductivity, which is usually applicable for loose, clean sands with a coefficient of uniformity, D_{60}/D_{10} , less than about 2;

$$K = C_H D_{10}^2 \tag{5.1}$$

where K is the hydraulic conductivity (cm/sec), C_H is the Hazen emprical coefficient, D_{10} is the particle size for which 10% of the soil is finer (cm).

Although Eq. (5.1) has been widely used in engineering applications, it may lead to errenous results since it is limited to quite narrow particle diameters such as 0.01 cm < D_{10} < 0.03 cm. Also, that Eq. (5.1) is only constructed on D_{10} in terms of gradation parameter restricts the practicability of this relationship, thus resulting in seeking of another equation. However, if one be in the condition of employing Eq. (5.1), there is no harm in applying it to interested soil masses.

- **Kozeny – Carman Formula**

Kozeny (1927) and Carman (1938) and (1956) derived the following relationship that predicts the hydraulic conductivity of porous media more accurately than Hazen's;

$$K(cm/sec) = \left(\frac{\gamma}{\mu}\right)\left(\frac{1}{C_{K-C}}\right)\left(\frac{1}{S_0^2}\right)\left(\frac{e^3}{1+e}\right) \tag{5.2}$$

where γ unit weight of permenant, μ viscosity of permenant, $C_{K\text{-}C}$ Kozeny – Carman empirical coefficient, S_0 specific surface area per unit volume of particles (1/cm), e void ratio.

Eq. (5.2) is rewritten as encompassing the related properties of water, thus yielding;

$$K = 1.99 * 10^4 \left(\frac{1}{S_0^2}\right)\left(\frac{e^3}{1+e}\right) \tag{5.3}$$

Measuring S_0 is rather troublesome process in that it is able to be simply estimated from particle size distribution and particle shape, leading to the equation;

$$K = 1.99 * 10^4 \left(\frac{100(\%)}{\left[\sum \frac{f_i}{D_{li}^{0.404} * D_{si}^{0.595}}\right]}\right)^2 \left(\frac{1}{SF^2}\right)\left(\frac{e^3}{1+e}\right) \tag{5.4}$$

where f_i fraction of particles between two sieve sizes, D_{li} larger sieve size, D_{si} smaller sieve size, SF shape factor, which is determined as 6.0 for spherical, 6.1 for rounded, 6.4 for worn, 7.4 for sharp and 7.7 for angular.

Also, two important points for Kozeny – Carman Equation should be declared; (1) This expression is reproduced for granular soils, thus it might not be appropriate for fine – grained soils. (2) The fact that this formula is not devised as taking anisotropy into consideration causes Kozeny – Carman Formula to compute only vertical permeability. However, horizontal hydraulic conductivity (K_h) is usually greater than vertical one (K_v) such an extent that ratio of K_h/K_v ranges from 1 to 10.

Also, Steiakakis, Gamvroudis and Alevizos (2012) demonstrate that Kozeny – Carman Relationship is also applicable for cohesive soils with a difference that specific surface (S_0) in Eq. (5.3) can be computed by means of a selected Atterberg limit. Chapuis and Aubertin indicates that specific surface is able to be associated with liquid limit (LL) such as;

$$\frac{1}{S_0} = 1.3513\left(\frac{1}{LL}\right) - 0.00089 \tag{5.5}$$

where S_0 is in m^2/g, LL is the liquid limit in percent (limited to LL < 60 %).

The 2_{nd} expression is proposed by Steiakakis, Gamvroudis and Alevizos (2012);

$$\frac{1}{S_0} = 6.152\left(\frac{1}{LL}\right) - 0.052 \tag{5.6}$$

Eq. (5.5) and Eq. (5.6) are substituted into Eq. (5.3) to calculate the vertical hydraulic conductivity for cohesive soils.

In addition to Steiakakis , Gamvroudis and Alevizos (2012), Carrier and Beckman (1984) enhanced an eq., said to encompass a wide variety of clay types;

$$K\,(m/sec) = \frac{\left\{\frac{e - 0.027[(PL) - 0.242(PI)]}{(PI)}\right\}^{4.29}}{1 + e} \tag{5.7}$$

where e is void ratio, PL is plastic limit and PI is plasticity index.

Also, calculated values of hydraulic conductivity for both granular and cohesive soils can be evaluated as whether it stays within the possible range presented in Table 5.1. As is known, clays or clayey soils generally possess such degree of imperviousness that there is no need for conducting any rainfall infiltration analysis for them. Each soil layer is thought to be as uniform in site but it is widely accepted that soils may be exposed to disintegration and may have lower hydraulic conductivity at shallow depths. Montgomery and Dietrich (1994) correspondingly states "*The saturated conductivity of the soil in Marin Country, California, varies from 10^{-3} m/sec at soil depths less than 1m to 10^{-10} m/sec for soil depths between 3 and 4 m*". This logic gives birth to the presumption of any reasonable value of hydraulic conductivity at shallow layers.

Table 5.1. Permeability ranges for soils classified with respect to USCS.

Major Divisions		Symbol	Name	K (cm/sec)
Coarse – Grained Soils	Gravel and Gravelly Soils	GW	Well-graded gravels or gravel sand mixtures, little or no fines	$K > 10^{-2}$
		GP	Poorly graded gravels or gravel sand mixtures, little or no fines	$K > 10^{-2}$
		GM	Silty gravels, gravel-sand-silt mixtures	$K = 10^{-3}$ to 10^{-6}
		GC	Clayey gravels, gravel-sand clay mixtures	$K = 10^{-6}$ to 10^{-8}
	Sand and Sandy Soils	SW	Well-graded sands or gravelly sands, little or no fines	$K > 10^{-3}$
		SP	Poorly graded sands or gravelly sands, little or no fines	$K > 10^{-3}$
		SM	Silty sands, sand-silt mixtures	$K = 10^{-3}$ to 10^{-6}
		SC	Clayey sands, sand-silt mixtures	$K = 10^{-6}$ to 10^{-8}
Fine – Grained Soils	Silts and Clays LL < 50	ML	Inorganic silts and very fine sands, rock flour, silty or clayey fine sands or clayey silts with slight plasticity	$K = 10^{-3}$ to 10^{-6}
		CL	Inorganic clays of low to medium plasticity, gravelly clays, sandy clays, silty clays, lean clays	$K = 10^{-6}$ to 10^{-8}
		OL	Organic silts and organic silt clays of low plasticity	$K = 10^{-4}$ to 10^{-6}
	Silts and Clays LL ≥ 50	MH	Inorganic silts, micaceous ordiatomaceous fine sandy or silty soils, elastic silts	$K = 10^{-4}$ to 10^{-6}
		CH	Inorganic clays of high plasticity, fat clays	$K = 10^{-6}$ to 10^{-8}
		OH	Organic clays of medium to high plasticity, organic silts	$K = 10^{-6}$ to 10^{-8}

The article published by Meiers, Barbour, Qualizza and Dobchouk (2011) gives place to this phenomenon and declares "*For fine-textured cover soils such as clays, physical processes, such as wet/dry and freeze/thaw cycles, can have a significant effect on hydraulic characteristics. These cycles cause volume changes (i.e., shrinkage and swelling) resulting in the creation of a secondary structure of macropores or fractures (Konrad and Morgenstern 1980) that cause an increase in the hydraulic conductivity of some soils. Watson and Luxmoore (1986), Wilson and Luxmoore (1988), and Dunn and Phillips (1991) reported that a high percentage of water is transported through the extremely small portion of the soil with macropores and fractures or preferred flow paths in structured, fine-textured materials. These findings suggest that the development of a secondary soil structure will strongly influence the hydraulic properties of fine-textured cover materials.*" and proceeds with the statement; "*A number of studies into the effects of wet/dry and freeze/thaw cycles for compacted clays have been published. Albrecht and Benson (2001) demonstrated that the hydraulic conductivity of compacted clay samples exposed to wet/dry cycles increased up to three orders of magnitude.*"

5.2.2. Calculation of Unit Weight and Friction Angle

As stated from Eq. (2.15) to Eq. (2.17) and also from Eq. (2.54) to Eq. (2.55), the quantification of γ_{sat} and φ is anticipated to proceed with the calculations of thresholds set forth for selected parameters such as A/b [contributing area per unit contour length (m)] and/or W (wetness parameter). In this document, all the decisions that should be made for determining the relevant shear strength parameters are left to the ones intending to exploit this methodology. However, available relationships for this process are presented in an attempt to display the logic that may be followed throughout the analysis.

Since Montgomery and Dietrich (1994) is constructed on the condition of local flux at a given steady – state rainfall, it is of importance to quote the passage given in Holtz and Kovacs (1981) in order that the role of shear strangth parameters in Montgomery and Dietrich (1994) Methodology can be grasped more properly; "*CD Conditions (Consolidated – Drained) are the most critical for the long – term steady – seepage case for embankment dams and the long – term stability of excavations or slopes in both soft*

and stiff clays." Thus, we are provided with a chance to define shear strength of interested soil as a function of φ (internal friction angle) within the context of this methodology;

$$\tau = \sigma \tan\varphi \tag{5.8}$$

The expected and most reliable process for attaining friction angle is to perform lab tests on soil samples but this might not be applicable for our situation. Thus, we appeal to either possible ranges of friction angles or some empirical relationships developed for related shear strength angle as a function of any given parameter for interested soil layer. Bowles (1996) proposes such ranges for relevant parameters in Table 5.2 and also, there exists quite amount of expressions for calculating friction angle of granular soils.

In the first place, relative density (D_r) is calculated for different depths by employing N'_{70} and/or N'_{60} values such as (Skempton, 1986);

$$\frac{N'_{70}}{D_r^2} = 32 + 0.288 P'_0 \tag{5.9}$$

Or, Yoshida *et al.* (1988)

$$D_r = 25 (P'_0)^{-0.12} * (N_{60})^{0.46} \tag{5.10}$$

where P'_0 is the overburden pressure, D_r is the relative density.

After that, internal friction angle can be attained through the formulation below; Mayerhoff (1959)

$$\varphi = 28 + 0.15\, D_r(\%) \tag{5.11}$$

Also, Shioi and Fukui (1982) proposes the following equations, each of which is recommended for different conditions such as;

$$\varphi = \sqrt{18N'_{70}} + 15 \text{ (for roads and bridges)} \quad (5.12)$$

$$\varphi = 0.36\, N_{70} + 27 \text{ (for buildings)} \quad (5.13)$$

$$\varphi = 0.36\, N_{70} + 20 \text{ (for general uses)} \quad (5.14)$$

In cohesive soils, as identical to Holtz and Kovacs (1981) and Skempton (1964) points out the pore pressure condition in clays slopes in that residual shear strength, φ_r, (or residual friction angle) (Figure 5.2) is suggested in order that compatibility is provided between back – calculation results of occurred landslide and that obtained from site observations for given event. For both NC and OC clays, the residual strength is thought to be in the same form of Eq. (5.8), thus resulting in the computation of φ_r by using Eq. (5.8). There are quite a few relationships proposed for finding residual friction angle with respect to any selected parameter, generally one of the Atterberg Limits for cohesive soils. Santamarina and Shin (2013) offers Table 5.3 for different Atterberg Limits and confining stress values, and Kanji (1974)' s Correlation was constructed on Plasticity Index (Ip), which is applicable for normal stresses ranging from 10 to 350 kPa (Figure 5.3);

$$\varphi_r = \frac{46.6}{I_p^{0.446}} \quad (5.15)$$

Table 5.2. Empirical values for φ, D_r and unit weight of granular soils based on the SPT at about 6 m depth and normally consolidated.

Description	**Very loose**	**Loose**	**Medium**	**Dense**	**Very Dense**
Relative Density, D_r	0	0.15	0.35	0.65	0.85
SPT – N'_{70}: Fine	1 – 2	3 – 6	7 – 15	16 – 30	?
SPT – N'_{70}: Medium	2 – 3	4 – 7	8 – 20	21 – 40	>40
SPT – N'_{70}: Coarse	3 – 6	5 – 9	10 – 25	26 – 45	>45
φ: Fine	26 – 28	28 – 30	30 – 34	33 – 38	
φ: Medium	27 – 28	30 – 32	32 – 36	36 – 42	
φ: Coarse	28 – 30	30 – 34	33 – 40	40 – 50	
γ_{wet} (kN/m^3)	11 – 16	14 – 18	17 – 20	17 – 22	20 - 23

In addition to this, Cancelli (1977) provided the following relationship, where LL (Liquid Limit) is in percent (Figure 5.4);

$$\varphi_r = \frac{453.1}{LL^{0.85}} \tag{5.16}$$

As can be considered, the fact that Eq. (5.15) and Eq. (5.16) are solely dependent on Atterberg Limits be undesirable situation due to the fact that shear strength parameters are mainly dominated by confining stress the soil has experienced. Luckily, Wright (2005) plugs this effect into his correlation to release an admissible relationship and also, granular soils is able to be quantified with the help of Table 5.4.

$$\varphi_r = 52.5 - 21.3\log_{10}(\omega_{LL}) - 3\log_{10}\left(\frac{\sigma'_{vo}}{P'_a}\right) \tag{5.17}$$

where ω_{LL} is the liquid limit, σ'_{vo} is the overburden stress, P'_a is the atmospheric pressure.

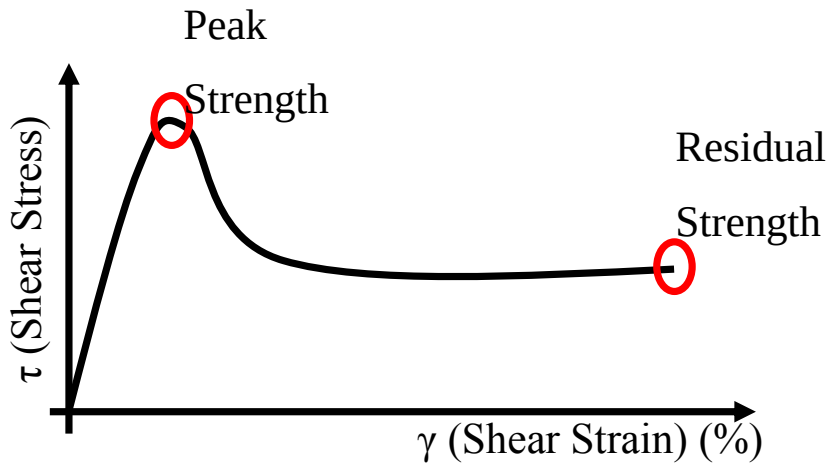

Figure 5.2. Variation of shear strength for different strain levels.

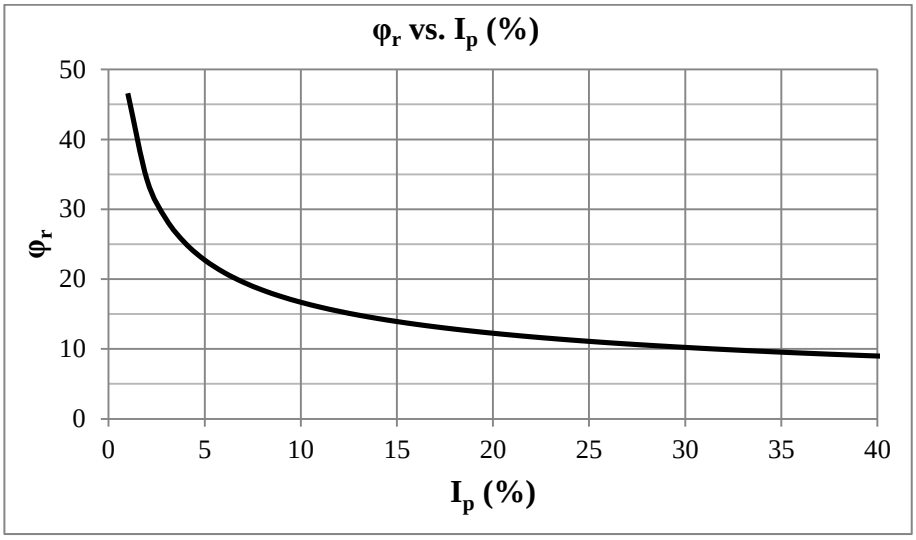

Figure 5.3. Φ_r with respect to I_p (Kanji, 1974).

In addition to this, utilizer of routines above is anticipated to use unit weight determined by lab tests but reasonable selections are also able to be performed by means of Table 5.2.

Table 5.3. Field residual strength of some english clays Santamarina and Shin (2013).

Site	**Stratum**	**w (%)**	**Index Properties (Average Values)**				**φ^{-1}_{rf}**		
			LL	**PL**	**CF**	**PI/CF**	**50 kPa**	**100 kPa**	**150 kPa**
Walton's Wood	Upper Carboniferous	29	57	27	70	0.43	13.8	13.2	12.8
Jackfield		21	44	22	36	0.61	16.8		
Bury Hill	Etnria Marl	30	60	27	52	0.63	13.4	12.5	12.1
Various	Upper Lias	29	64	28	52	0.69	12.7	11	9.9
M4, near Swindon	Gault	36	64	29	47	0.74	14	14	-
Sevenoaks bypass	Athetfield	35	75	29	58	0.79	13.4	12	11.1
Various	London Clay	34	80	29	55	0.93	13.3	12.3	11.8

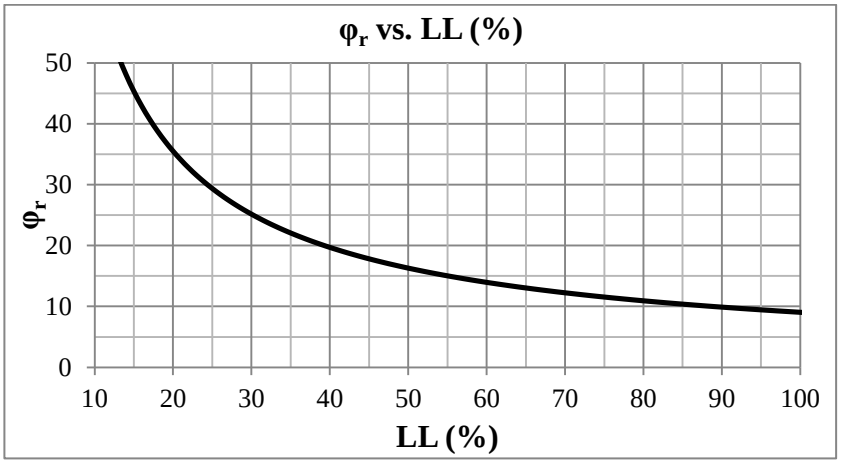

Figure 5.4. Φ_r with respect to LL (Cancelli, 1977).

Table 5.4. Friction angles of granular soils (After Lambe and Whitman, 1979).

Soil Type	Friction Angle, ϕ (Degrees)	
	Residual	Peak
Medium – dense silt	26 - 30	28 – 32
Dense silt	26 - 30	30 – 34
Medium – dense, uniform fine – to – medium Sand	26 - 30	30 – 34
Dense, uniform fine – to – medium Sand	26 - 30	32 – 36
Medium – dense, well – graded sand	30 - 34	30 – 34
Dense, well – graded sand	30 - 34	38 - 46
Medium – dense sand and gravel	32 – 36	36 – 42
Dense sand and gravel	32 - 36	40 – 48

5.2.3. Determination of Hydraulic Diffusivity

As stated, parameters expected to apply this routine be K_z, H, A, θ, d_Z, φ, D_0, I_z, and T such that almost each of them is assessed in Montgomery and Dietrich (1994) in terms of how it can be obtained except D_0 and H. H is able to be defined as the depth to the impermeable layer and totally dependent on the available geology. However, D_0 should be designated properly in order to go ahead with transient groundwater response calculations, which is computed in Iverson (2000) as;

$$D_0 = \frac{K_{sat}}{C_0} \tag{5.18}$$

Where C_0 is the minimum value of $C(\psi)$, typically observed when the soil becomes saturated, $C(\psi) = d\omega/d\psi$ is the change in volumetric water content per unit change in pressure head.

There are a great number of SWCC (Soil Water Characteristic Curve), which is expressed as the variation of volumetric water content with respect to matric suction, and is generally designed as a function of certain parameters extracted from fitting process of test results. Fredlund, Rahardjo and Fredlund (2012) presents that one of the most prominent equation is Gardner (1958b) such as;

$$\Theta_d = \frac{1}{1 + \mu_g \psi^{n_g}} \tag{5.19}$$

where,

$$\Theta_d = \frac{w(\psi)}{w_{sat}} \tag{5.20}$$

μ_g is the fitting parameter which is a function of air – entry value of the soil, n_g is the fitting parameter which is a function of rate of water extraction from soil once air – entry value of soil has been exceeded.

Brooks and Corey (1964) derived the relationship between water content and matric suction as;

$$w(\psi) = w_{sat} \text{ or } \Theta_d = 1 \text{ for } \psi \leq \psi_{aev} \tag{5.21}$$

$$\Theta_d = \left(\frac{\psi}{\psi_{aev}}\right)^{-\lambda_{bc}} \text{ for } \psi > \psi_{aev} \tag{5.22}$$

where,

$$\Theta_d = \frac{w(\psi) - w_r}{w_{sat} - w_r} \tag{5.23}$$

ψ_{aev} is the air – entry value of soil, λ_{bc} is the pore – size distribution index, w_r is the residual water content located through trial – and – error process that yields straight line on semi – log plot of degree of saturation versus suction.

Finally, Van Genuchten (1980)' s equation is frequently referred in articles, related to this issues such as;

$$\Theta_d = \frac{1}{\left[1 + \left(\mu_g \psi\right)^{n_g}\right]^{m_g}} \tag{5.24}$$

where,

$$\Theta_d = \frac{w(\psi) - w_r}{w_{sat} - w_r} \tag{5.25}$$

$$m_g = (1 - 1/n) \tag{5.26}$$

Fredlund and Xing (1994) revealed the fact that S, saturation, value is usualy employed instead of normalized water content, Θ_d, and Papa, Medina, Ciervo and Bateman (2013) explained that C_0 can be investigated through the derivation of Van Genuchten (1980) equation. As can be seen, key parameters included in presented SWCC should be accounted for by carrying out lab tests but this might not be appropriate for most conditions, in which limited amount of data can be provided. Hence, it might be feasible to look forward to data from literature, which is expected to be based on common rule, or methodology. Hydrologic Properties of Final Cover Soils from the Alternative Cover Assessment Program (2003) was carried out to develop relevant parameters for Van Genuchten (1980) expressed as compatible with USCS (Unified Soil Classification System) and USDA Soil Classification (United States Department of Agriculture) and given in Table 5.6.

Ghanbarian-Alavijeh , Liaghat, Guan-Hua and Van Genuchten (2010) also complied lab test results from literature in an attempt to find Van Genuchten parameters for selected two groups of soil samples classified as USDA Soil Classification System, (Table 5.5, Table 5.7 and Table 5.8). Utilisers is supplied with adopting appropriate m_g, n_g and μ_g values from these tables by pursuing their soil types, which can be classified both USCS and/or USDA Specifications.

All in all, all the assigned parameters are presented in Table C.1.

Table 5.5. 1_{st} group of soil for determination of Van Genuchten parameters.

#	Texture	# of Samples	m_g		μ_g	
			Max	Min	Max	Min
					kPa^{-1}	
1	Sand	6	0.85	0.47	1.28	0.20
2	Loamy sand	8	0.68	0.16	1.30	0.30
3	Sandy loam	6	0.73	0.11	5.61	0.09
4	Sandy clay loam	5	0.39	0.07	1.60	0.20
5	Sandy clay	3	0.26	0.11	0.24	0.01
6	Loam	8	0.34	0.08	1.97	0.09
7	Silt loam	7	0.29	0.09	1.47	0.13
8	Silty clay loam	10	0.48	0.09	1.51	0.01
9	Clay loam	5	0.26	0.05	2.46	0.21
10	Silt	1	0.25	-	0.10	-
11	Silty clay	8	0.50	0.05	16.30	0.04
12	Clay	8	0.13	0.02	50.30	0.01

Table 5.6. Soil types used during alternative cover assessment program (2003).

#	Location	USCS	G (%)	S (%)	F (%)	LL	PL	PI	w
1	Sacramento, CA	SC	30.60	28.10	41.40	31.50	14.00	17.50	15.30
2	Sacramento, CA	CL	2.10	19.20	78.80	39.80	17.70	22.20	14.70
3	Sacramento, CA	CL	16.60	29.60	53.80	34.00	14.20	19.80	15.60
4	Helena, MT	SC	21.70	51.00	27.40	31.50	17.00	14.50	15.80
5	Helena, MT	CH	2.00	53.00	45.04	65.80	19.90	45.80	14.00
6	Polson, MT	ML-NP	4.00	52.90	43.10	29.00	22.00	7.00	15.30
7	Polson, MT	ML-NP	5.40	53.70	40.90	29.00	22.00	7.00	16.20
8	Polson, MT	ML	0.90	8.20	90.90	27.30	20.90	6.40	16.10
9	Polson, MT	ML-NP	7.40	51.40	41.30	27.00	20.00	7.00	15.50
10	Polson, MT	ML	0.80	6.00	93.20	28.70	21.40	7.30	15.10
11	Polson, MT	ML-NP	4.90	50.50	44.60	27.00	20.00	7.00	16.40
12	Albany, GA	SC	5.00	68.00	25.00	26.00	14.50	11.50	16.80
13	Albany, GA	SC	8.40	63.40	30.80	27.80	14.40	13.40	16.80
14	Albany, GA	SC	4.40	60.10	36.20	27.50	14.50	13.00	16.60
15	Albany, GA	SC	9.80	61.90	32.50	26.50	15.50	11.00	15.70
16	Albany, GA	SC-SM	4.80	67.70	31.50	25.80	16.30	9.50	17.20
17	Albany, GA	SC	9.20	60.80	36.30	24.00	14.00	10.00	16.50
18	Omaha, NE	CL	0.00	3.40	96.60	46.80	17.00	29.80	14.00
19	Omaha,NE	CL	0.00	0.90	99.20	44.00	17.00	27.00	14.80
20	Omaha, NE	SP	0.00	98.20	1.80	0.00	0.00	0.00	15.20
21	Omaha, NE	CL	0.00	1.50	98.50	40.00	19.50	20.50	15.10
22	Cedar Rapids, IA	CL	4.50	47.80	51.80	34.50	18.30	16.30	15.60
23	Cedar Rapids, IA	CL	4.80	52.30	51.10	28.80	15.40	13.40	17.20
24	Cedar Rapids, IA	CL	3.20	50.80	50.60	31.30	16.70	14.70	17.40
25	Boardman, OR	CL-ML	0.20	37.50	86.90	25.50	18.90	6.50	14.50
26	Boardman, OR	ML	0.10	37.60	82.20	22.30	19.70	2.70	14.10
27	Altamont, CA	CL	2.50	8.60	91.20	47.30	26.50	20.80	16.70
28	Altamont, CA	CL	1.90	12.20	87.50	45.10	26.10	19.00	16.20
29	Altamont, CA	CL	1.50	14.80	86.00	47.00	25.80	21.30	15.80
30	Monterey, CA	SC	15.90	55.00	33.50	29.50	14.50	15.00	16.70
31	Monterey, CA	SP	0.10	92.20	8.60	0.00	0.00	0.00	16.40
32	Monticello, UT	CL	2.90	22.30	74.80	31.50	14.50	17.00	15.10

Table 5.7. Van Genuchten parameters for soils above.

Group #	USCS Group Symbol	Number of Samples	μ_g (kPa-1)		n_g	
			Geometric Mean	σlnα	Mean	σ_n
1	SC	2	0.00641	0.12	1.20	0.05
2	CL	12	0.00351	1.15	1.32	0.10
3	CL	5	0.01030	0.79	1.37	0.11
4	SC	2	0.00879	0.05	1.36	0.02
5	CH	13	0.00346	1.42	1.19	0.02
6	ML-NP	4	0.01019	0.07	1.41	0.01
7	ML-NP	4	0.01013	0.14	1.42	0.04
8	ML	8	0.00266	0.29	1.25	0.05
9	ML-NP	4	0.00938	0.06	1.40	0.01
10	ML	7	0.00271	0.32	1.27	0.03
11	ML-NP	8	0.01035	0.05	1.44	0.04
12	SC	2	0.00357	2.20	1.42	0.28
13	SC	5	0.00244	1.23	1.58	0.42
14	SC	2	0.00126	0.87	1.79	0.40
15	SC	4	0.00408	1.26	1.39	0.09
16	SC-SM	4	0.00233	0.52	1.49	0.14
17	SC	2	0.00197	0.29	1.52	0.07
18	CL	4	0.00095	1.15	1.61	0.39
19	CL	4	0.00291	1.09	1.97	1.24
20	SP	3	0.37888	0.09	7.12	0.17
21	CL	4	0.00581	1.04	1.28	0.10
22	CL	8	0.00159	0.55	1.63	0.26
23	CL	8	0.00266	0.69	1.40	0.09
24	CL	3	0.00261	1.03	1.47	0.23
25	CL-ML	13	0.01398	0.46	1.48	0.10
26	ML	3	0.02528	0.31	1.35	0.02
27	CL	4	0.00761	0.83	1.30	0.06
28	CL	7	0.00296	0.56	1.42	0.05
29	CL	4	0.00789	0.94	1.32	0.08
30	SC	11	0.00408	0.76	1.40	0.10
31	SP	8	0.48279	0.08	3.92	0.74
32	CL	8	0.00281	0.91	1.38	0.11

Table 5.8. 2_{nd} Group of soil for determination of Van Genuchten parameters.

#	Texture	# of samples	Clay content		m_g		μ_g	
			Max	Min	Max	Min	Max	Min
			g kg^{-1}				kPa^{-1}	
1	Sand	2	18	14	0.61	0.55	0.28	0.27
2	Loamy sand	10	108	23	0.61	0.25	0.45	0.24
3	Sandy loam	11	178	70	0.58	0.11	0.50	0.13
4	Sandy clay loam	15	349	208	0.46	0.06	0.40	0.15
5	Loam	7	260	122	0.49	0.19	0.50	0.18
6	Silt loam	5	270	120	0.20	0.12	0.98	0.15
7	Silty clay loam	8	390	280	0.30	0.12	0.90	0.10
8	Clay loam	6	348	304	0.39	0.05	0.50	0.08
9	Sandy clay	5	421	352	0.33	0.09	0.50	0.18
10	Silty clay	2	460	420	0.09	0.08	0.65	0.55
11	Clay	1	452	-	0.34	-	0.09	-

5.2.4. Computation of Topographical Properties of Interested Site

One of the most significant and demanding process of Montgomery and Dietrich (1994)' s Methodology is to delineate the catchment area, which is also divided by b and then called as "*contributing area per unit length (m^2/m)*", or "*specific catchment*", such that interested site is required to be partitioned into smaller areas bounded by the trajectories drawn from lower contour to upper one. The logic declares that subsurface flux is composed of both infiltrated rain water and existing steady – state groundwater and is assumed to be deeply affected by catchment topography. Consider the hypothetical topography in Figure 5.5 to illustrate the aforementioned topic. Hypothetical catchment (in black color) and relevant contours (in red colors) are generated to typify what are expected to perform throughout the topographical operations in Montgomery and Dietrich (1994) and the longitudinal section of one of the trajectories (in green color) in Figure 5.6 is

provided in an attempt to sketch the assumption laying the foundation of this methodology; wetness parameter includes both percolated rain water and existing groundwater .

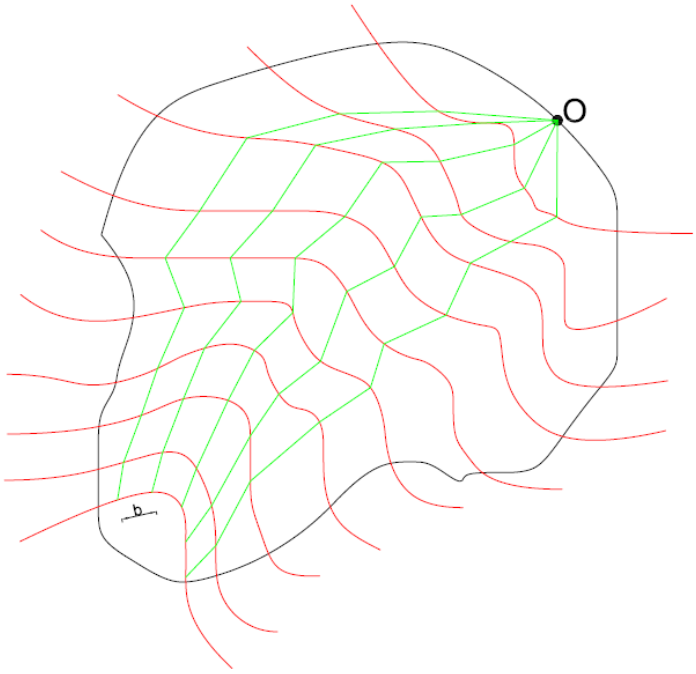

Figure 5.5. Catchment area and compete set of uphill trajectories for hypothetical topography.

To begin with the topographical treatments as visualized in Figure 5.5, each contour line is divided into certain number of end point coordinates, which is also dependent on a selected b value. Assigned value of b is totally related to such an extent of precision determined for results that both amount of time spent for and accuracy of calculations specifies the selection of b. After the disintegration of contour lines with with respect to prescribed b parameter, boundaries are started to be drawn from lower contour to upper one in an attemp to constitute an area, which is the indication of subsurface flux route. Each path should be concluded at watershed peak (either local or global) and ought to be computed by pursuing the minimum steeper distance between respective contour segments. Also, it is of significance to quote this passage from O'Loughlin (1981) "*The contour resolution and contour element length b used in the analysis dictate the precision of the result. In any case, their choice should allow calculation of the partial catchment areas and slopes everywhere with a precision consistent with the map scale. Experience has indicated that a good match can be achieved between the resolution of the predicted wet areas and their real size and location if the contour density is such that 30 or more*

contours are available to describe the terrain, and a contour element length of 10 units (rescaled computer units) is used."

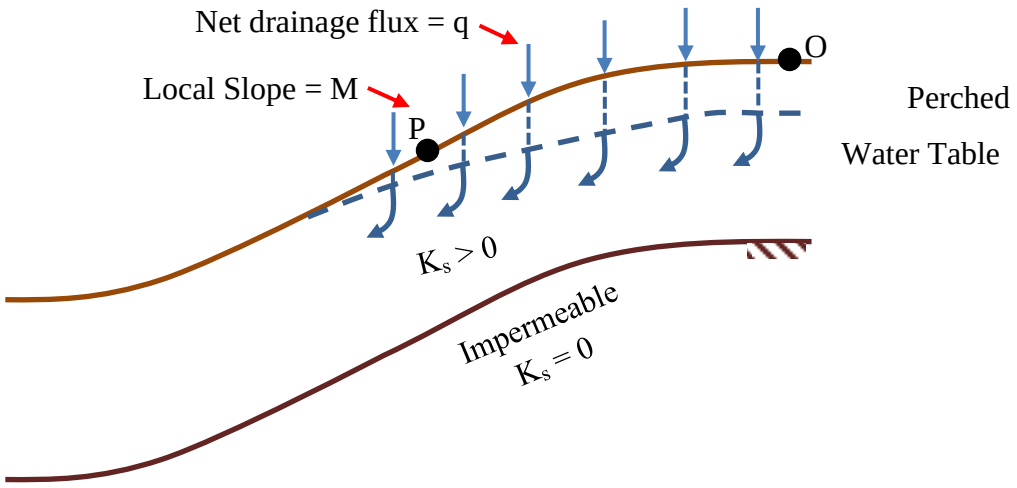

Figure 5.6. Definition skecthes for section along transect of partial catchment area.

This process is able to be achieved by the model coded by Papatheodorou and Tzanou (2014), which only demands the DEM (Digital Elevation Model) of study area to map specific catchment area and slope values for each cell by 30 X 30 m. The routine developed by Papatheodorou and Tzanou (2014) should be operated in QGIS environment, freely downloadable on net and is schematized in Figure 5.7.

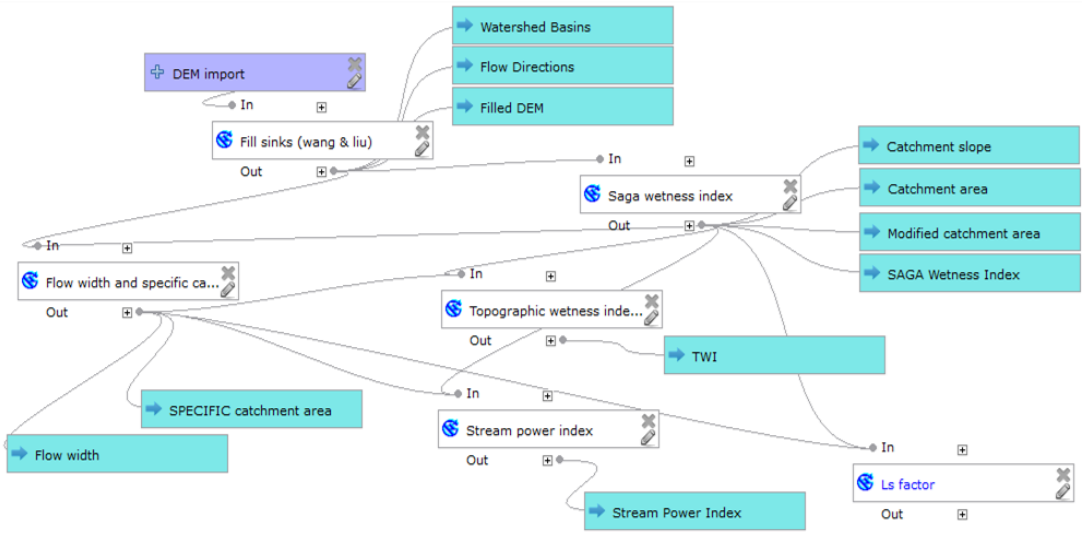

Figure 5.7. Procedural steps of Papatheodorou and Tzanou Methodology (2014).

5.2.5. Determination of Rainfall Intensity

Up to this point, it is struggled for attaining the parameters, which be constant in nature, through empirical correlations or comparisons from soils tested in lab but incoming rainfall can statistically be predicted for rainfall – induced landslide forecasting process. Should Montgomery and Dietrich (1994) be taken into consideration to unfold the behaviour of relevant site under steady – state rainfall effect, the statistical characteristics of rainfall is able to be modelled by distribution functions properly fitted to previous intensity measurements. Incorporating the rainfall amount into the analysis by such way is presumed as more logical and favored by researchers since the risk, containing both hazard and vulnerability within itself, of site is usually apprehended as a probabilitistic quantity rather than a deterministic one.

Figure 5.8. The location of meteorological stations and study area in red boundary.

There exists plenty of probability distribution functions in literature in that different types of them is assessed to provide statistical coherence between number of measurements divided by total one given for certain rainfall intensity interval and the corresponding value derived by distribution function. To that end, the measurements extracted from 4 different meteorological stations in Tekirdağ Region (Tekirdağ, Malkara, Çorlu and Çerkezköy) are both daily and monthly scrutinized so as to decide on which can be employed for Montgomery and Dietrich (1994). It can be deduced from the map in Figure 5.8 that the most closest Tekirdağ Meteorological Station ought to be adopted throughout the analysis.

Then, daily measurements can only be represented by exponential distribution Eq. (5.27) as presented in Figure 5.9 because of the fact that dry days govern the rainfall characteristics of Tekirdağ Region. Eq. (5.27) is also recasted into more usable form so that rainfall amount tallying with prescribed degree of exceedence probability can be extracted from cumulative distribution in Eq. (5.28).

$$P(x,\lambda) = \begin{cases} \lambda e^{-\lambda x} & x \geq 0 \\ 0 & x < 0 \end{cases} \tag{5.27}$$

$$F(x,\lambda) = \begin{cases} 1 - e^{-\lambda x} & x \geq 0 \\ 0 & x < 0 \end{cases} \tag{5.28}$$

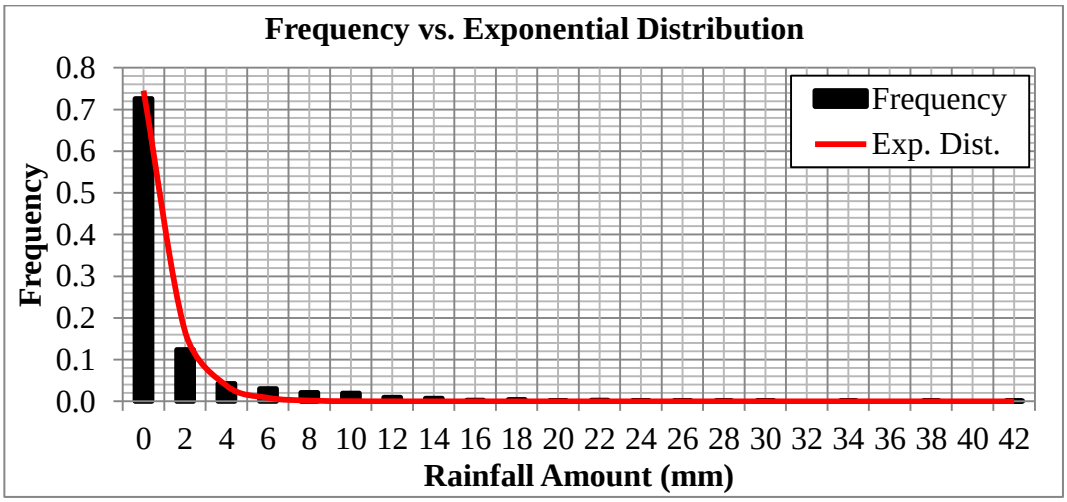

Figure 5.9. Daily rainfall frequency vs. exponential distribution function.

The bottom line of this statistical route paves the way for conducting probabilistic assessment within the context of Montgomery and Dietrich (1994) as illustrated in Figure 5.10.

Table 5.9. Exceedence probability (%) with respect to daily rainfall amount (DRA).

Exceedence Prob (%)	**DRA (mm)**
EP of 2%	5.25
EP of 10%	3.09

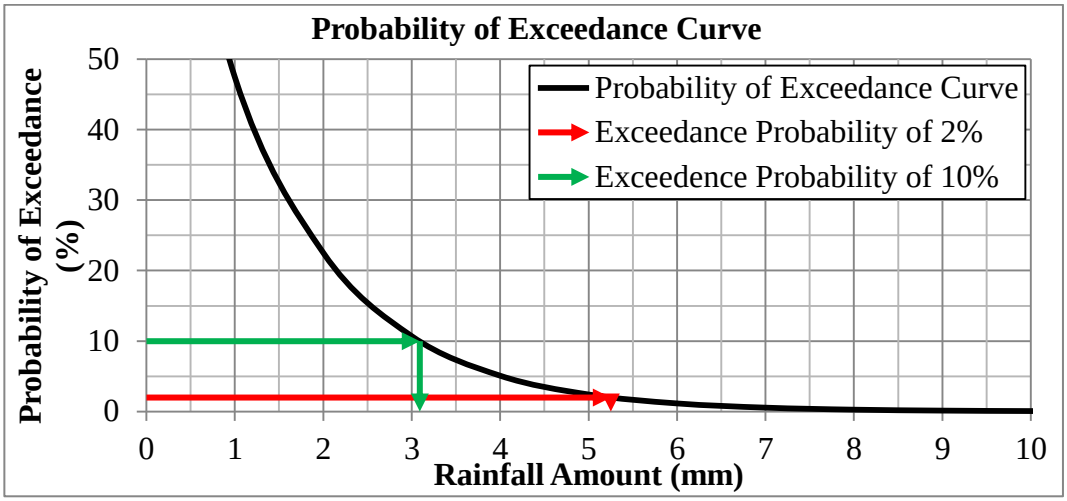

Figure 5.10. Exceedence probability curve with respect to rainfall amount (mm).

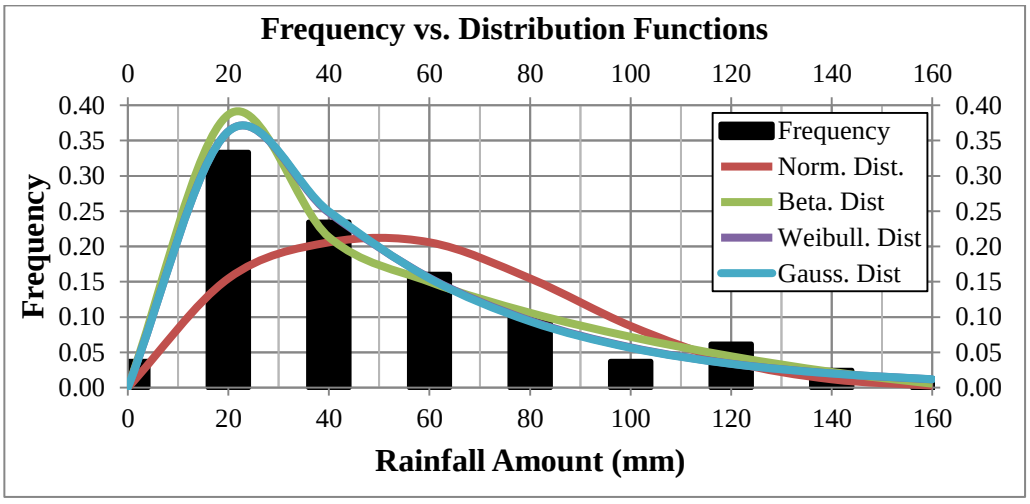

Figure 5.11. Monthly rainfall frequency vs. distribution functions.

Same procedure is embraced for monthly rainfall data with a difference that Normal Eq. (5.29), Beta Eq. (5.30), Weibull Eq. (5.31) and Gamma Distributions Eq. (5.32) are exploited to supply goodness of fit between data and simulated statistical model.

$$P(x,\mu,\sigma) = \frac{1}{\sigma\sqrt{2\pi}} e^{-\frac{(x-\mu)^2}{2\sigma^2}} \tag{5.29}$$

$$P(x,\alpha,\beta) = \frac{x^{\alpha-1}(1-x)^{\beta-1}}{B(\alpha,\beta)} \tag{5.30}$$

$$P(x,\lambda,k) = \begin{cases} \frac{k}{\lambda}\left(\frac{x}{\lambda}\right)^{k-1} e^{-(x/\lambda)^k} & x \geq 0 \\ 0 & x < 0 \end{cases} \tag{5.31}$$

$$P(x,k,\theta) = \frac{x^{k-1}e^{-\frac{x}{\theta}}}{\theta^{k}\Gamma(k)} \tag{5.32}$$

As can be inferred from Figure 5.11, normal distribution is not appropriate for monthly rainfall frequency and cannot be optimized due to its dependence on mean (μ) and standard deviation (σ). What is the benefited from other types of distributions is to provide compatibility between data and those in Figure 5.11 by means of arranging parameters included in these relationships. The methodology bear on the logic that the sum of square of difference between frequency value and that obtained from distribution function corresponding to certain range of rainfall amount is attempted to be minimized by changing the *parameters* in from Eq. (5.30) to Eq. (5.32). The results given in Table 5.10 reveal that the most suitable one can be deduced as Weibull Distribution and what is inferred from exceedence probability curve generated for Weibull Distribution is proposed in Figure 5.12 and Table 5.11.

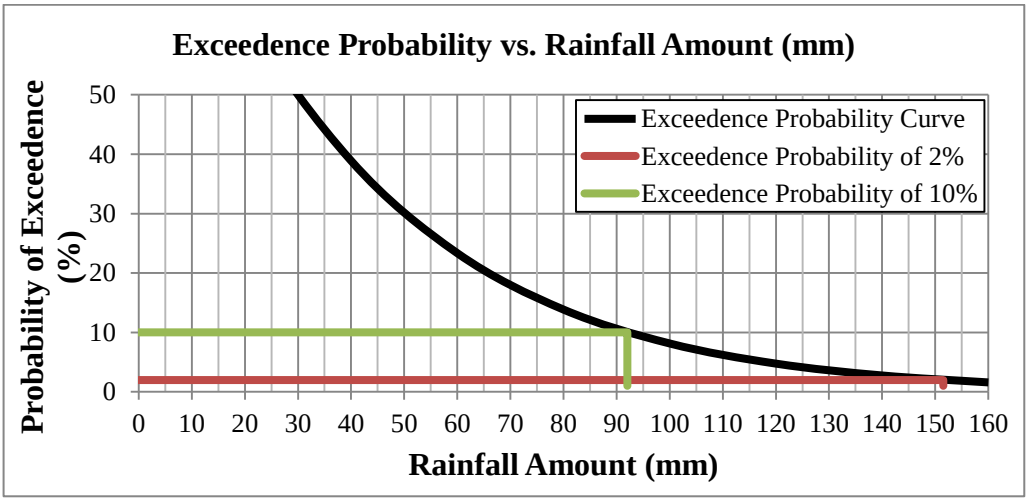

Figure 5.12. Probability of exceedence curve with respect to rainfall amount (mm).

Table 5.10. The sum of square of difference between frequency value and that obtained from distribution functions.

RD	RD Array	Normal	Beta	Weibull	Gamma
MRA	0 - 160 by 20	0.08544	0.00444	0.00358	0.00368

Table 5.11. Exceedence probability (%) with respect to Monthly Rainfall Amount (MRA).

Exceedence Prob (%)	MRA (mm)
EP of 2%	151.5
EP of 10%	92

In contrast to adopted in the application of Montgomery and Dietrich (1994) and Iverson (2000) methodology included in developed routine is performed by sequence of rainfall data, hence probabilistic approach might not be appropriate for a logic pledging to calculate time – dependent pressure heads and factor of safety values. Thus, the most detrimental amount of rainfall occurred in a definite day is sorted out among the measurements in order that the minimum factor of safety values, which in turn overlaps with the maximum pore water pressures, can be gained throughout the analysis.

5.3. The Results of Montgomery and Dietrich (1994) Methodology

Since Montgomery and Dietrich Methodology (1994) is composed of carrying out two simple equations as given from Eq. (2.14) to Eq. (2.17), the capability of Mapinfo to perform such operations is exploited within the context of this algorithm. In the first case, specific catchment area (Figure 5.13) and slope angles (Figure 5.14) as 30 X 30 m cells are transferred from QGIS media as shapefiles and converted into the desired form to go ahead with the calculations. After this step, permeability (Figure 5.15), soil depth (Figure 5.16) and daily rainfall data are projected onto each grid cell in that the latter one is considered as both exceedence probability of 2% and 10% in wetness computations. The fact that Montgomery and Dietrich (1994) is based on “steady – state condition” prevents utilizers from simulating the pore pressure patterns developed under different rainfall conditions but it successfully represents the potential waterlogging zones in area. This is what we anticipate from this methodology to detect water accumulation zones at the expense of omitting transient rain water effects and factors rather than topography.

Figure 5.13. Specific catchment areas for Tekirdağ City Center.

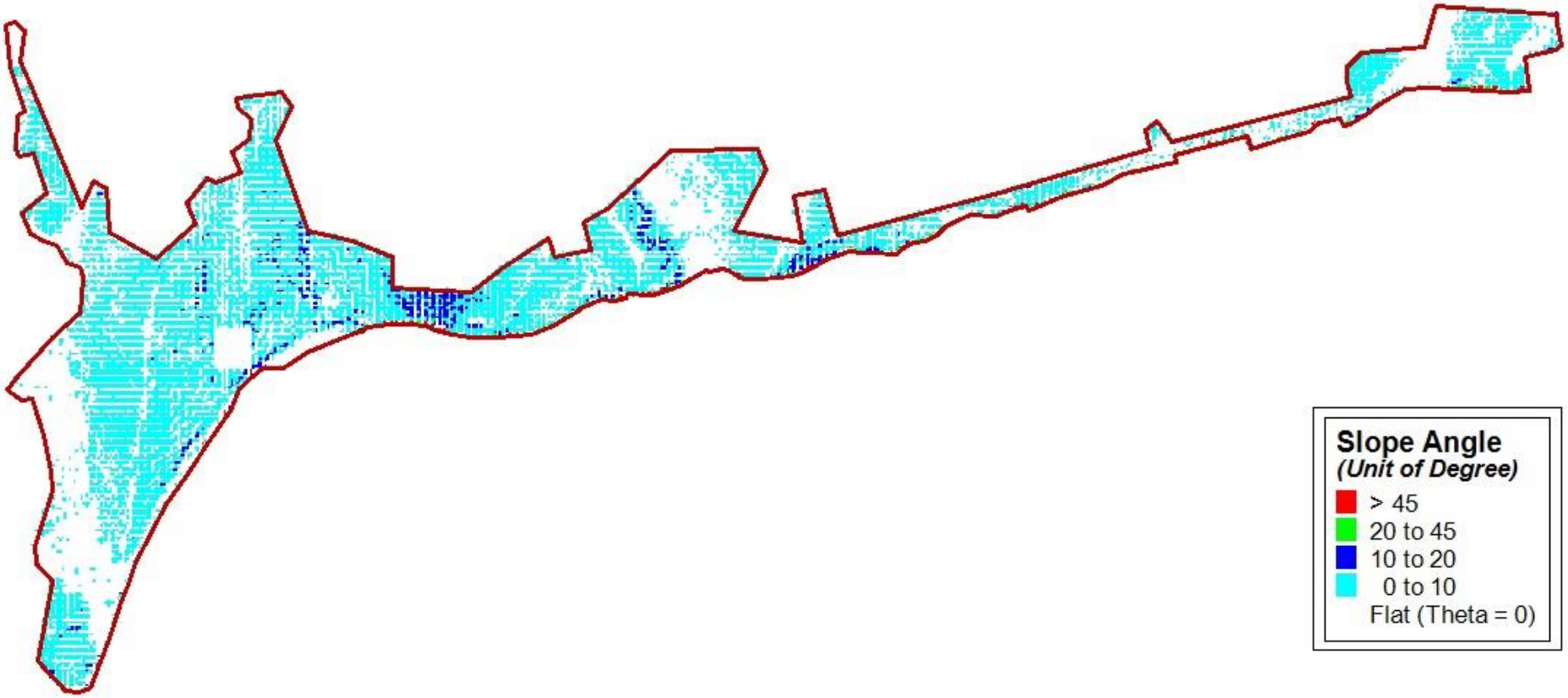

Figure 5.14. Slope angles for Tekirdağ City Center.

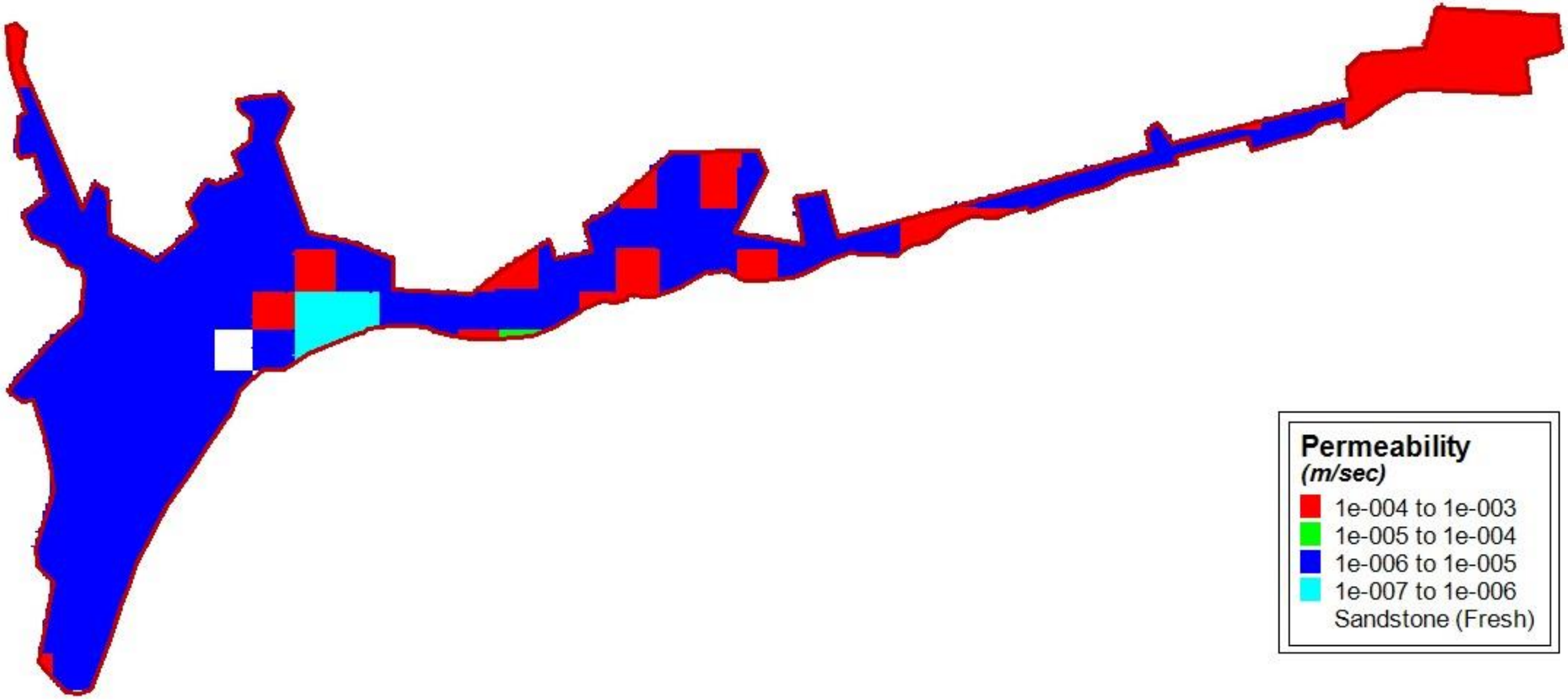

Figure 5.15. Permeability values for Tekirdağ City Center.

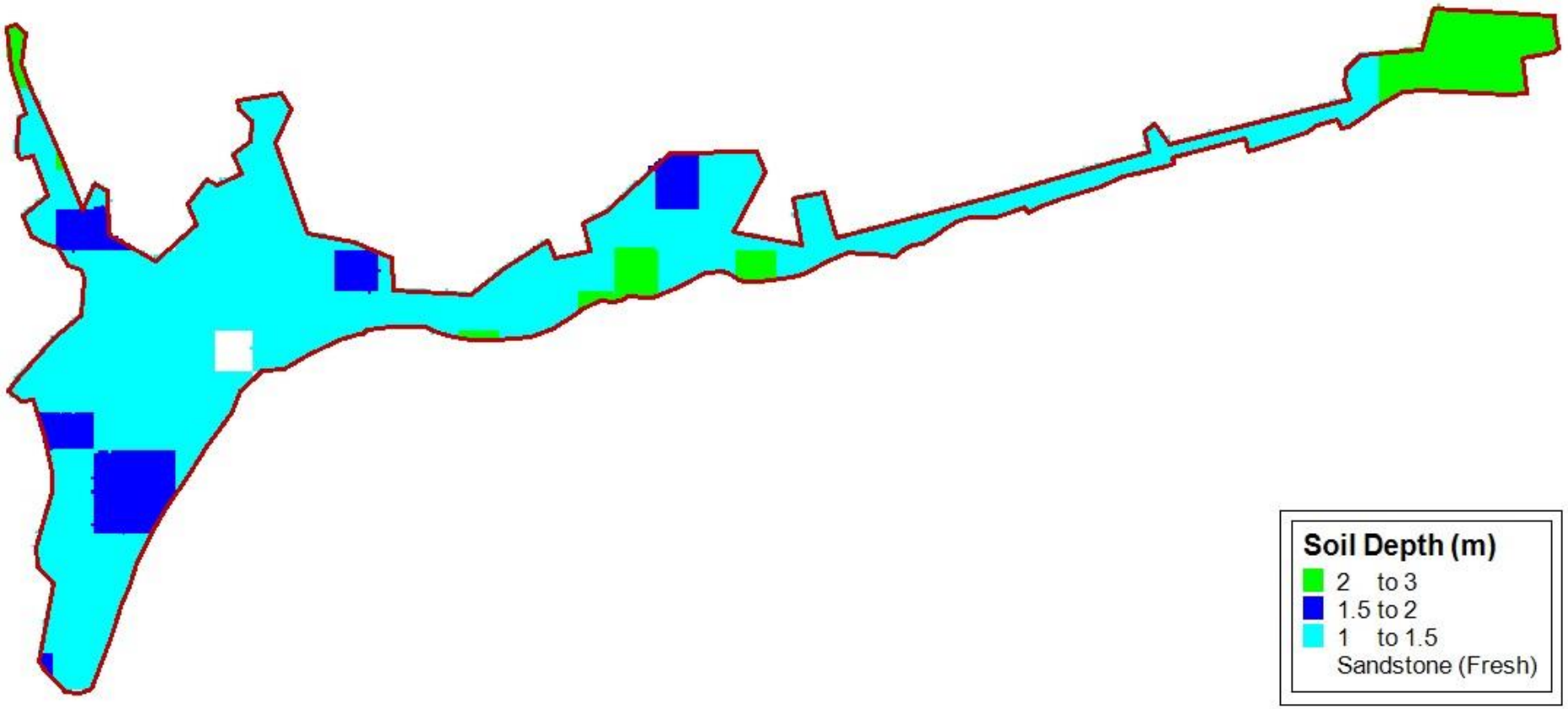

Figure 5.16. Soil depths for Tekirdağ City Center.

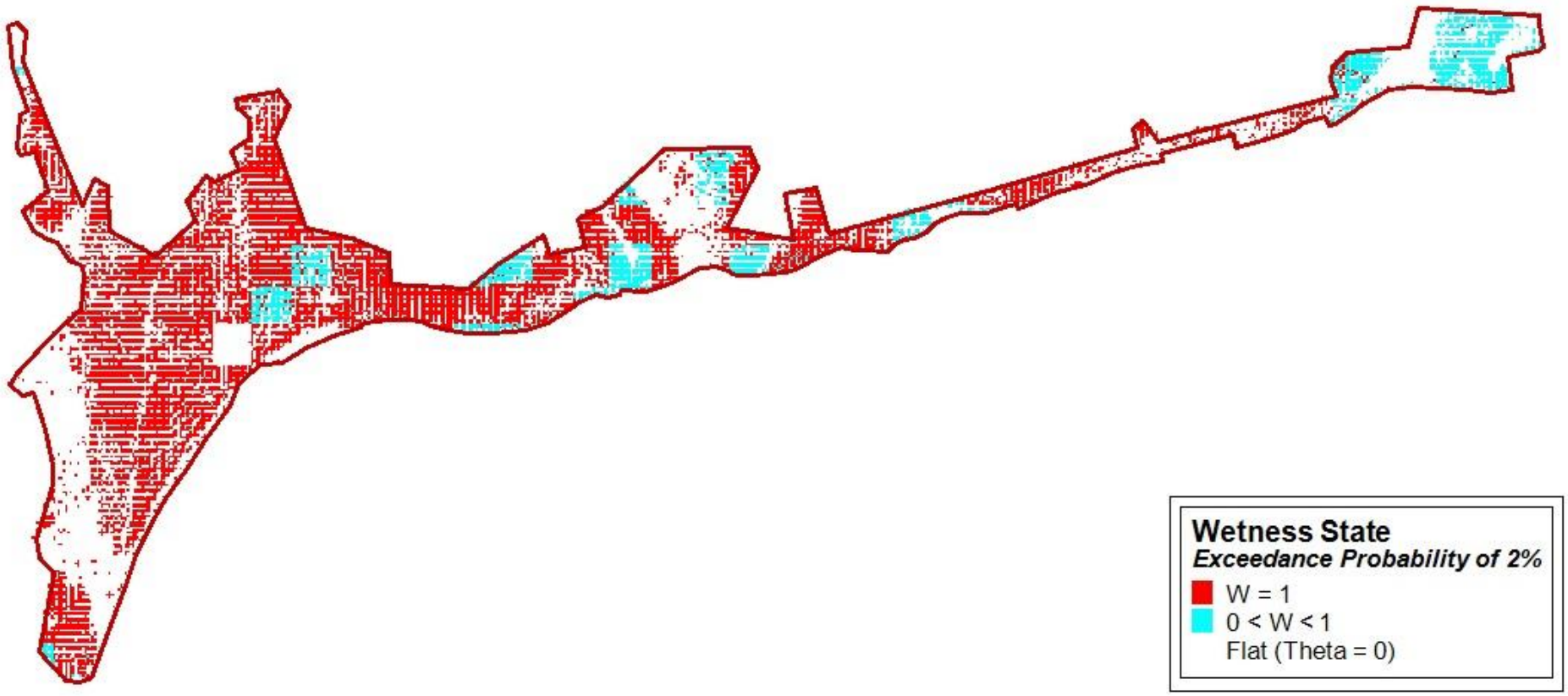

Figure 5.17. Wetness state for rainfall amount corresponding to exceedence probability of 2%.

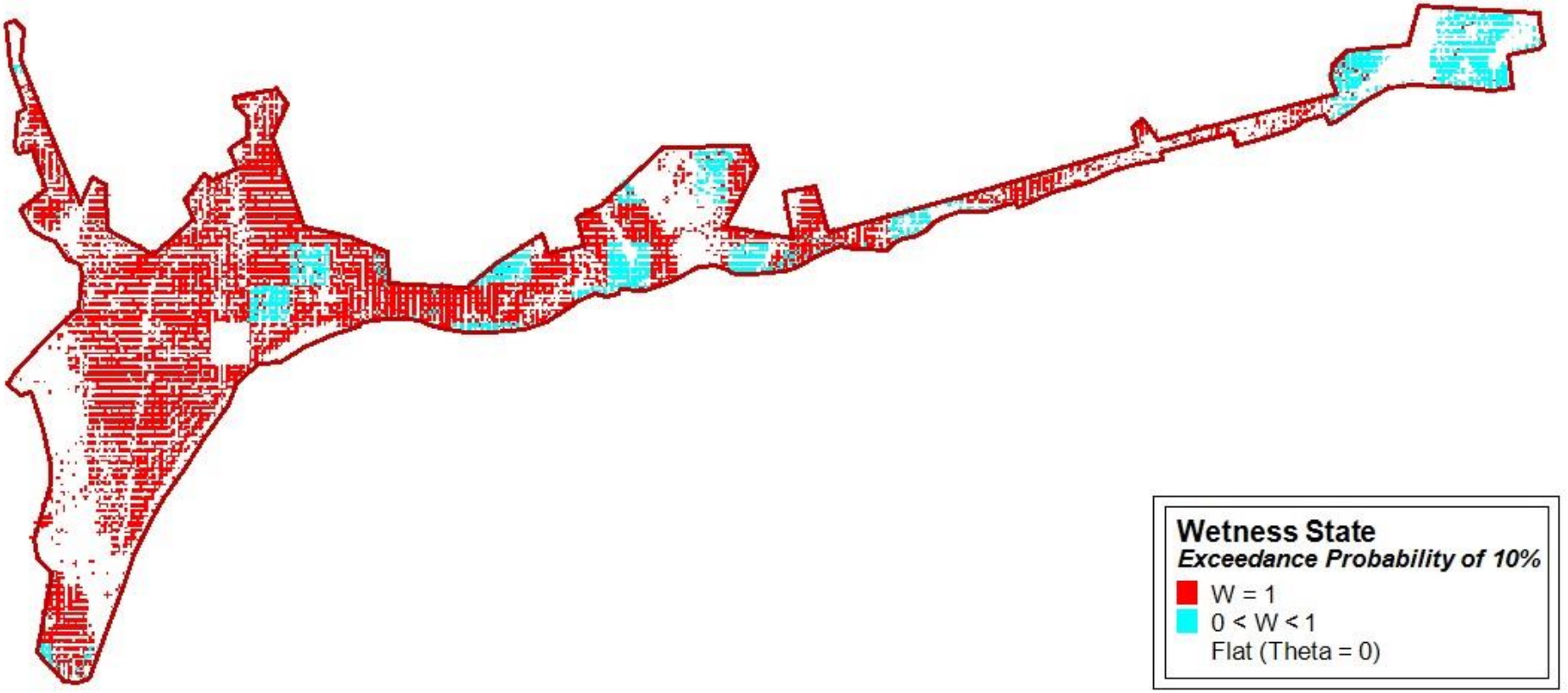

Figure 5.18. Wetness state for rainfall amount corresponding to exceedence probability of 10%.

Before evaluating the FoS maps, should the wetness state maps be investigated, it can be stated that wetness parameter is dominantly specified by the degree of permeability and slope angles for given cells rather than specific catchment areas in this case (The corollary of overlapping between cells quantified as clay in terms of permeability in Figure 5.15, Figure 5.17 and Figure 5.18). In other words, although most of the regions possess lower values of A/b, these cells are exposed to full saturation since slope values computed for them lie within the low (0^0 to 10^0) extent and again most of site is quantified as clay type of soil, which in turn indicates the lower capability of soil transmissivity.

What is deduced from the FoS Maps are that (1) the regions where residual friction angles are assigned as lower than slope angle be unconditionally unstable under whichever exceedence probability value is embraced for rainfall amount in wetness parameter (2) the white zones stands for the unconditional stable zones due to slope angle value of 0 (3) the distribution of failure (FoS < 1) and on the verge of failure ($1 \leq FoS < 1.5$) zones concentrating on the middle and partially left side of Figure 5.19 and Figure 5.20 is substantially determined by soil properties for Tekirdağ City Region. This bottom line is able to be verified by employing right side of Figure 5.19 and Figure 5.20 such that even though specific cathcment areas and slope angles are approximately similar for both left and right sides, areas situated onto the latter stays within the safe side since the greater permeability permits soil to conduct subsurface flux, thus decreasing the wetness state, in turn, groundwater level. The second component is the greater residual shear strength angles in these cells at such an extent that failure is not be monitored even if full saturation arises after significant amount of rainfall.

Number of failed cells is obtained as 995/11819 and 997/11819 for Exceedence Probability of 10% and 2% (approximately %8.41 of total cells) by means of this methodology, respectively. This result indicates that coastal area (middle part) and relatively left side of Tekirdağ City Center may be exposed to instability under aforementioned amount of rainfall if assigned soil parameters govern the response of encountered soil.

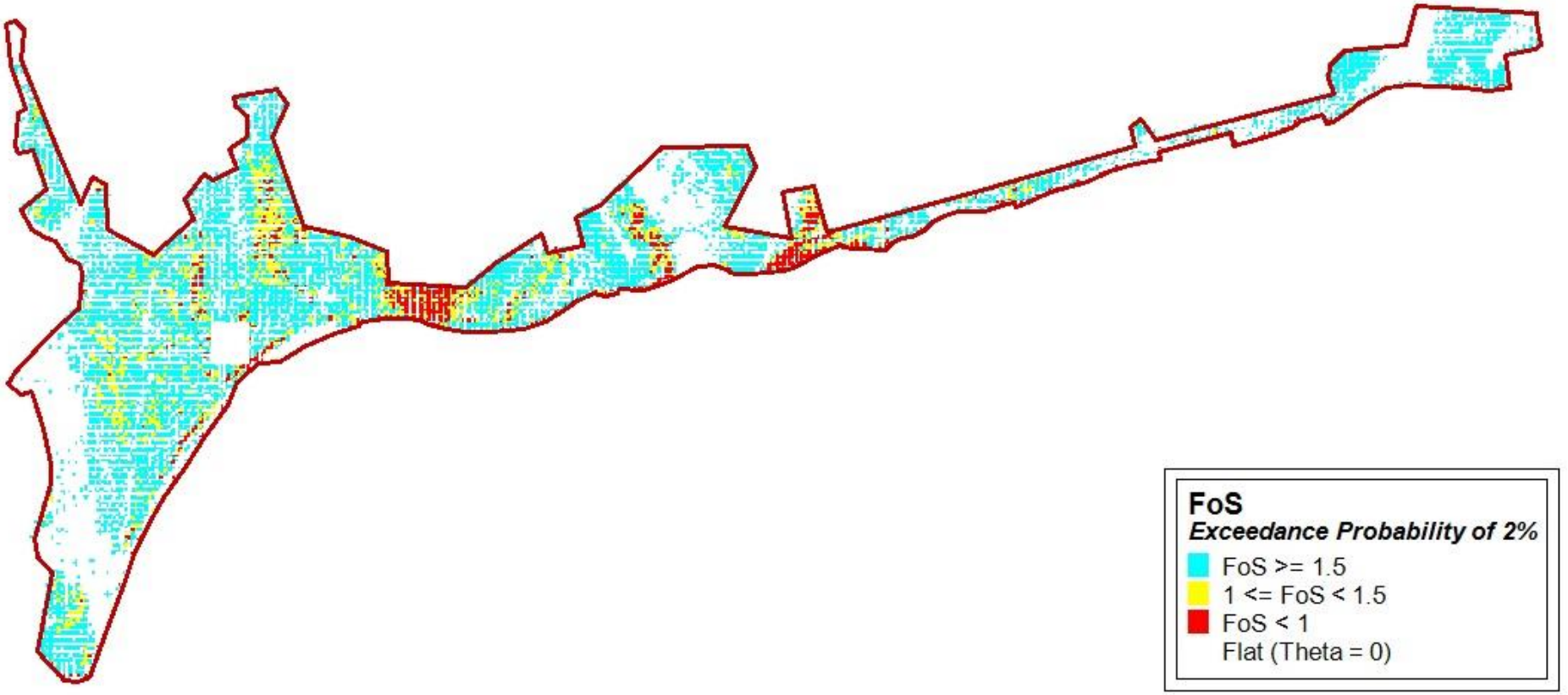

Figure 5.19. FoS for rainfall amount corresponding to exceedence probability of 2%.

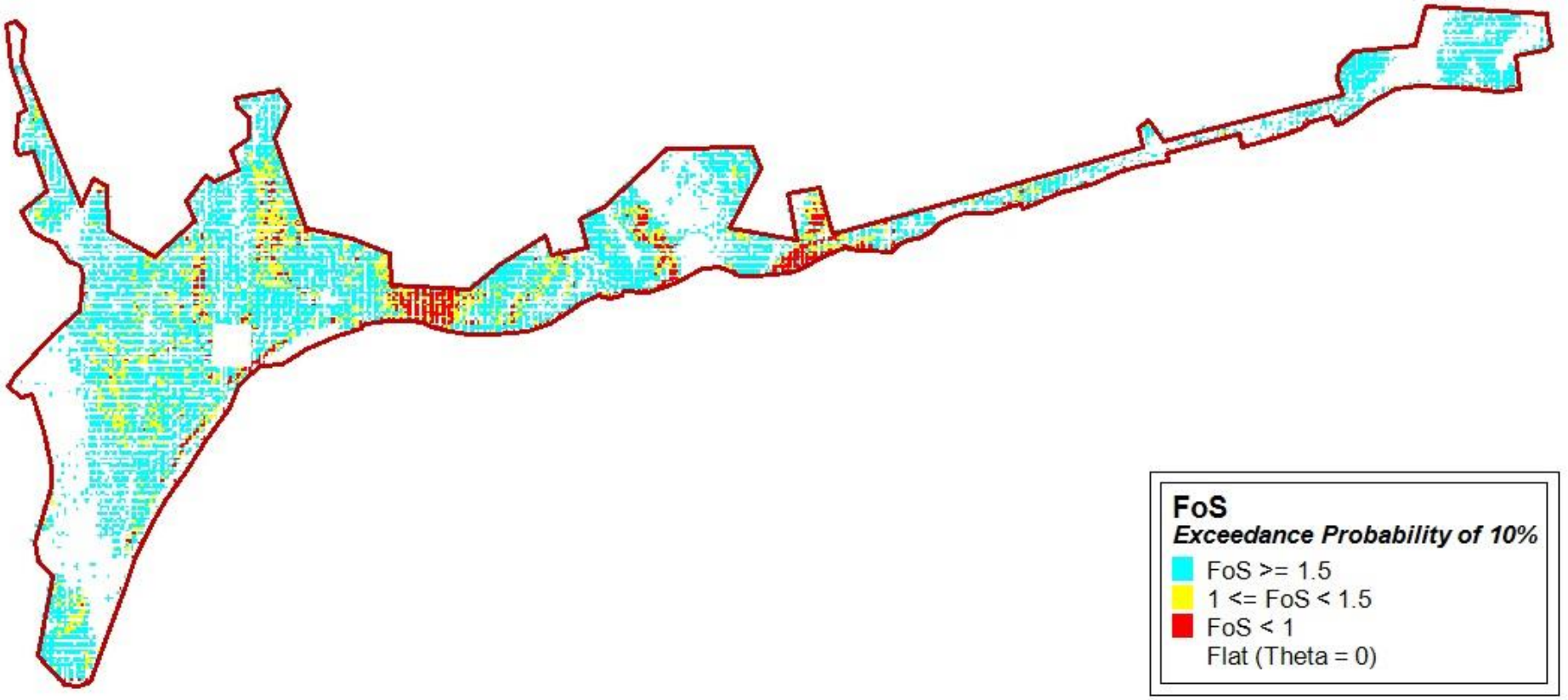

Figure 5.20. FoS for rainfall amount corresponding to exceedence probability of 10%.

5.4. The Results of Developed Methodology

As stated in Chapter THEORETICAL BACKGROUND OF DEVELOPED METHODOLOGY, it would be possible to monitor the pore pressure fluctuation under rainfall sequence in that the increase or decrease (overlapping with the condition of no rainfall) in pressure head values can be mimicked through exact solution of partial differential equation given from Eq. (2.48) to Eq. (2.53).

In this context, the procedure is commenced by the procurement of the maximum daily rainfall amount within the measurement conducted between the date of 10.11.2007 and that of 31.08.2014. The total value for this day is found as 41.8 mm on 28.10.2010 and each quantity is plotted with respect to respective time interval (Figure 5.21). Before 00:00, it is thought that Tekirdağ City Center be in hydrostatic condition and factor of safety calculations are carried out in regard to static groundwater table for each cell (Figure 5.22). The accumulation of pore water pressures (PWP) are able to be simulated by a logic that corresponding FoS values are attained during rise in pressure heads and minimum estimation is mapped for each time interval (From Figure 5.23 to Figure 5.45). Also, the condition of no rainfall, which is usually called as relaxation process, is regarded and projected into the analysis as decay and grow in PWP and FoS, respectively.

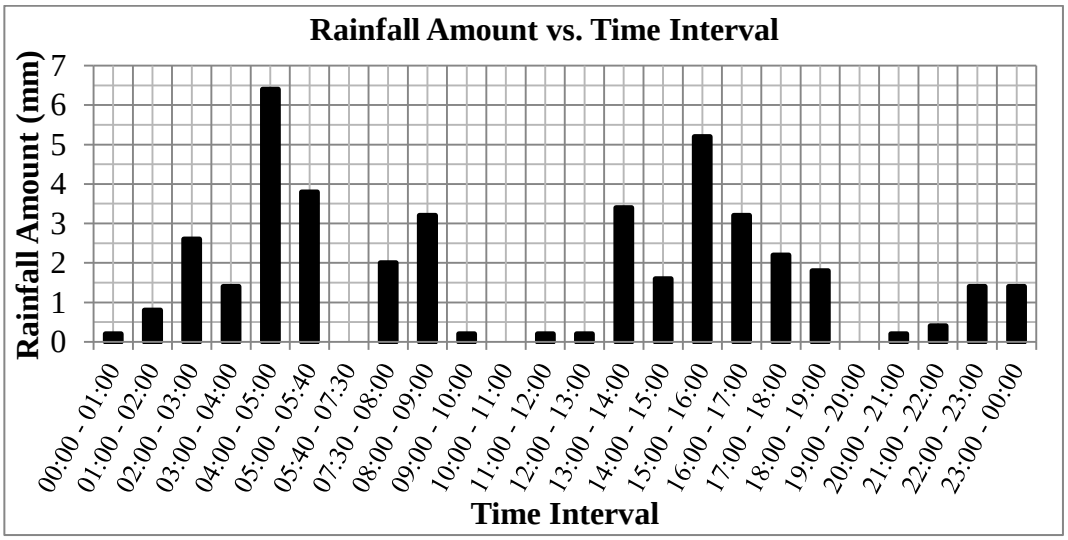

Figure 5.21. Rainfall amount vs. time interval for maximum daily rainfall obtained from measurements of Tekirdağ Meteorological Station.

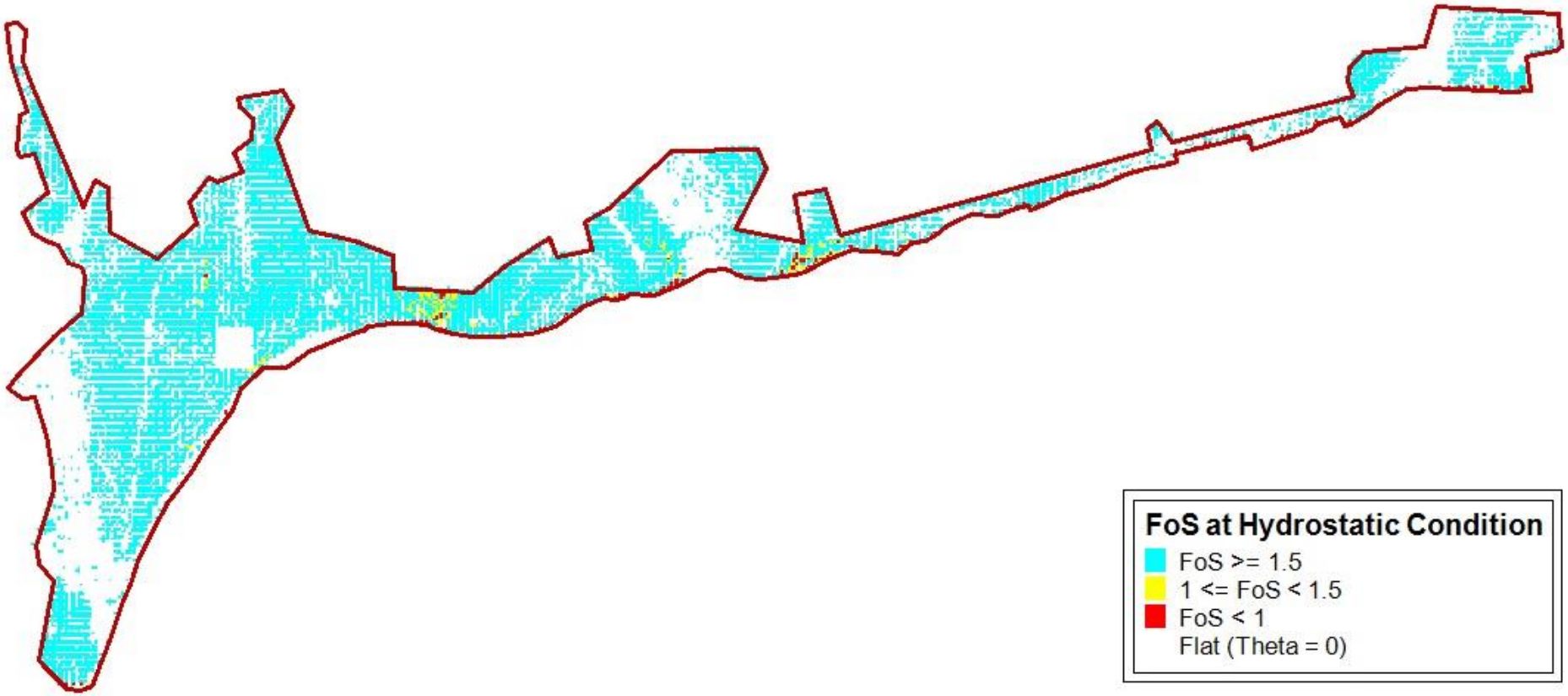

Figure 5.22. Factor of safety values at hydrostatic condition.

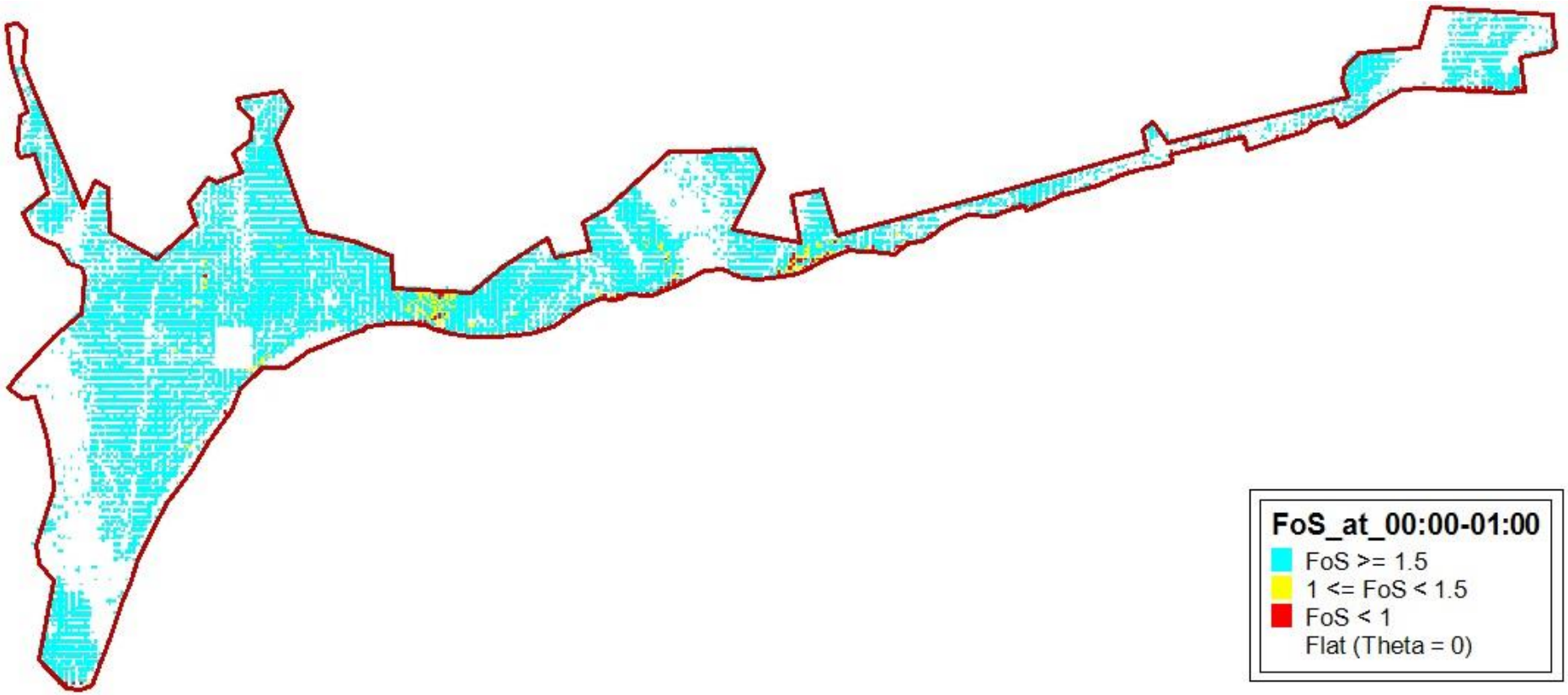

Figure 5.23. Minimum factor of safety values at 00:00 – 01:00.

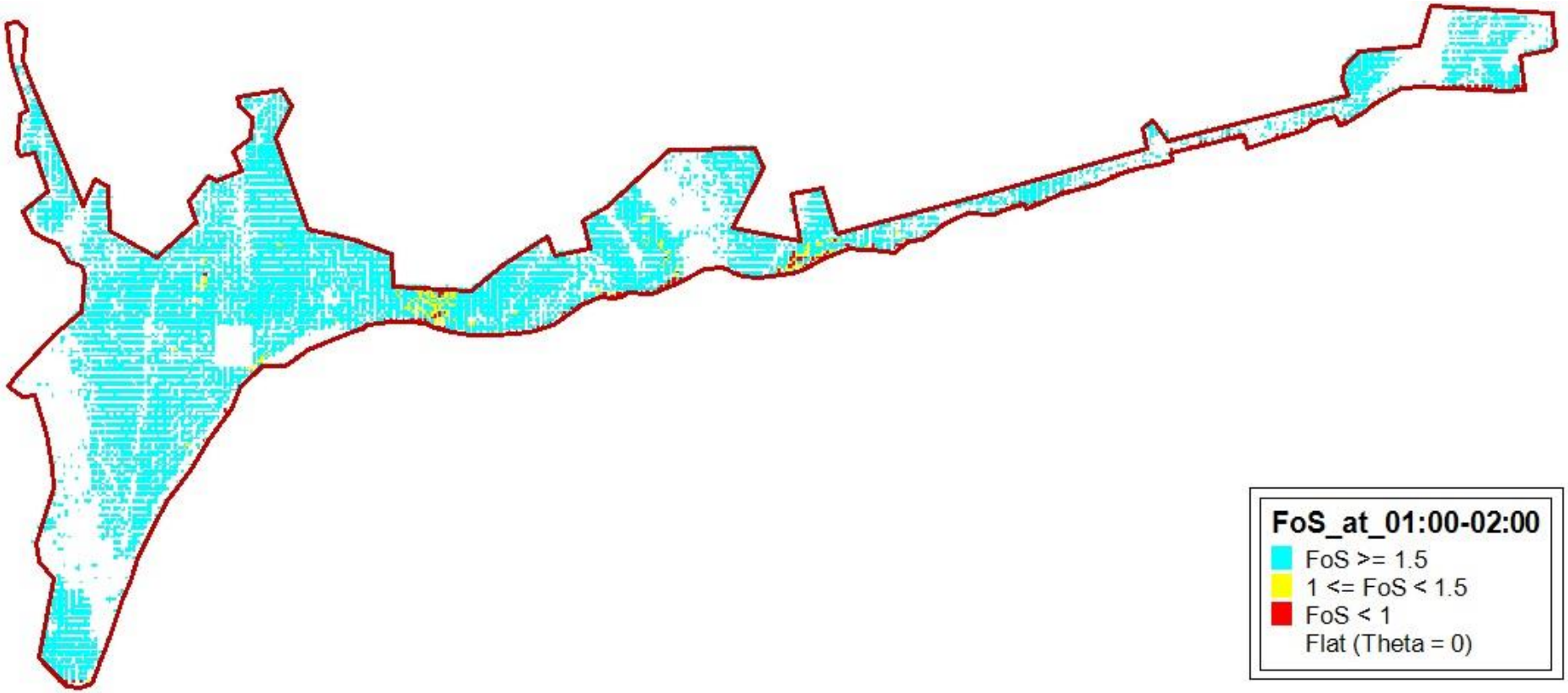

Figure 5.24. Minimum factor of safety values at 01:00 – 02:00.

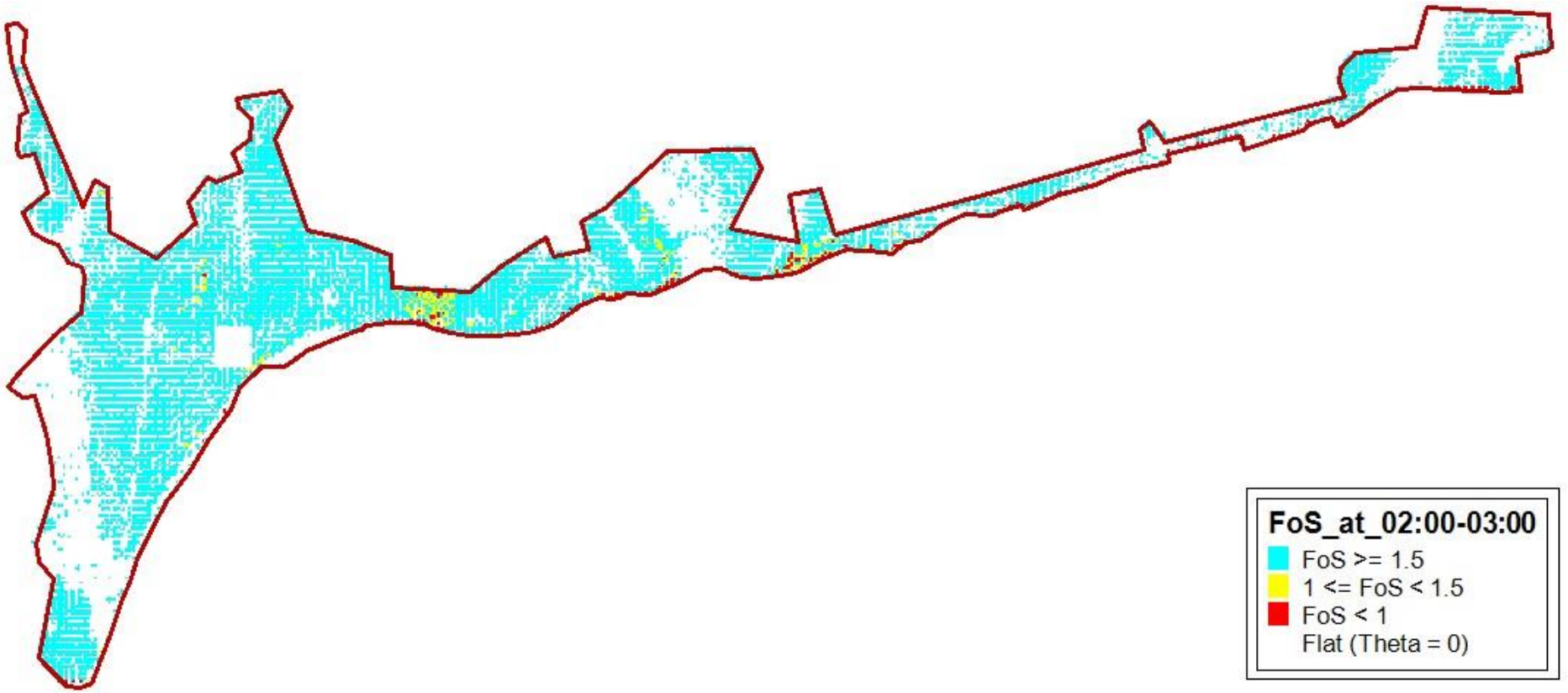

Figure 5.25. Minimum factor of safety values at 02:00 – 03:00.

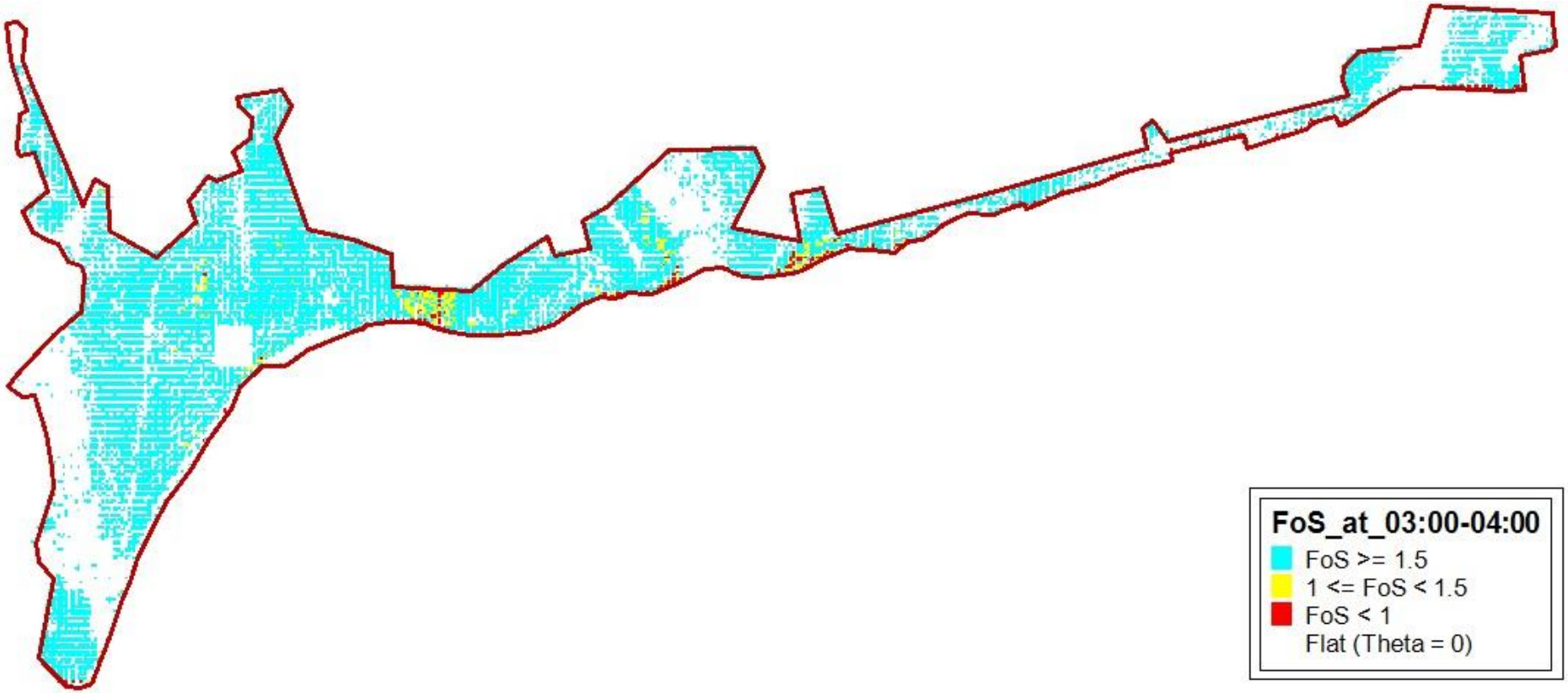

Figure 5.26. Minimum factor of safety values at 03:00 – 04:00.

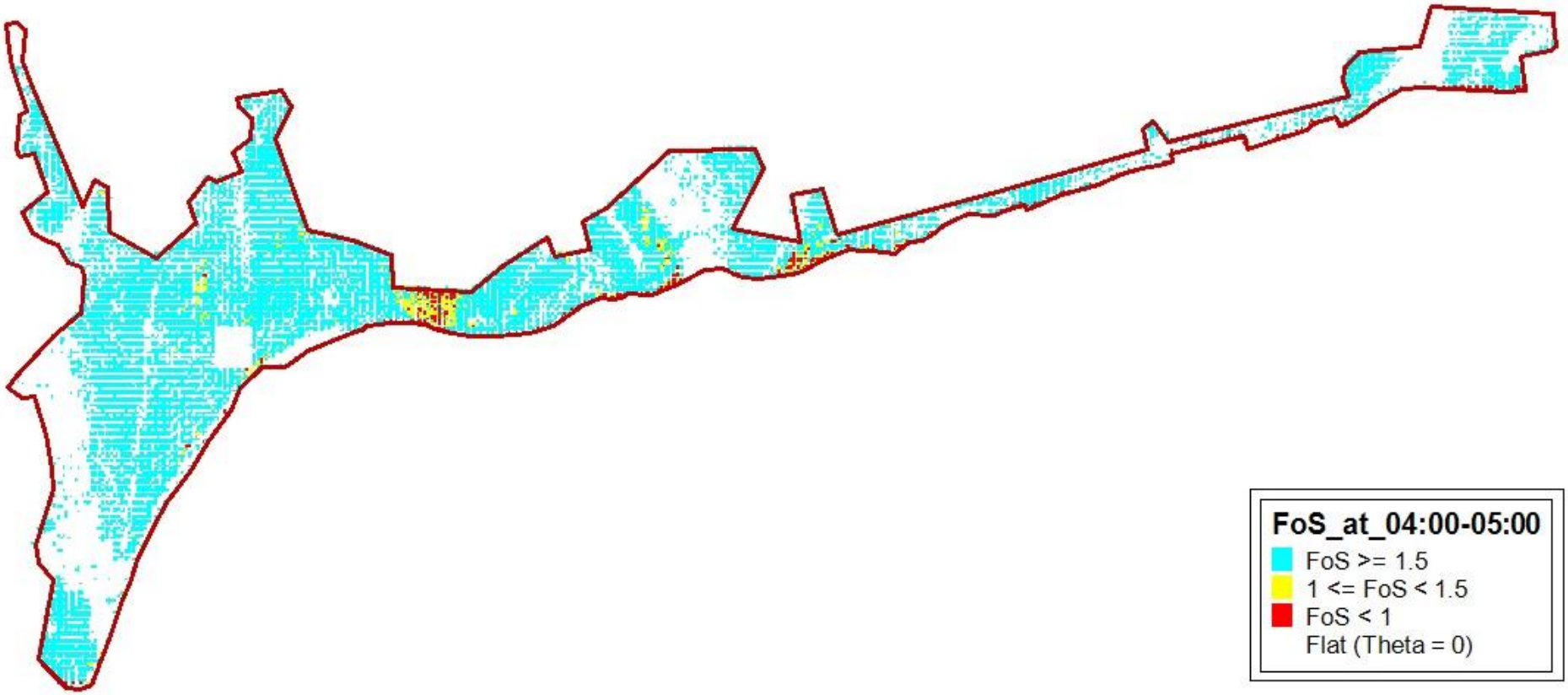

Figure 5.27. Minimum factor of safety values at 04:00 – 05:00.

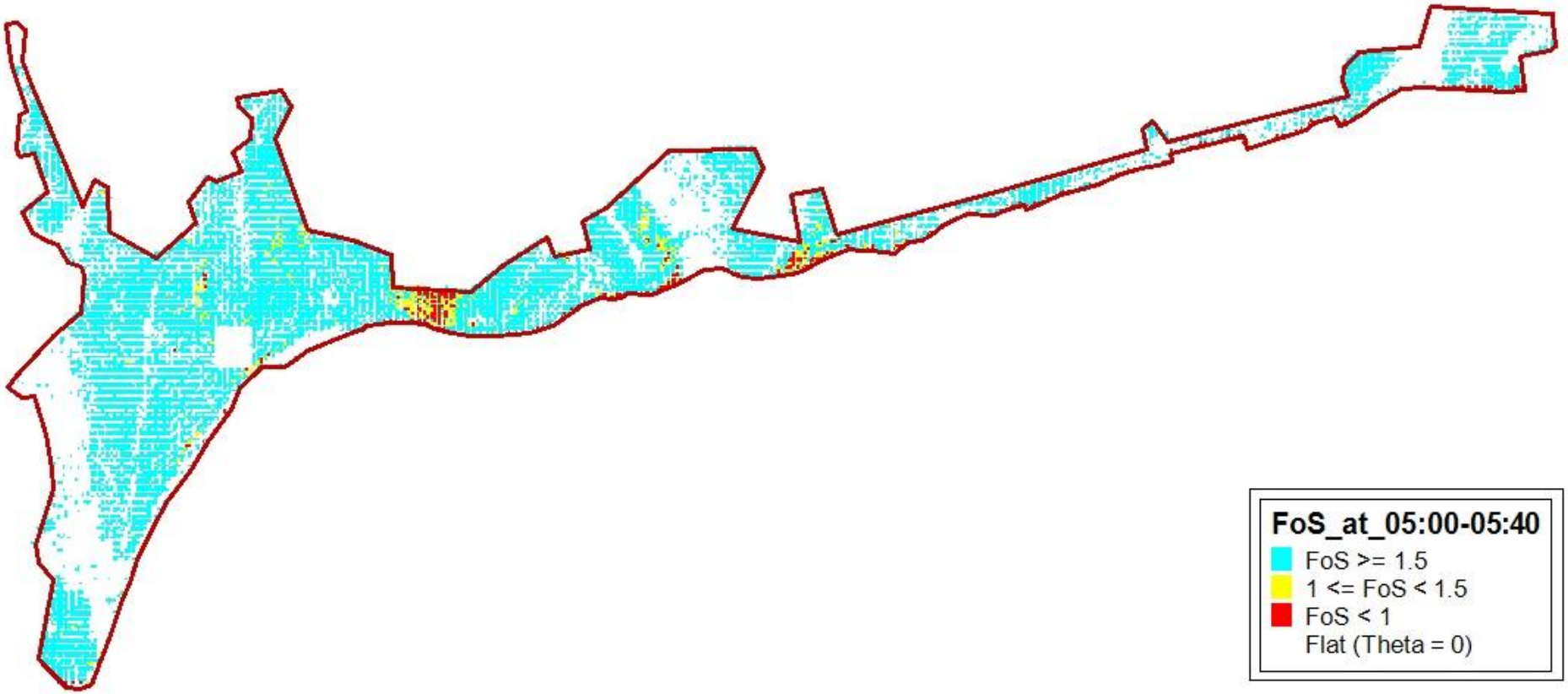

Figure 5.28. Minimum factor of safety values at 05:00 – 05:40.

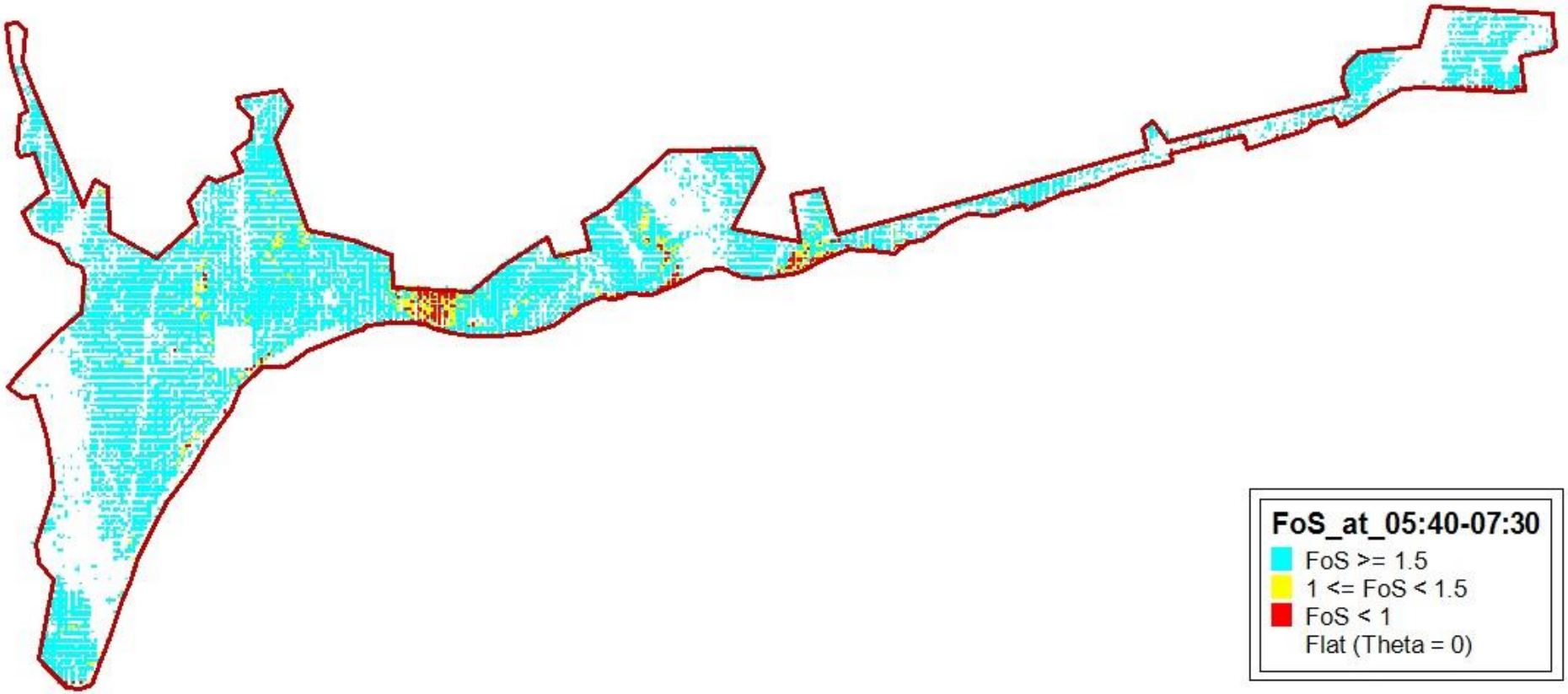

Figure 5.29. Minimum factor of safety values at 05:40 – 07:30.

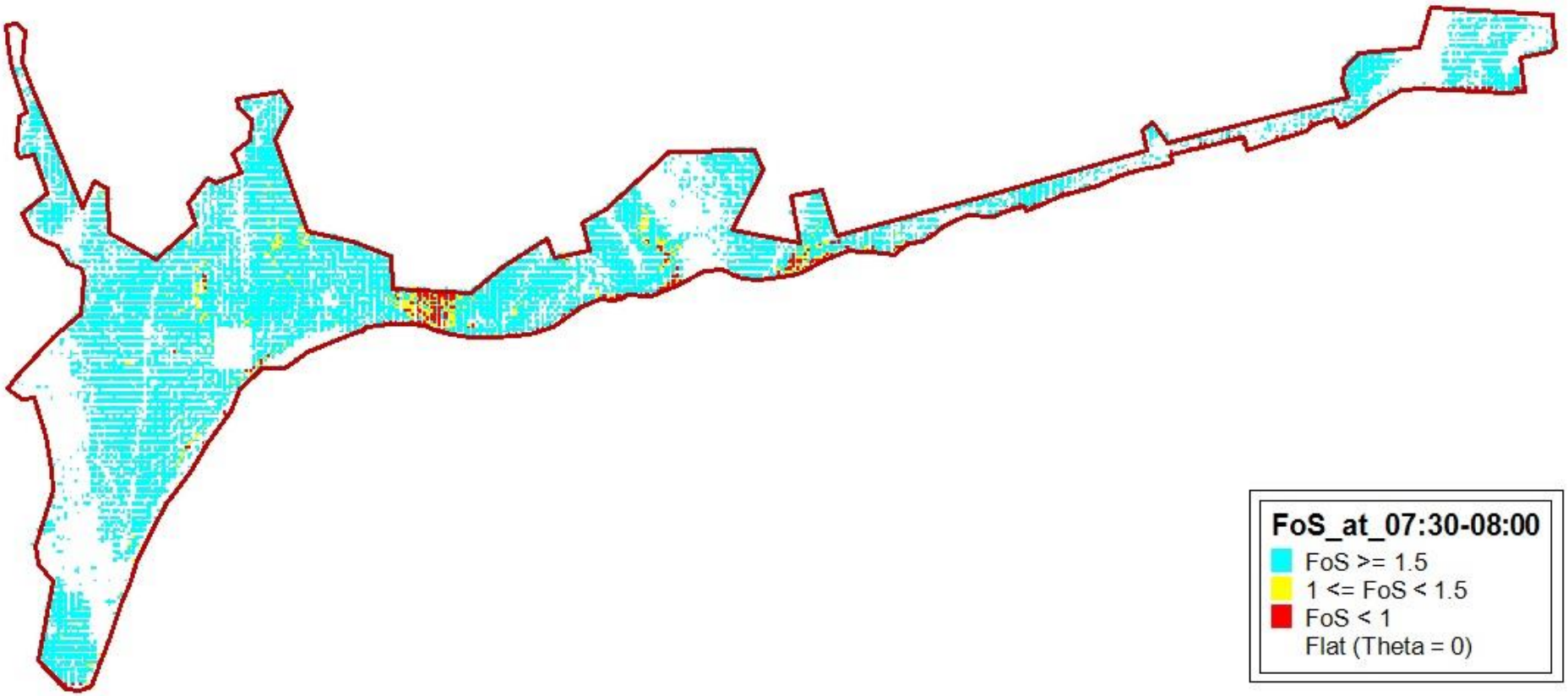

Figure 5.30. Minimum factor of safety values at 07:30 – 08:00.

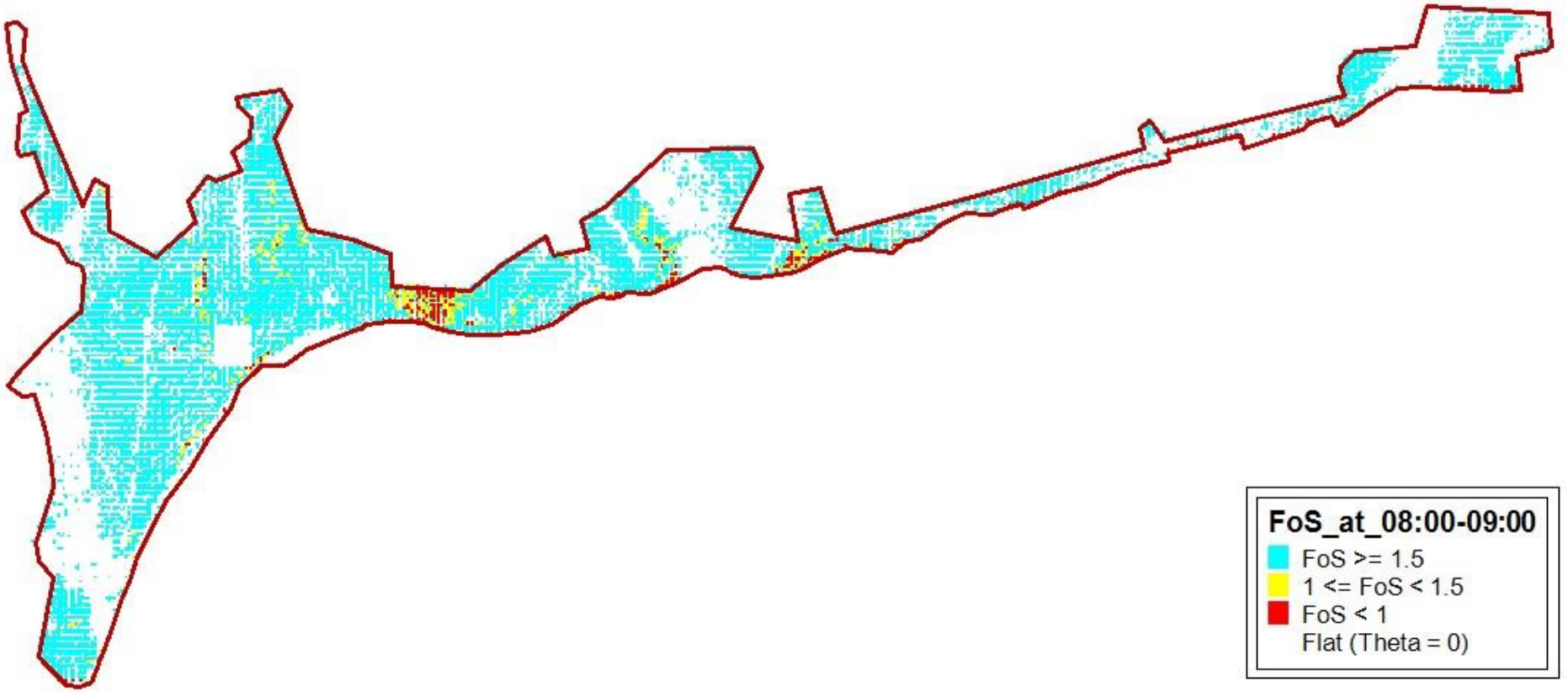

Figure 5.31. Minimum factor of safety values at 08:00 – 09:00.

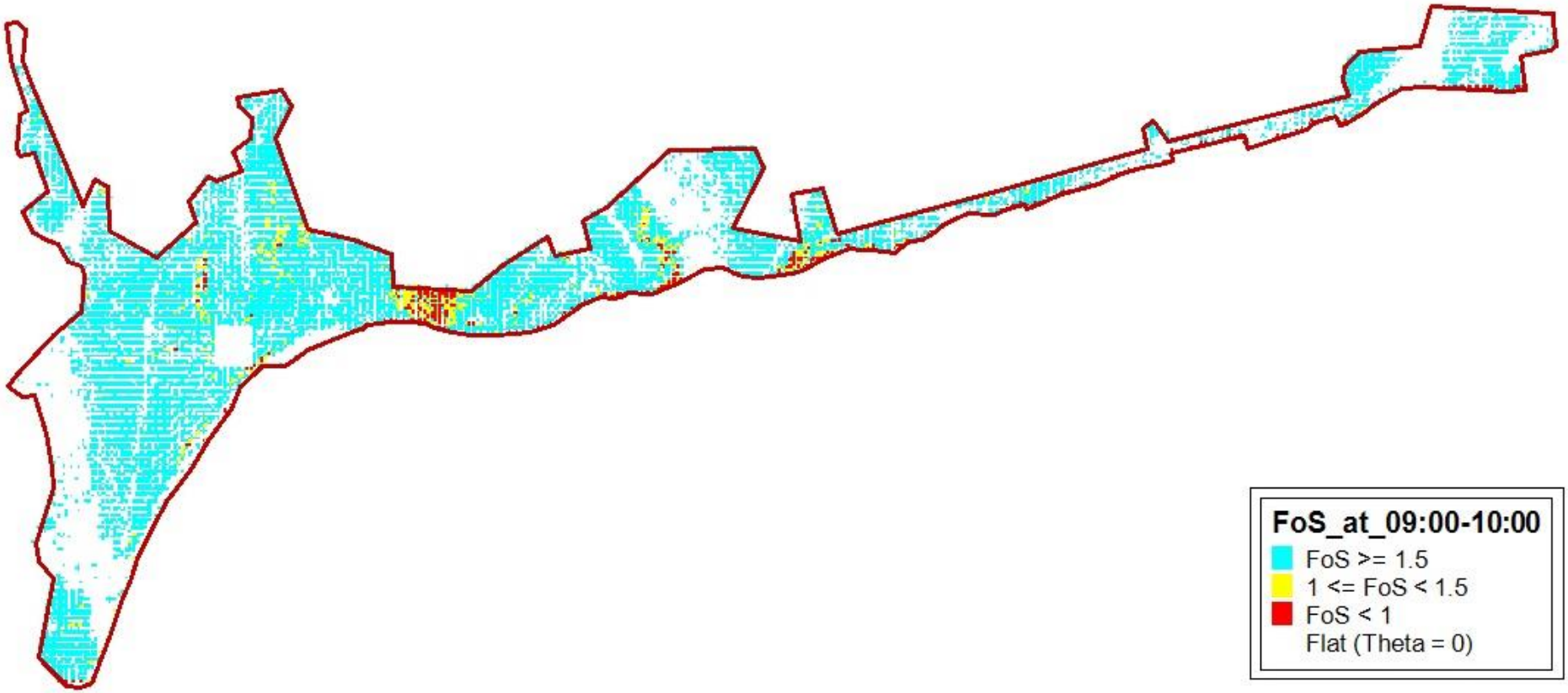

Figure 5.32. Minimum factor of safety values at 09:00 – 10:00.

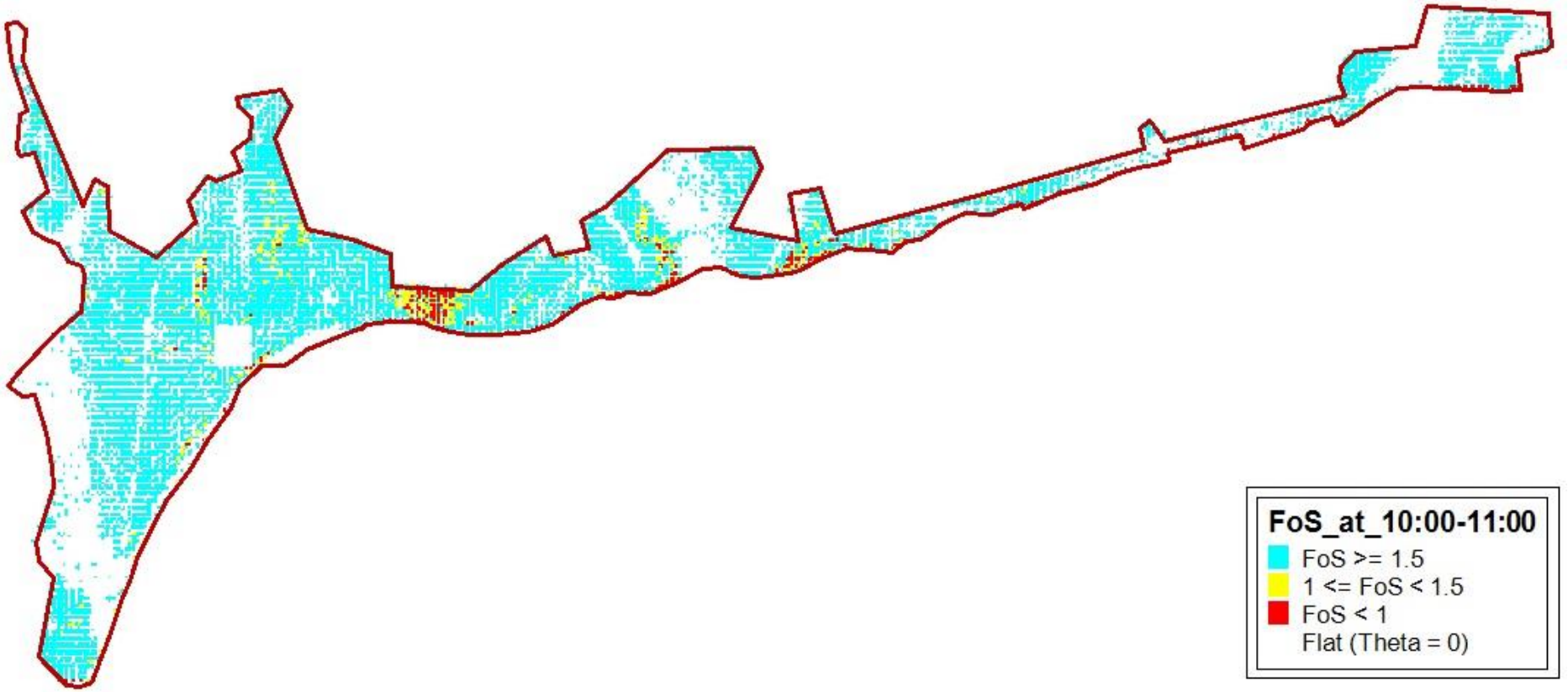

Figure 5.33. Minimum factor of safety values at 10:00 – 11:00.

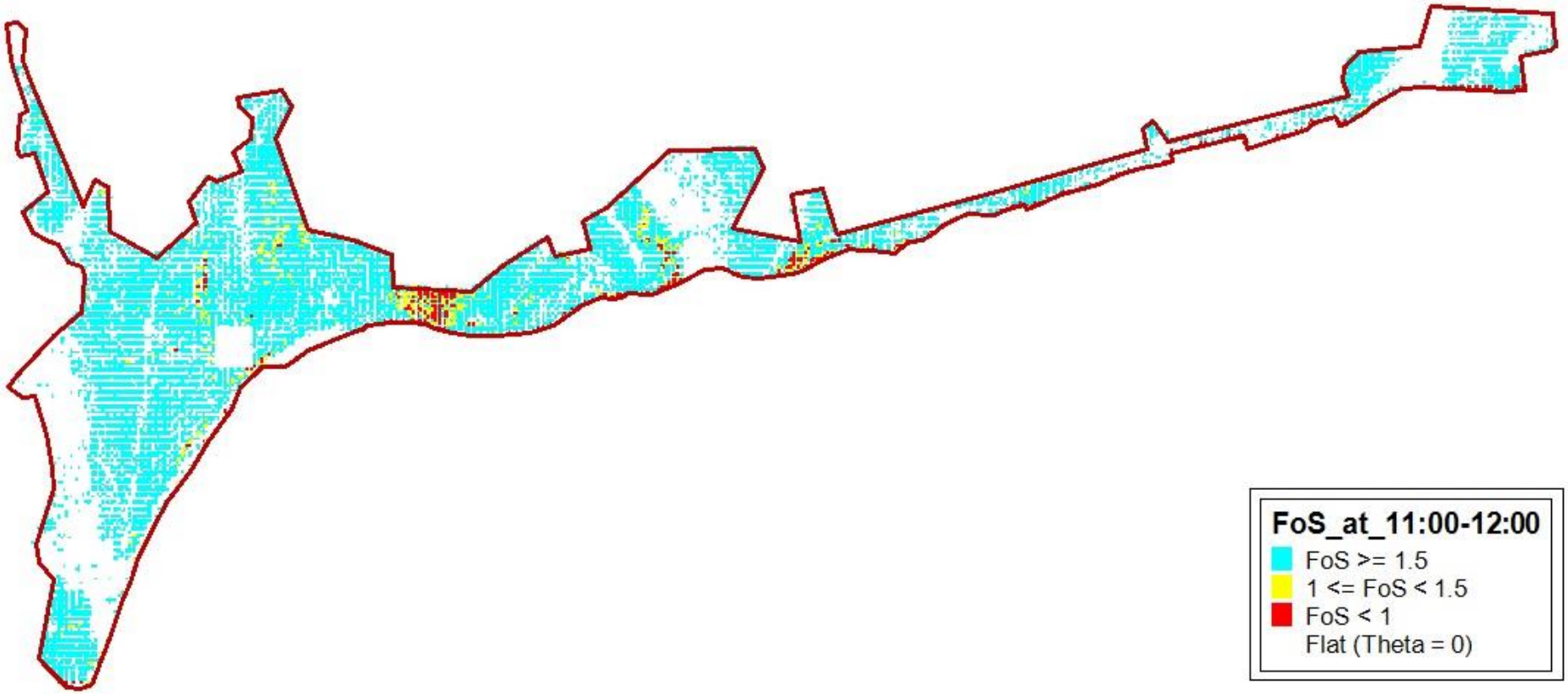

Figure 5.34. Minimum factor of safety values at 11:00 – 12:00.

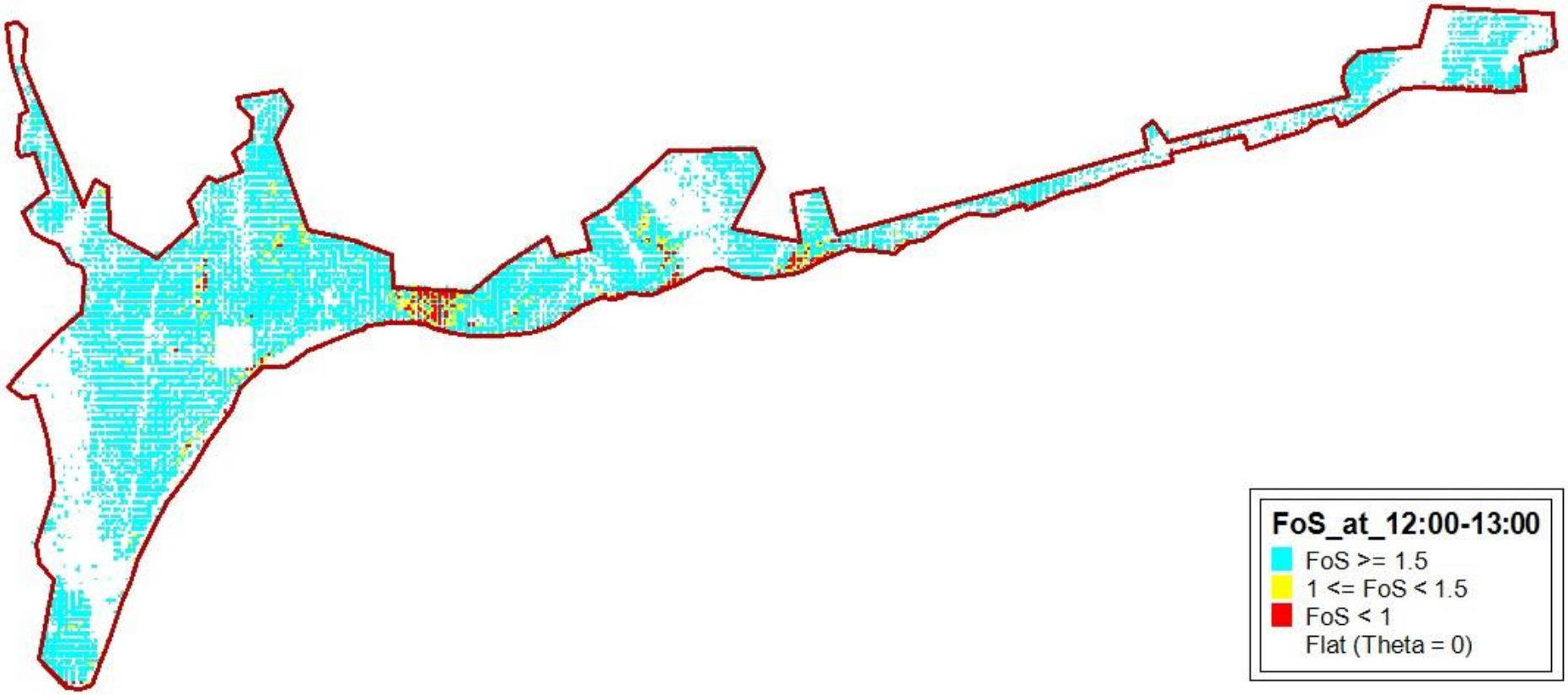

Figure 5.35. Minimum factor of safety values at 12:00 – 13:00.

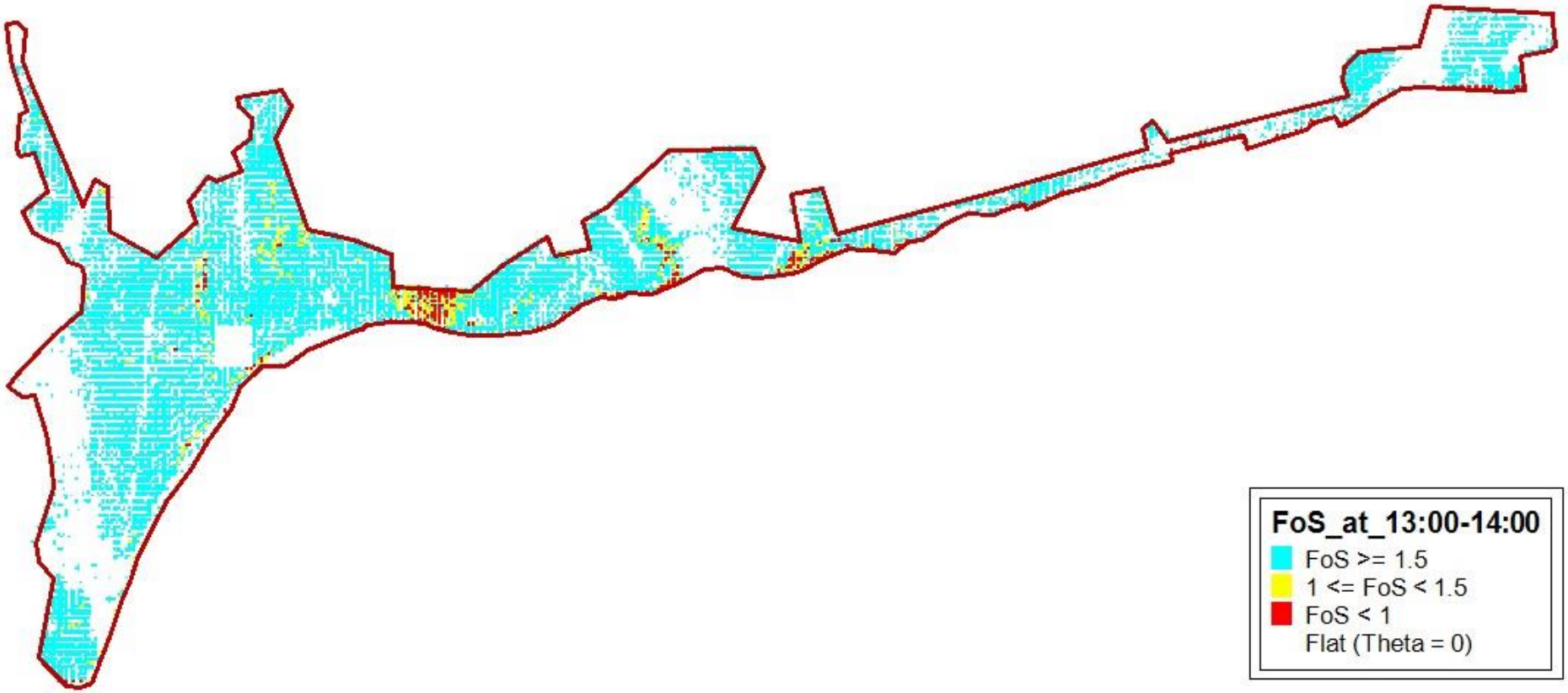

Figure 5.36. Minimum factor of safety values at 13:00 – 14:00.

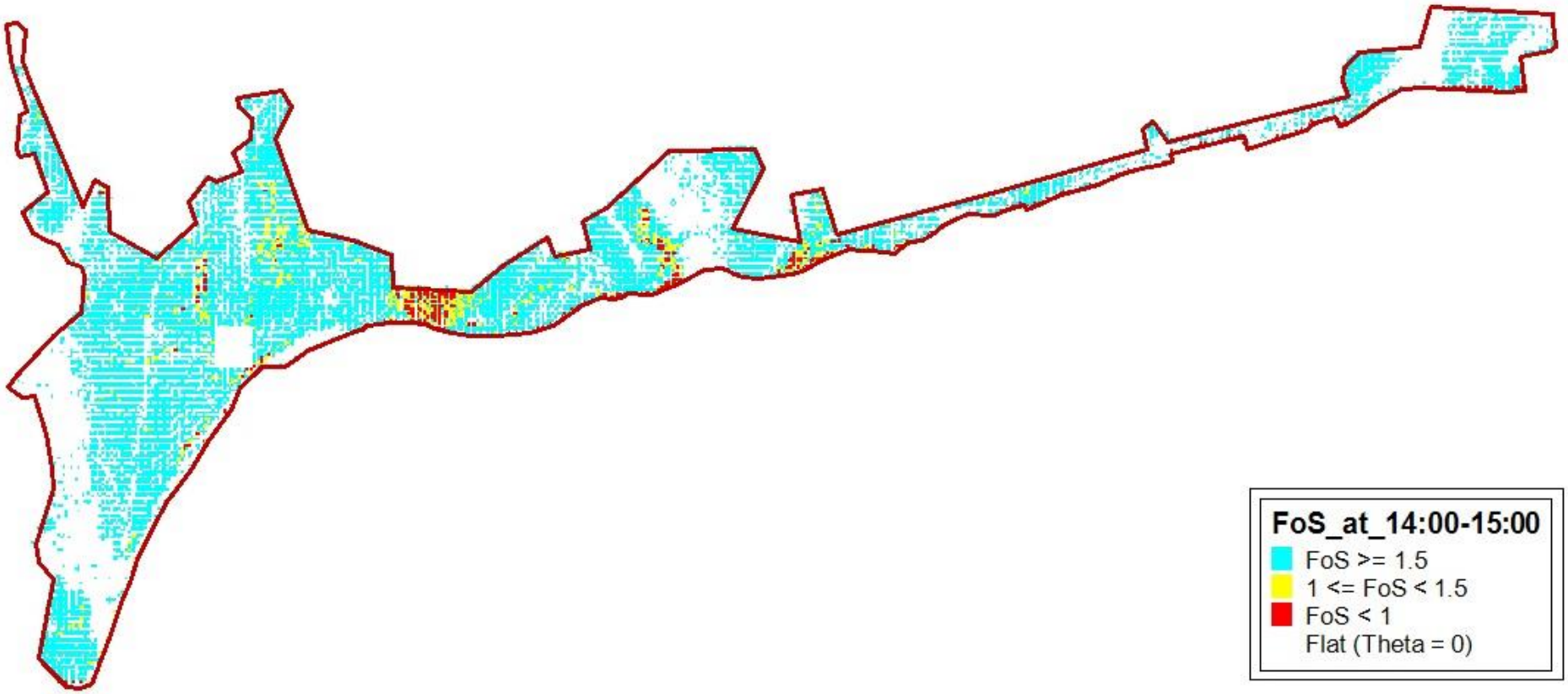

Figure 5.37. Minimum factor of safety values at 14:00 – 15:00.

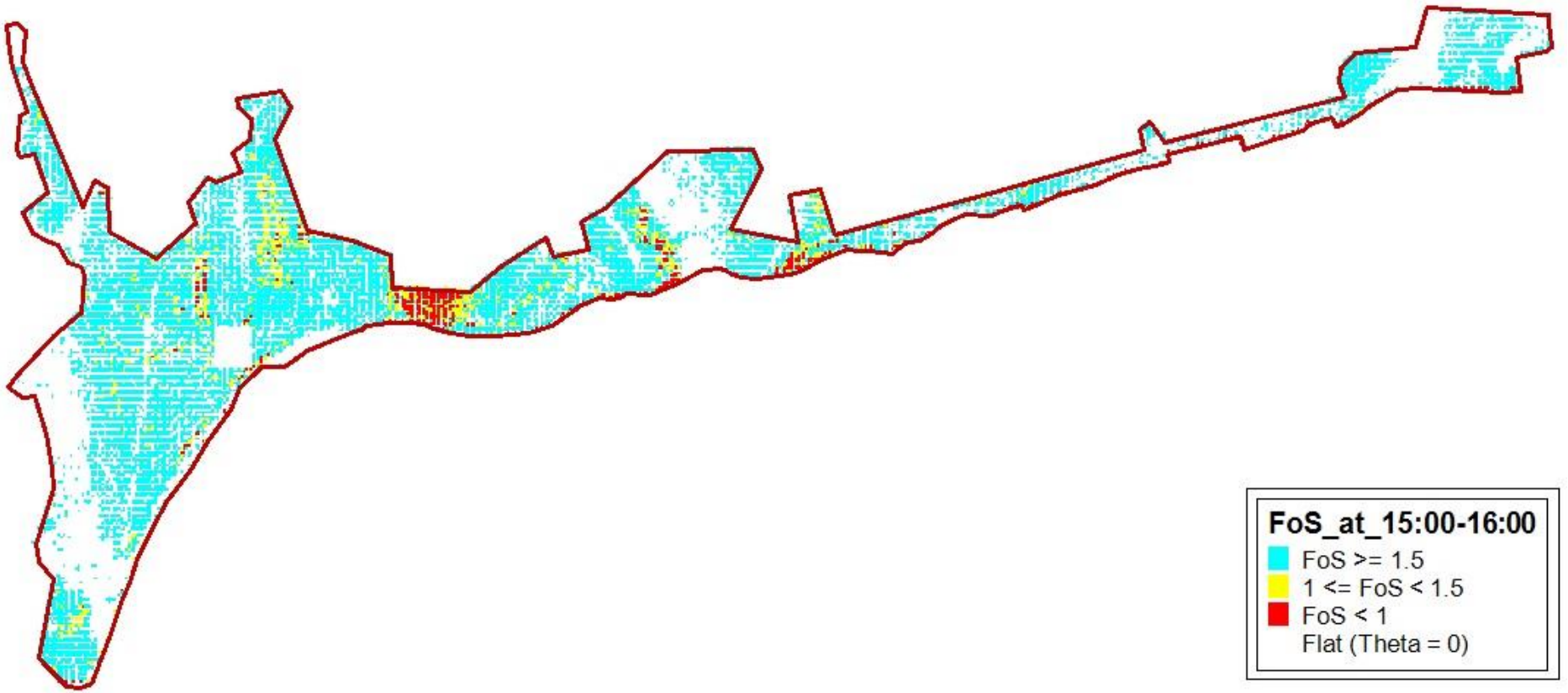

Figure 5.38. Minimum factor of safety values at 15:00 – 16:00.

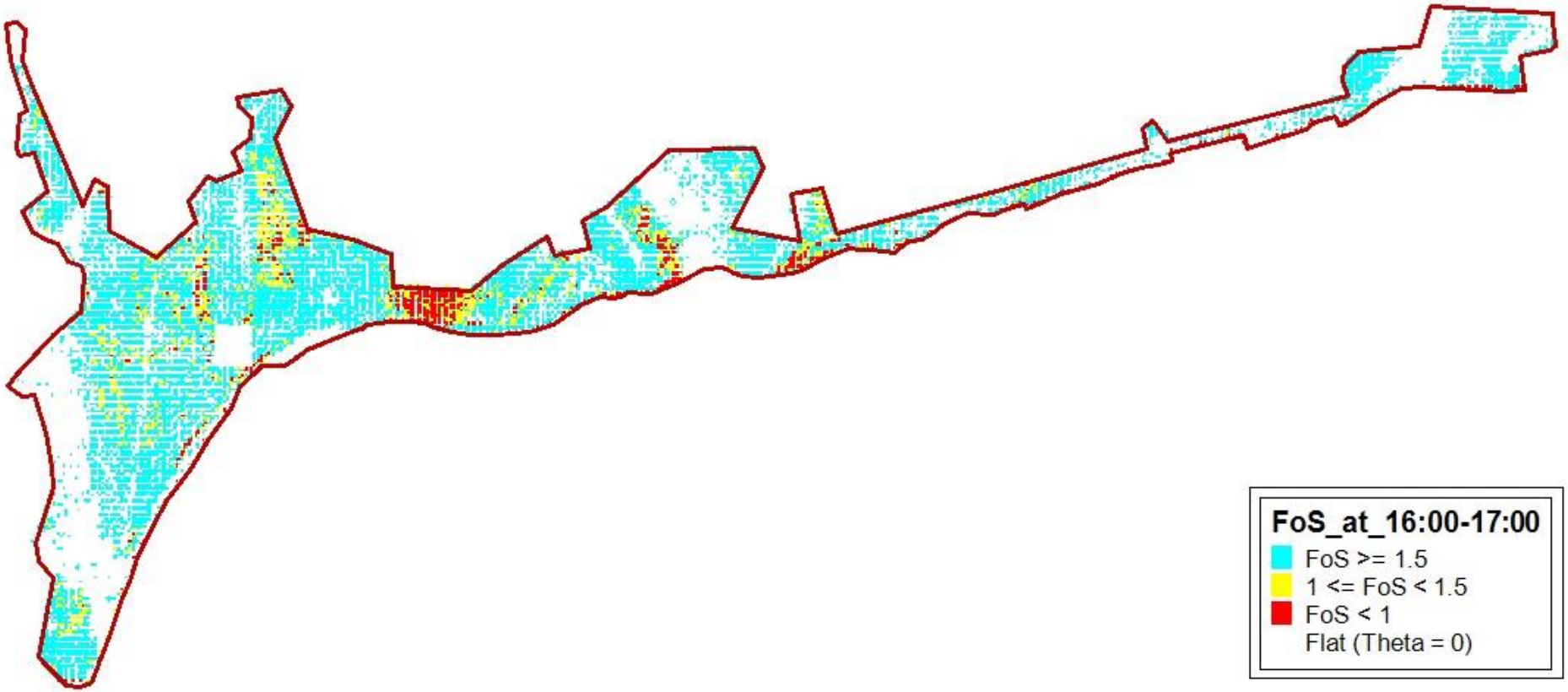

Figure 5.39. Minimum factor of safety values at 16:00 – 17:00.

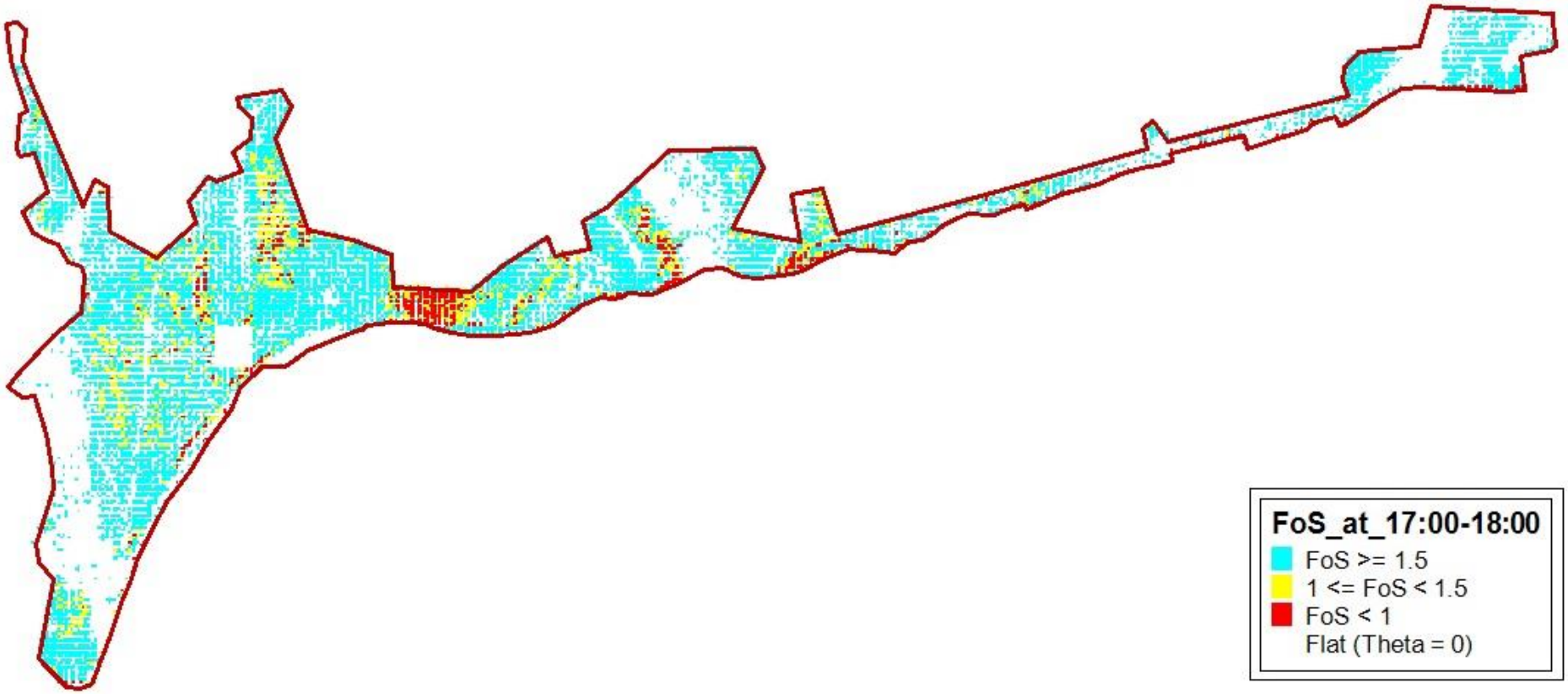

Figure 5.40. Minimum factor of safety values at 17:00 – 18:00.

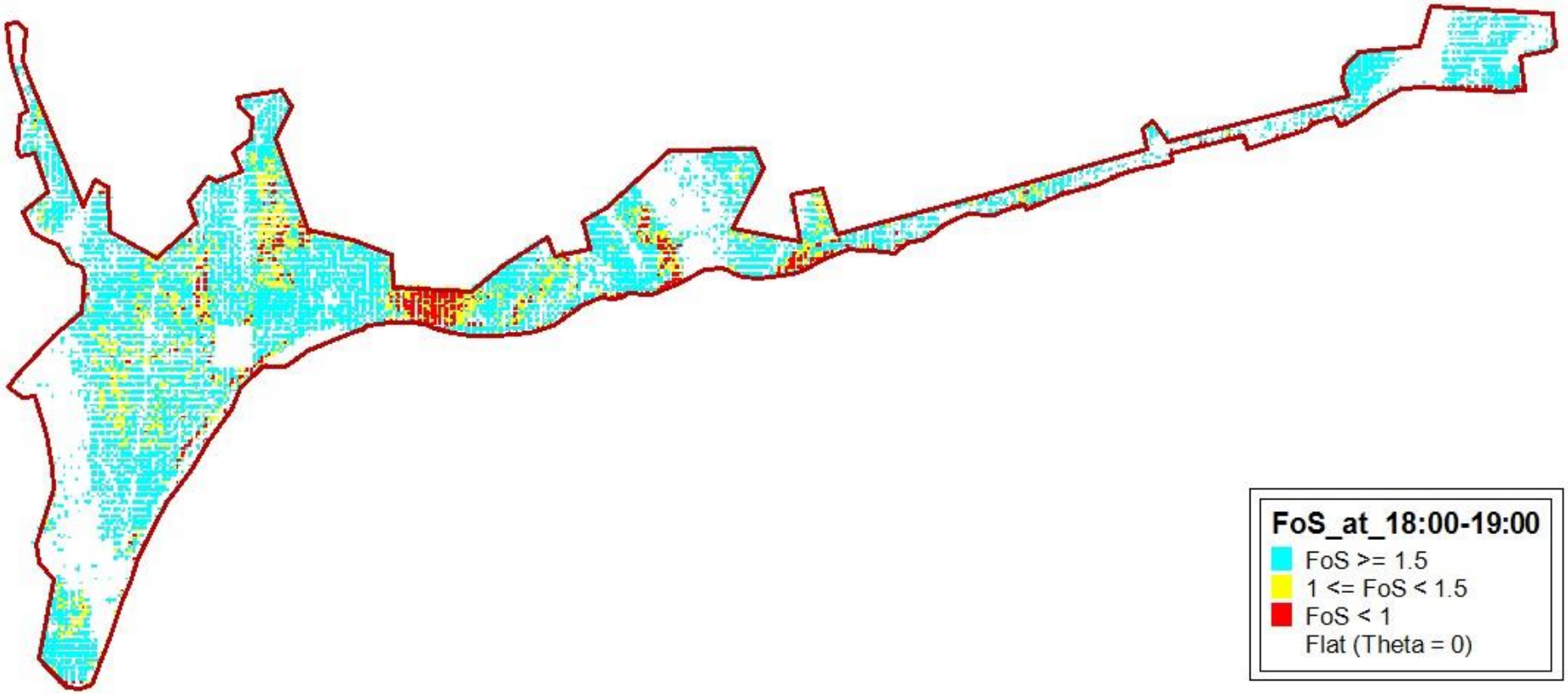

Figure 5.41. Minimum factor of safety values at 18:00 – 19:00.

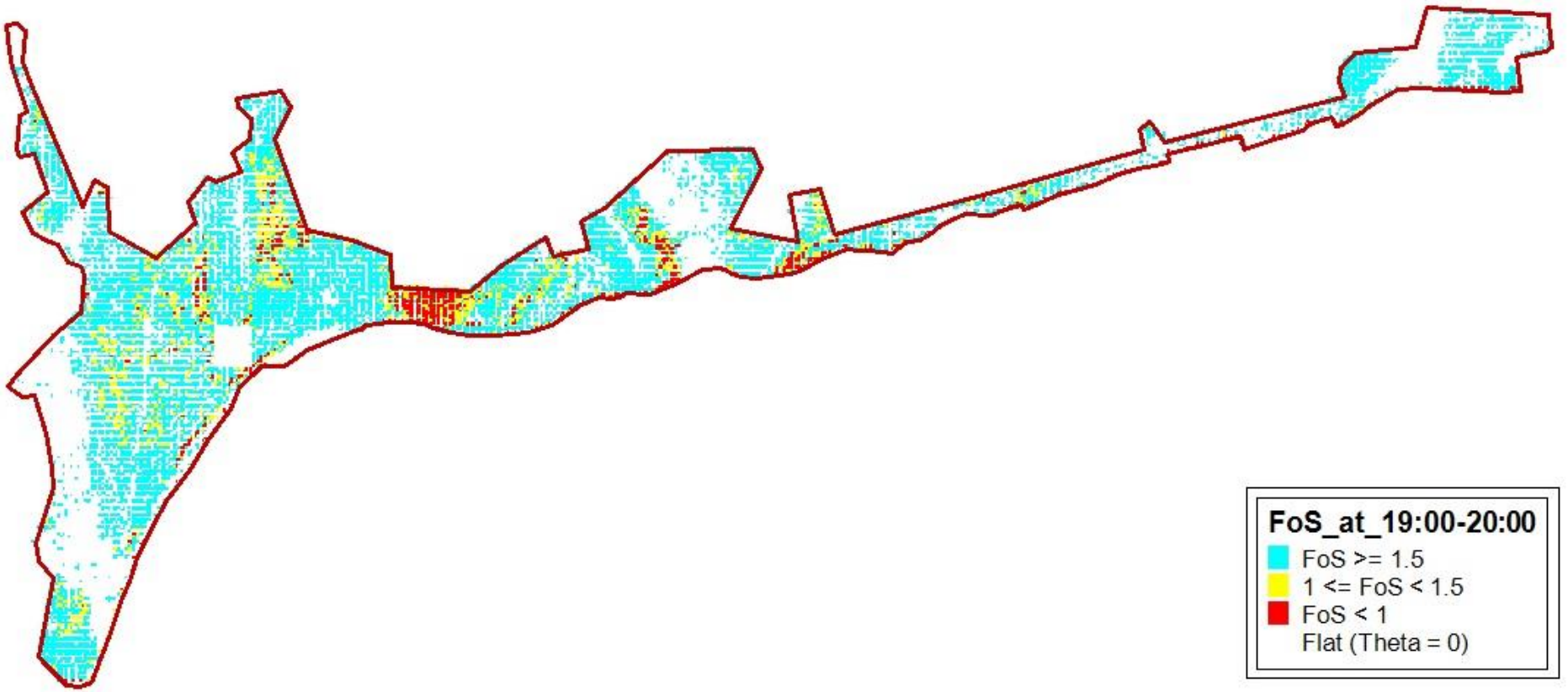

Figure 5.42. Minimum factor of safety values at 19:00 – 20:00.

Figure 5.43. Minimum factor of safety values at 20:00 – 21:00.

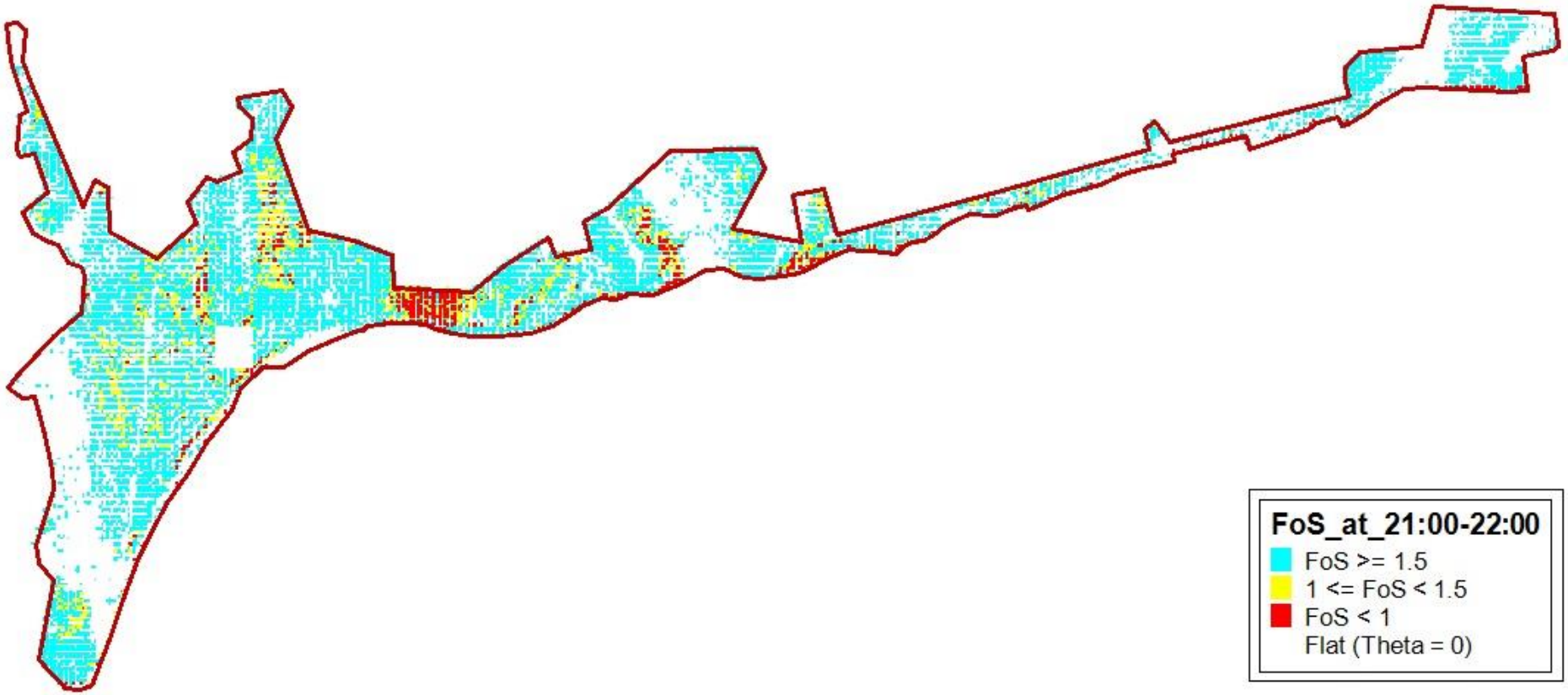

Figure 5.44. Minimum factor of safety values at 21:00 – 22:00.

Figure 5.45. Minimum factor of safety values at 22:00 – 23:00.

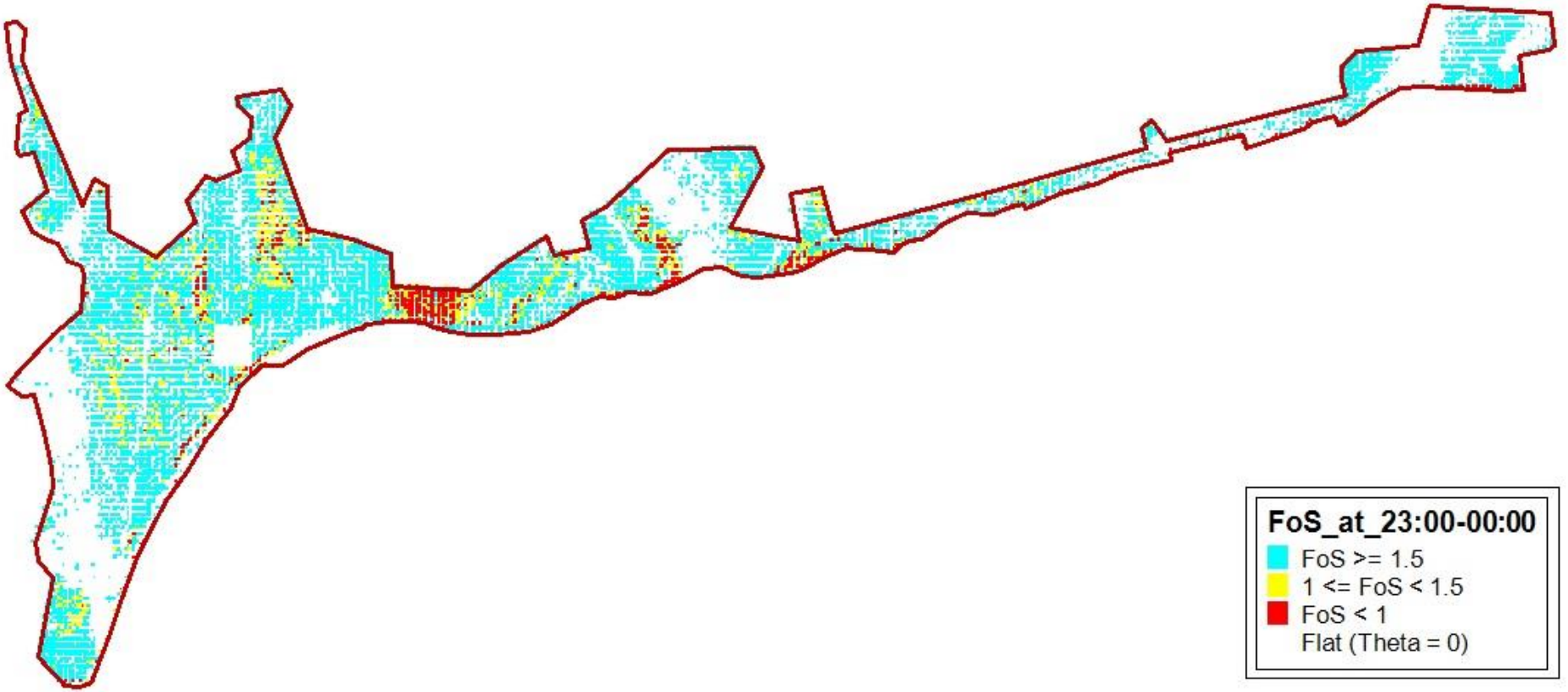

Figure 5.46. Minimum factor of safety values at 23:00 – 00:00.

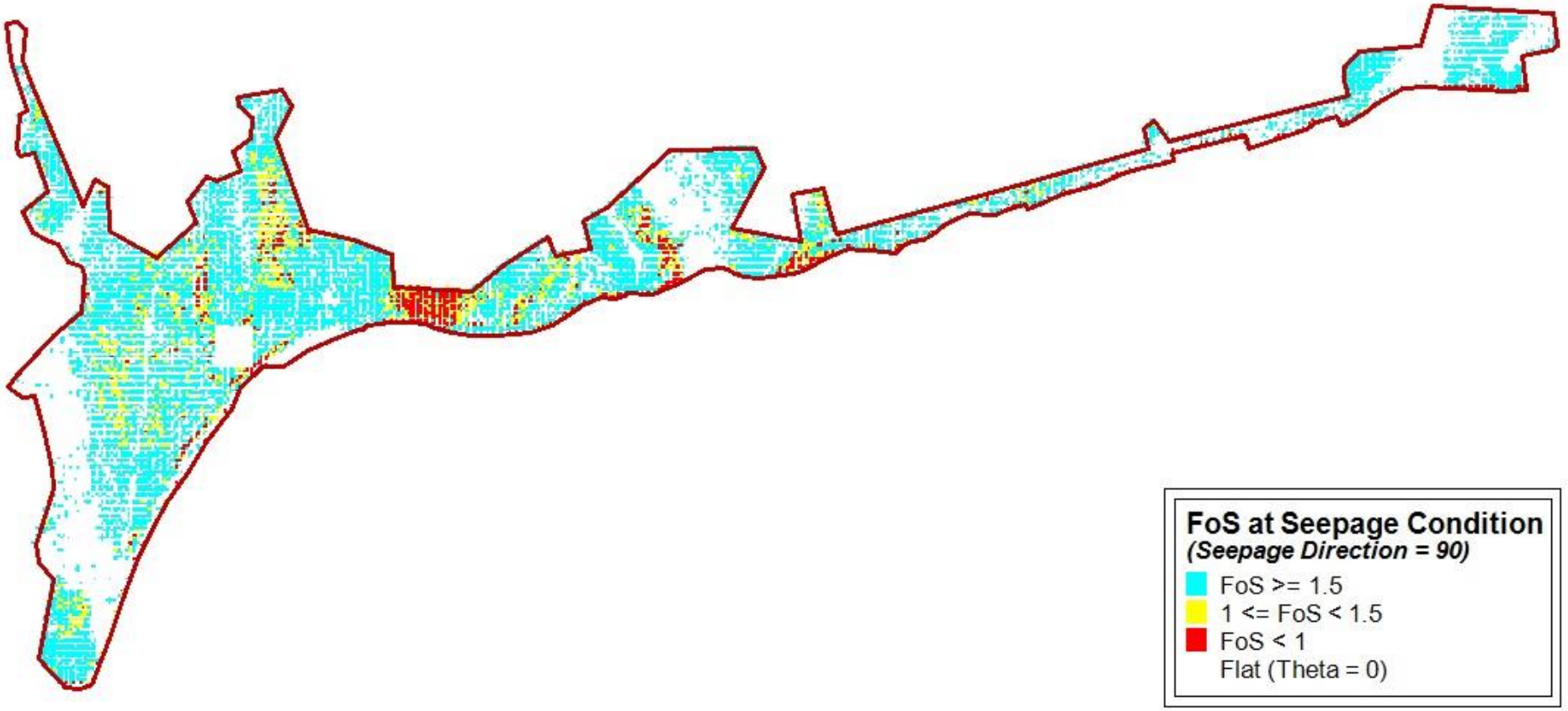

Figure 5.47. Minimum factor of safety values at seepage condition ($\lambda = 90^0$).

Figure 5.48. Groundwater table depth at each cell at the end of computations.

What follows the end of transient, or short – term response, hydrological response of interested site is that accrued groundwater table tends to flow in downslope direction, which is dependent on the analogy elaborated in Seepage Condition of THEORETICAL BACKGROUND OF DEVELOPED METHODOLOGY. Seepage direction is thought to act on soil continuum at an angle of either or 90^0 in order that possible FoS values can be evaluated during the implementation of recommended algorithm (Figure 5.47).

In the first place, Figure 5.22 is able to be interpreted that there exists unstable cells at hydrostatic condition, resulting from the slope angle values exceeding those of prescribed residual shear strength parameters. This might not be the situation in site but computations on transient rainfall effect are proceeded with for the sake of both desire to conclude the process and to stay within the safe side.

Short – term response points out the pore pressure buildup, which can be distinguished by executing the comparison between Figure 5.22 and Figure 5.46, results in the degradation of FoS estimations such an extent that the rise in rainfall amount is accomodated by the anticipated degree of attenuation in FoS. Also it is expected that either the recovery of or no considerable change in FoS is encountered in the time intervals where there is no rainfall and generally denoted as *pore pressure relaxation*.

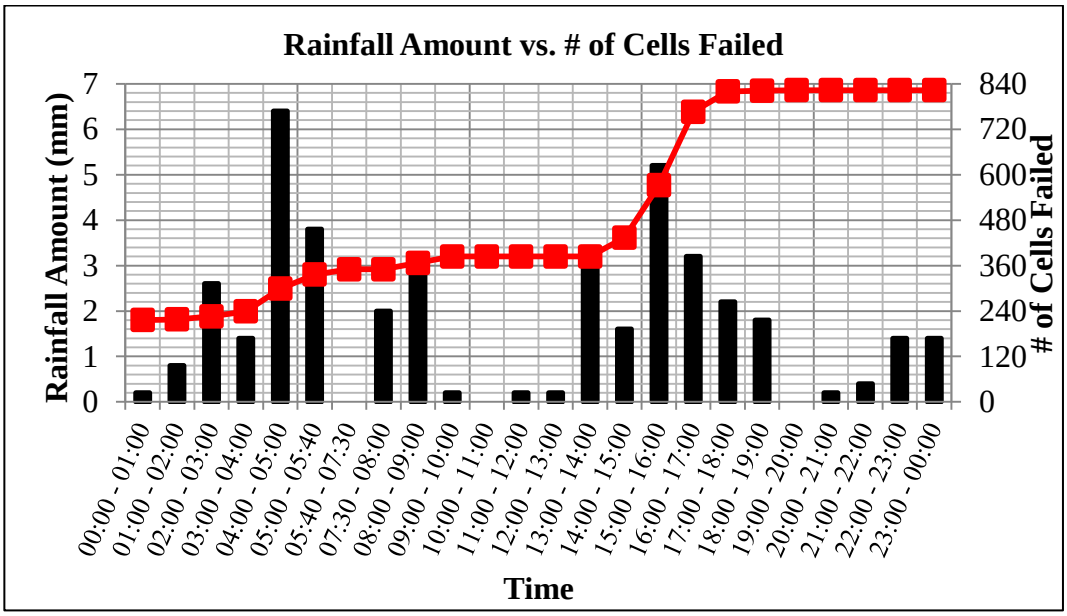

Figure 5.49. # of cells failed for each time interval.

Figure 5.49 is plotted to illustrate the # of cells failed at each corresponding rainfall amount for given time interval. It can be seen that there is no gradual growth in # of cells failed from 00:00 – 01:00 to 13:00 - 14:00 but once the rainfall effects accumulate through time, the boost in number of failure reveals itself at 15:00 – 16:00. The essence of this statement indicates the significant effect of pore pressure build-up on hillslope masses but such an increment cannot be observed in each time interval due to the fact that either slope angle for given soil mass is too low to lead to failure or groundwater level reaches to ground surface (Figure 5.48), which means that there is no possibility for attaining lower FoS values, and both of these conditions may govern the response of interested cells.

As a result, the failure percentage (FP) of % 1.78 (210/11819) at hydrostatic condition (defined as the ratio of the number of cells included within FoS < 1 range to the total number of cells) grows to that of % 6.96 (823/11819) at 23:00 – 00:00 but it is concluded in the FP of % 7.07 (836/11819) due to the excitation of seepage drag at angle of 90^0. What is faced with after the seepage calculation is that $\lambda = 90^0$ imposes no significant influences on hillslope mass stability.

5.5. The Results of Mora and Vahrson (1994) Methodology

As a last stage of rainfall – instigated landslide evluation of Tekirdağ City Center, Mora and Vahrson (1994) algorithm be adopted with the hope that the aforementioned analysis can be justified. This intent stems from the fact that Mora and Vahrson (1991) is designated to produce hazard index, which indicates the tendency of interested hillslope to collapse and both rainfall and earthquake triggering factors co – exist in hazard assessment Thus, its qualitative characteristics enable researchers to weigh up their computations in order to come up with credible and reliable results.

The first step in Mora and Vahrson (1994) Methodology is to determine the relative relief value within each 1 km^2 area of interested site, which is defined as "*difference between summit level, the highest altitude for a given area, and base level, lowest altitude for a given area*". To that end, the contour lines (Figure 5.50) are converted into elevation points (Figure 5.51) so that the difference between max and min elevations is able to be

computed for each 500X500 m cell. Then, these values are divided by the distance between the max and min points to obtain the most steepest slope in considered cell. The Relative Relief (RR) intervals are concordantly adjusted by using such a logic that RR ranges in Table 5.12 are divided by 1000 m to attain S_r with the help of comparison between maximum degree of slope and related RR boundaries (Figure 5.52 and Table 5.12).

Table 5.12. Converted Relative Relief.

Relative Relief	**Susceptibility**	**Parameter, S_r**
0 – 0.075m/km^2	Very Low	0
0.076 – 0.175	Low	1
0.176 – 0.3	Moderate	2
0.301 – 0.5	Medium	3
0.501 – 0.8	High	4
> 0.8	Very High	5

After that, the parameter, S_h, is proposed as 1 due to the fact that the average monthly precipitation for measurements extracted from 2007 to 2014 is declared as 40 mm. Also, the S_l value is obtained through the geology exposing itself in site (Figure 5.53 and Figure 5.54). The respective S_l values for given geological structures is presented in Table 5.13.

Table 5.13. S_l values for each geological structure.

Geological Structure	**S_l**
Danişmen Formation – Clay (DFC)	3
Danişmen Formation – Sand (DFS)	3
Man – Made Fill (MMF)	3
Ergene Formation (EF)	4
Trakya Formation (TF)	4
Quaternary Alluvium (QA)	5

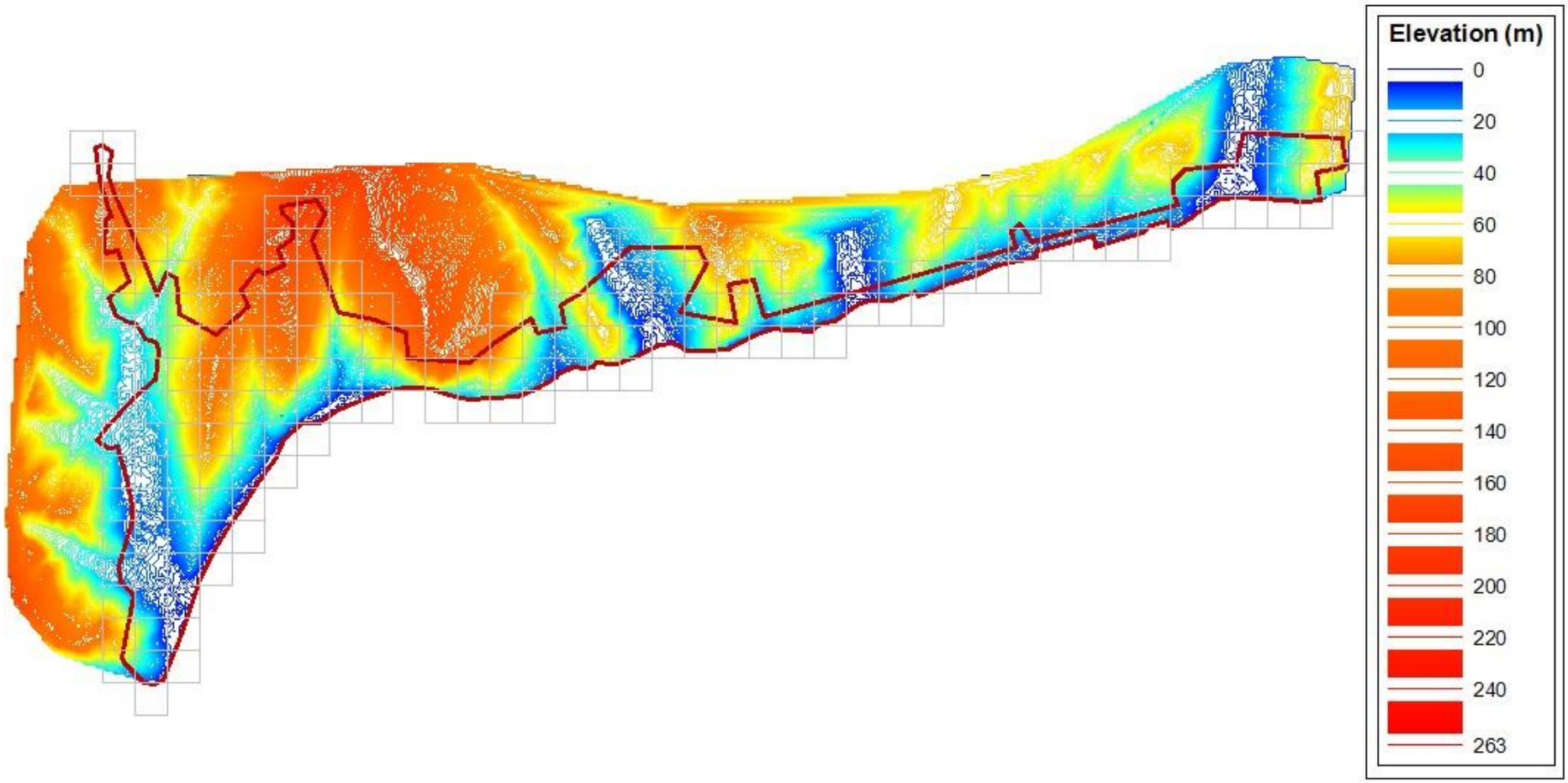

Figure 5.50. Contour map of Tekirdağ City Center.

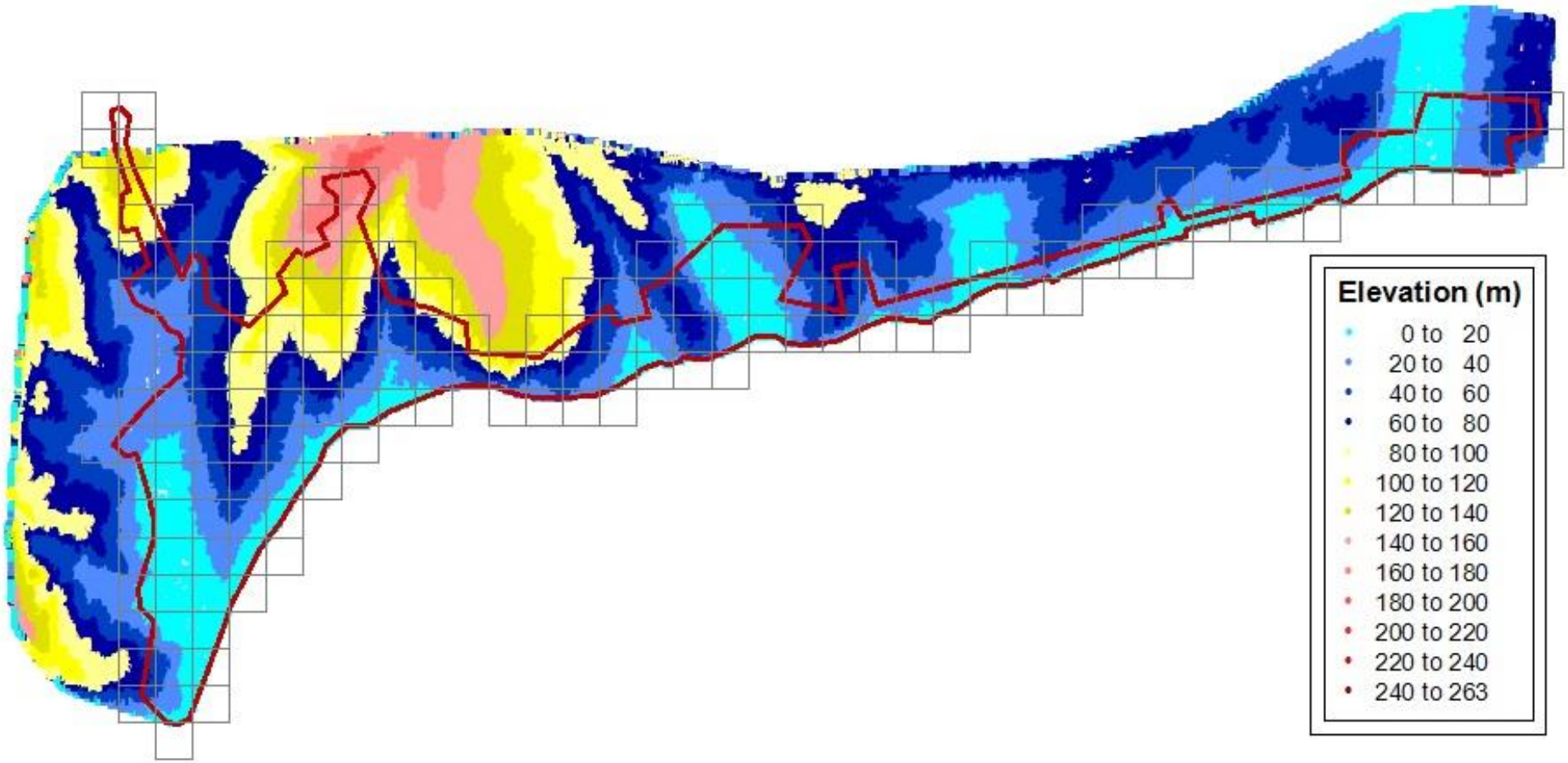

Figure 5.51. Converted contour map of Tekirdağ City Center.

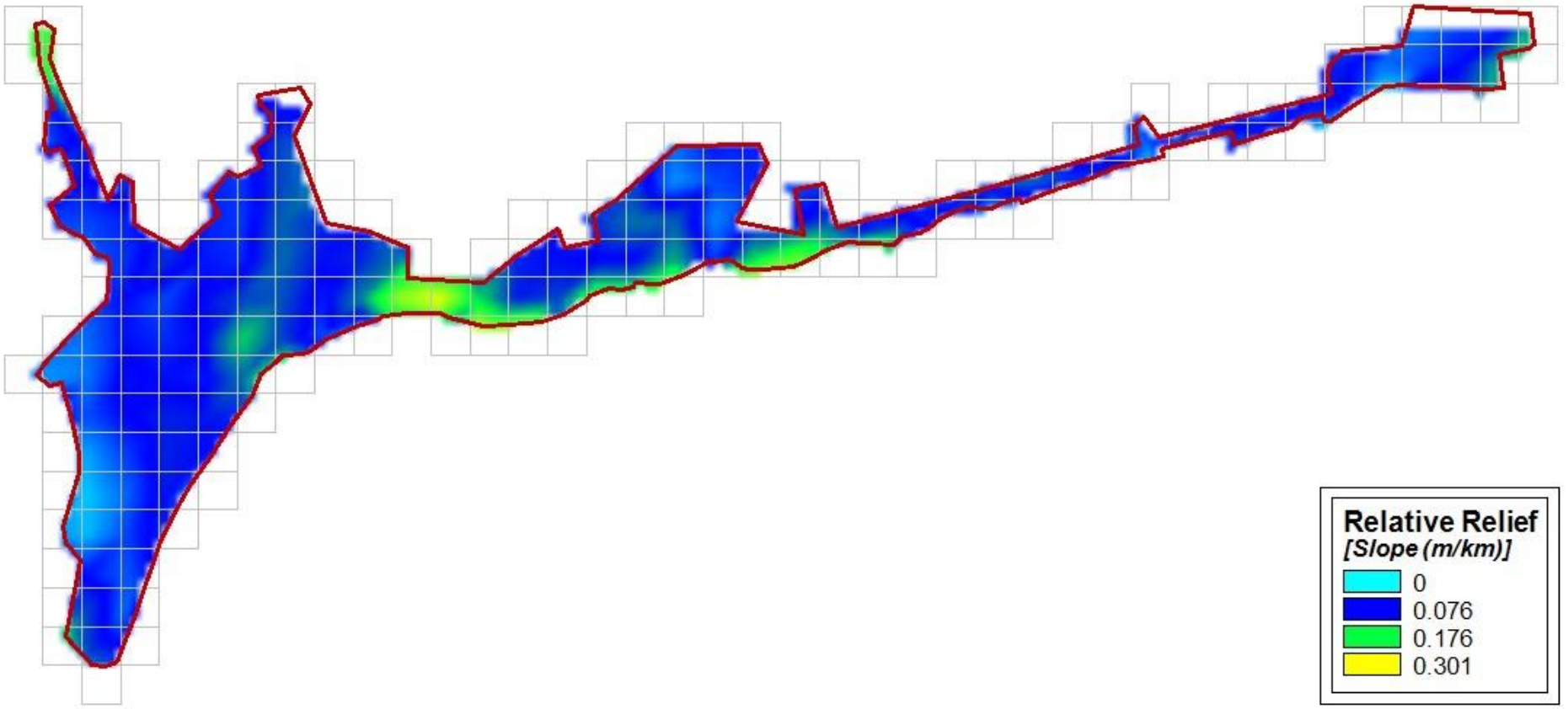

Figure 5.52. Converted Relative Relief.

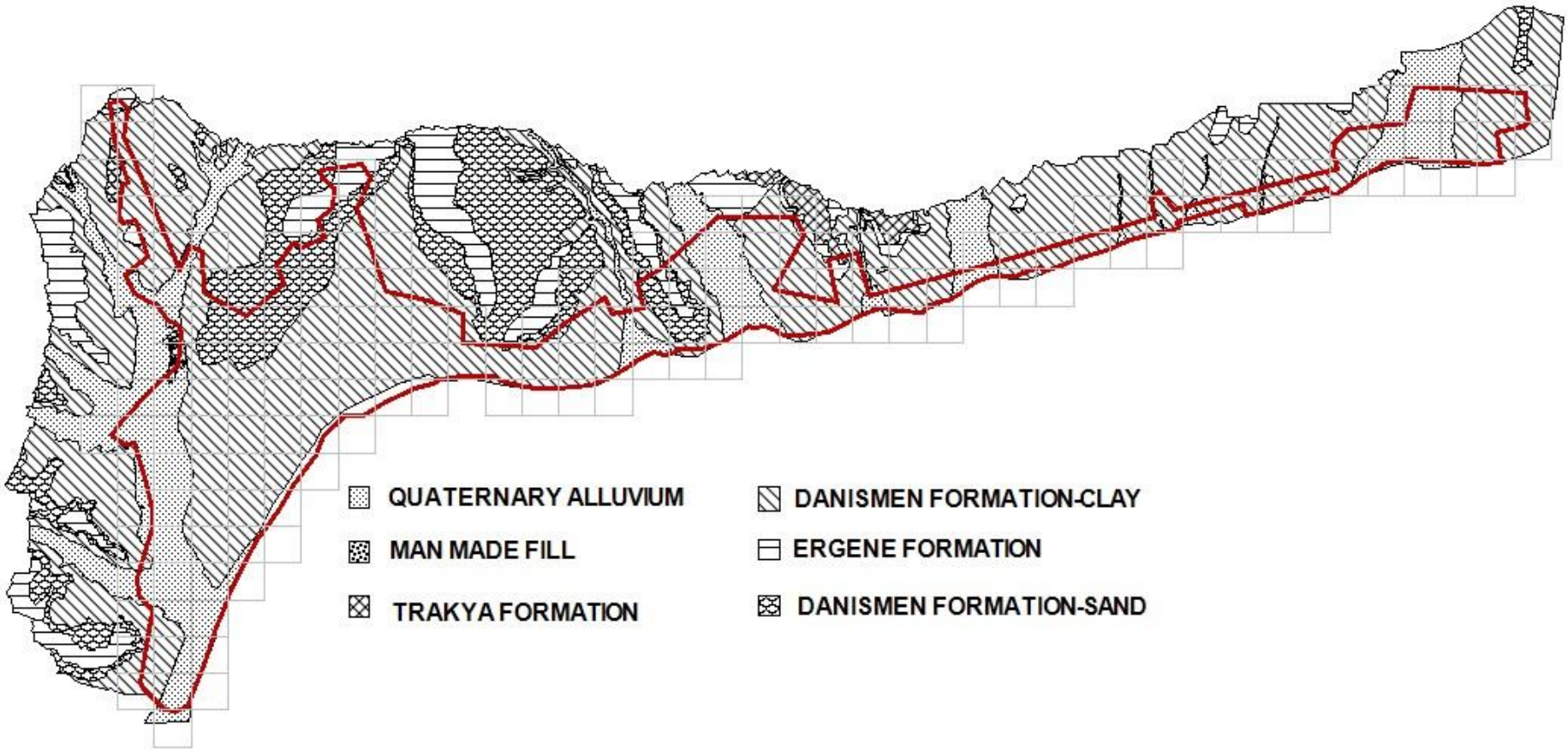

Figure 5.53. Geology of Tekirdağ Region.

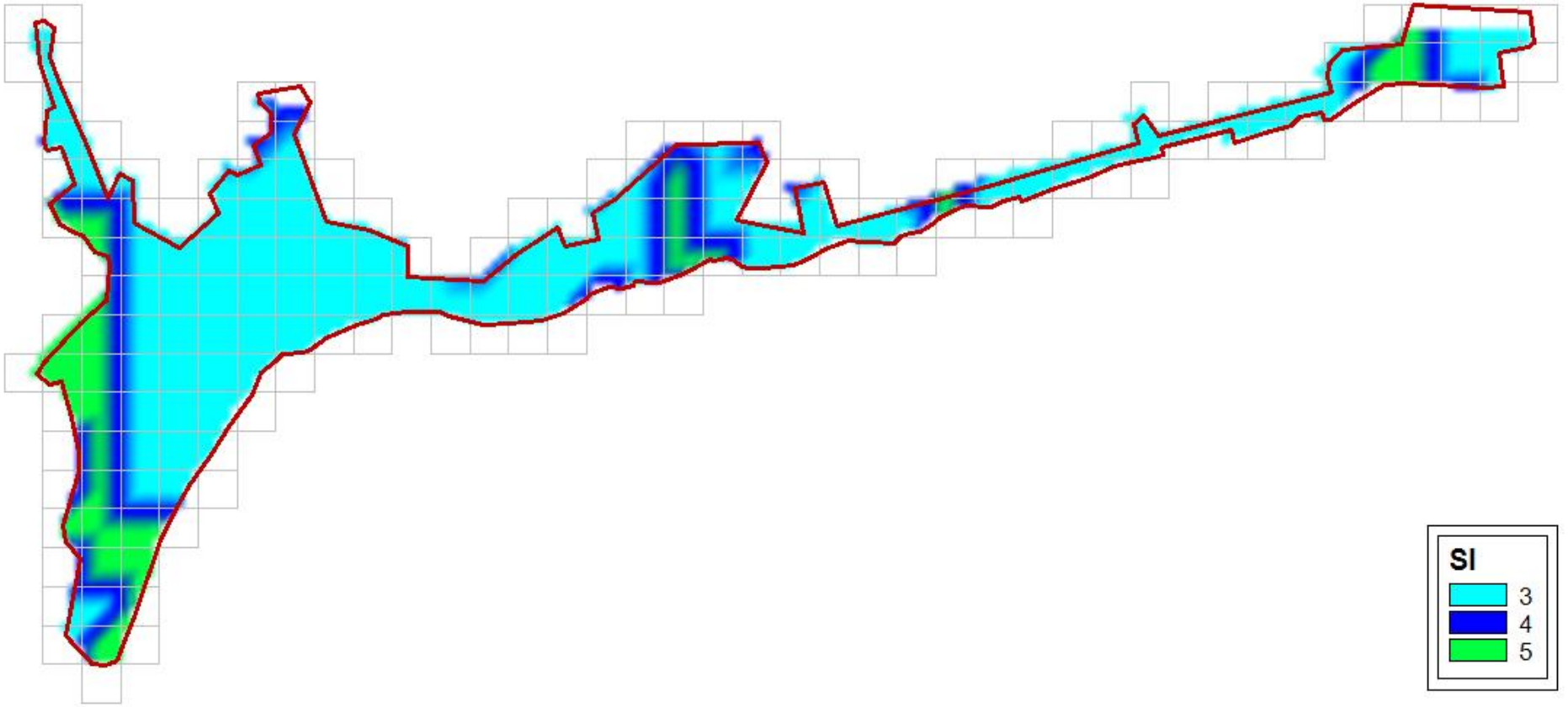

Figure 5.54. S_I values.

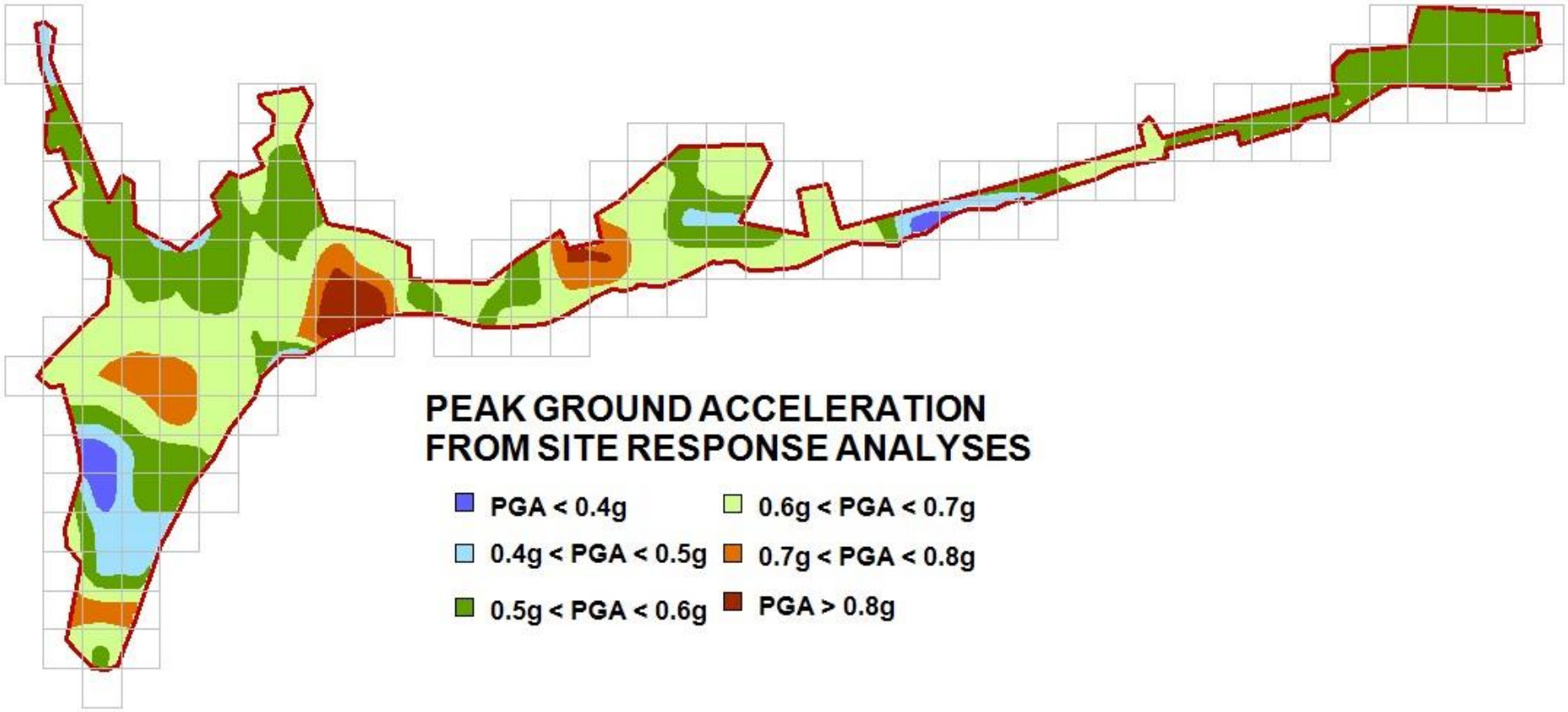

Figure 5.55. Peak ground acceleration from site response analyses for Tekirdağ Region.

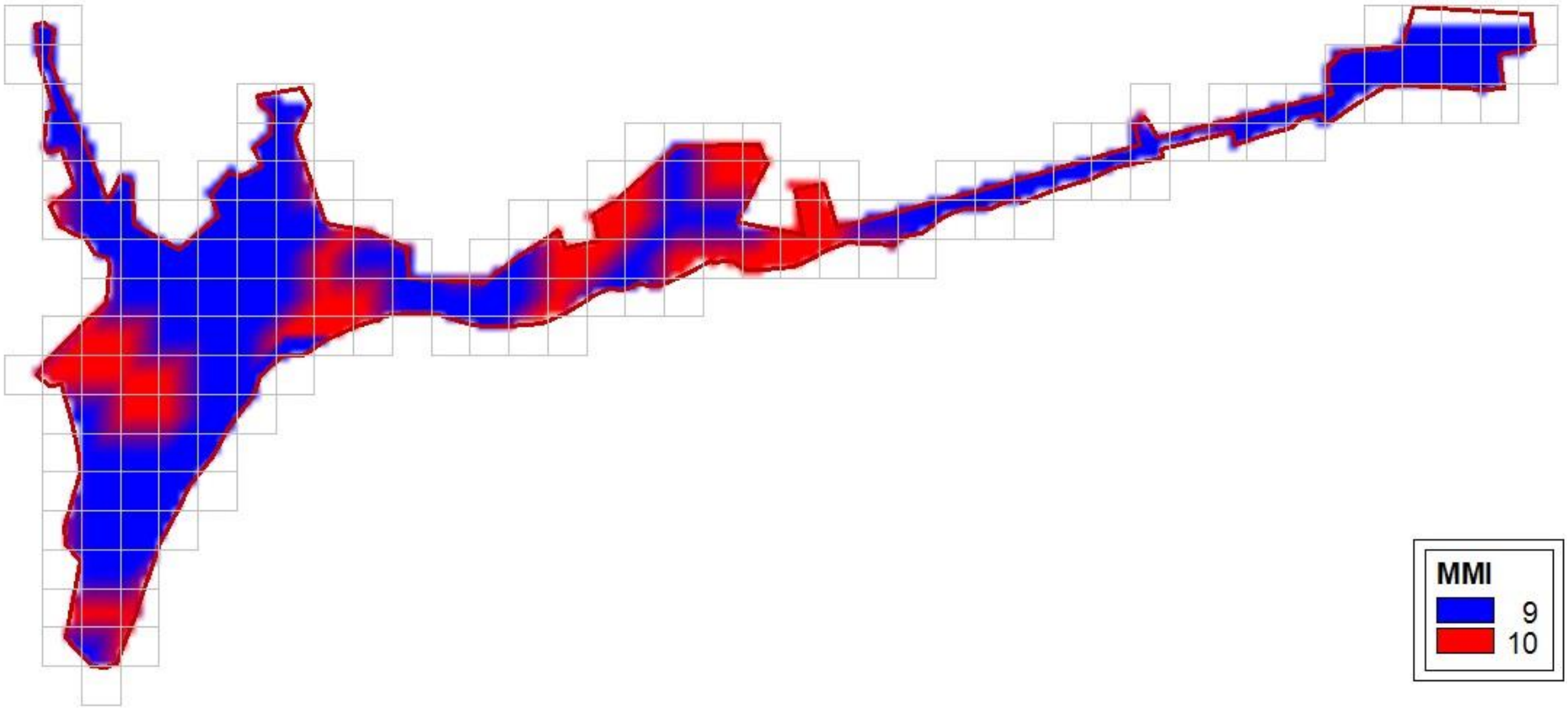

Figure 5.56. MMI for Tekirdağ Region.

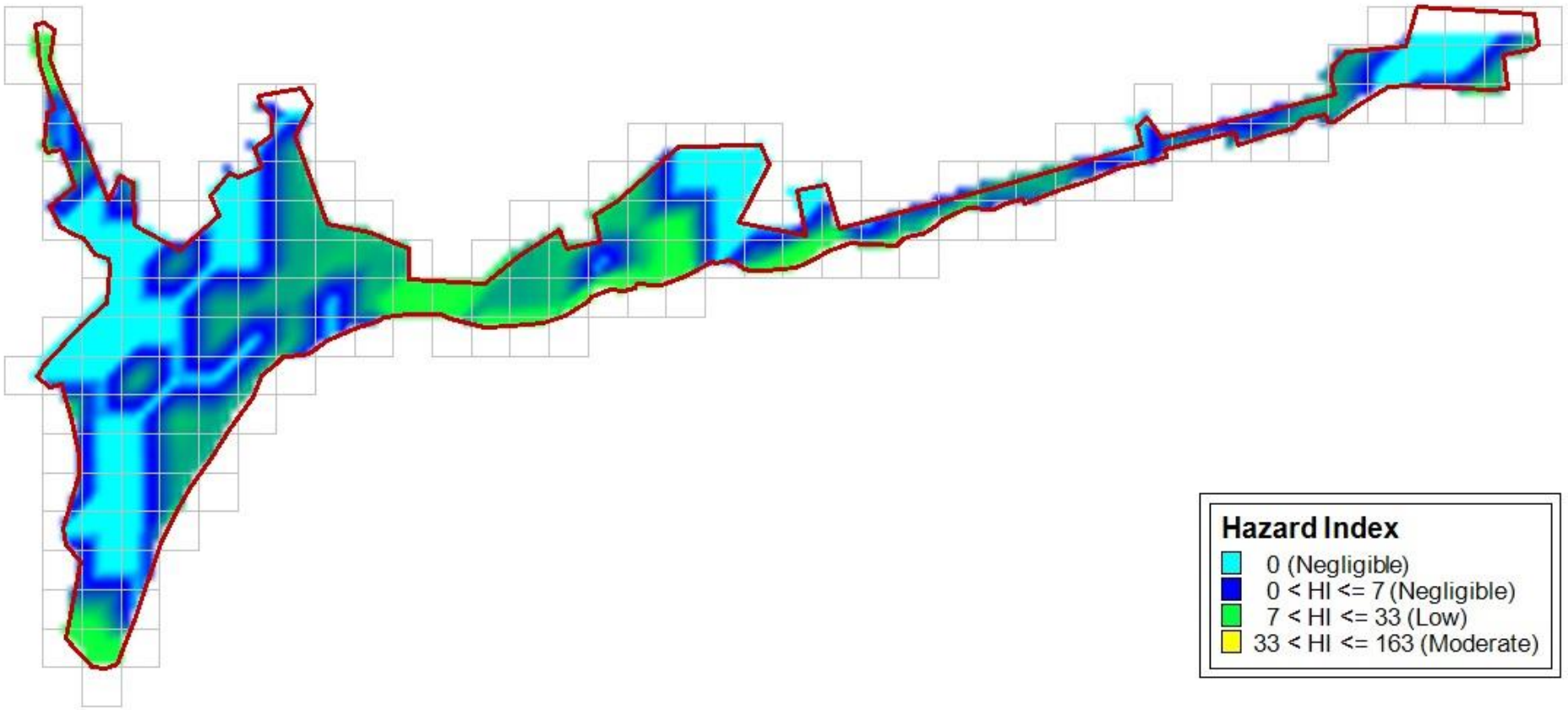

Figure 5.57. Hazard index.

On the other side of the spectrum, the triggering effects, rainfall (T_p) and earthquake (T_s), are determined such that T_p is selected as 1 since maximum daily rainfall was gauged as 41.8 mm in ten years. Modified Mercalli Index (MMI) is computed with the help of relationship Eq. (5.33), which is proposed by Gama – Garcia and Gomez – Bernal (1999) between PGA values attained through site response calculations (Figure 5.55) and MMI (Figure 5.56). T_s values are selected through Table 2.5 and Ultimate Hazard Map is given in Figure 5.57 along with input parameters in Table D..

$$\mathrm{MMI} = 3.0262 \log[\mathrm{PGA}(\mathrm{cm}^2/\mathrm{sec})] + 1.0195 \tag{5.33}$$

The bottom line inferred from the application of Mora and Vahrson Methodology (1994) on Tekirdağ City Center reveals that considerable % of site is considered as negligible in but middle parts and cells at coastal region may be subjected to rainfall and/or earthquake hazard (II and III degrees of hazard) since Tekirdağ may be assumed as "dry region" with respect to high rainfall zones such as Central America and so on. Also, Figure 5.57 is justified or is able to be further explained by the quotation from Manual for Zonation on Seismic Geotechnical Hazards (Revised Version) "*The maximum value of the landslide index predicted for areas of no rainfall would be around 200 under this method, suggesting that the likelihood of slope failures would only reach Class III or IV in dry countries*".

6. CONCLUSION

In this document, endeavour is made on devising a microzonation method, intended to be concise, apparent and trouble – free in that (1) no numerical instability is encountered during calculations, (2) it is easily able to be applied by researchers (3) parameter selection should not be troublesome to commence the computations. This context holds down the adoptation of different techniques in solution of Richards' Equation, which portrays the variation of pore water pressure under rainfall percolation, such as finite – difference and/or finite – element methods. This is because exact solution is pursued for degraded form of Richards' Relationship, which is succeeded by the horizontal flow of infiltrated rain water towards different parts of soil continuum. Exact solution is achieved through the assumption that the portion above groundwater level be initially wet but this might not be the situation encountered in site. The second limitation is the water flux directly proportional to the percolation of total rainfall amount through soil, which regrettably leads to the overestimation of pore water pressures but computed pressure heads are bounded by the maximum capacity of soil mass to hold water so as to get rid of absurd values calculated throughout the analysis. Also, the following stage, seepage condition, is totally dependent on the uniform seepage and hydraulic gradients are merely thought to occur as a result of topographical attributes in site. If it is not presumed that soil is homogeneous and hydraulic conductivity of soil does not converge to saturated one, (in turn corresponds to initially wet assumption), this presumption loses its validity and suction effect prevails over that of topography.

To display the pros and cons of the proposed methodology, a hypothetical topograpy is firstly generated to evaluate how varying soil conditions response the fluctuated amount of rainfall. What is deduced from this logic is that intensity of rainfall be quite dominant in the development of pressure heads and similarly that shower condition on site is the most detrimental one among others. In addition to this, If the seepage direction angle be not governed by topographical feaures of relevant area, that is, it is not at angle of 90^0, the degradation of FoS due to horizontal flow in hillslope is quite sharp and may lead to hazardous conditions.

On the other hand, Tekirdağ City Center is selected to test the improved algorithm but Montgomery and Dietrich Methodology (1994) is at first embraced to assess the interested site in that required parameters are attained by some empirical correlations. This is readily implemented procedure with two simple equations but compels utilizers to consult on GIS Programs to derive specific catchment area, slope angle, and so on. What is deduced from this methodology is that the patterns indicating FoS < 1 (failure) and 1 ≤ FoS < 1.5 (on the verge of failure) at the coastal zones (middle part) and partially left side of Tekirdağ City Center ought to be focused on.

Then, prescribed routine is executed on Tekirdağ in an attempt to reveal whether there is compatibility between the results Montgomery and Dietrich (1994) yield and those computed by developed methodology. It seems that even though the locations of failed cells is able to be mimicked by the former one, the selection of the value of exceedence probability should be carried out cautiously to produce compatible results between these routines (the response observed in 48.1 mm daily amount of rainfall approximately catches up with that obtained in 5.25 mm amount of rainfall in a day). In other words, although most of the cells declared as failed or on the verge of failure at coastal area (middle part) and relatively left side through developed routine are quite similar to those in Montgomery and Dietrich (1994) the rainfall amount in latter one should be selected as greater as that leading to same hazard proposed by former. Hence, the corollary inferred from Montgomery and Dietrich (1994) should be verified by aforementioned algorithm to lie within the safe side.

The last but not the least is the exploitation of Mora and Vahrson (1994) Methodology in terms of a justification tool so as to supply previous methods with a chance to unleash their capabilities to model the effects of incoming rainfall influence on study area. Since this method is only dependent of the visual inspection of quantities incorporated into the analysis and qualitative approach rather than appealing to more detailed computations, the exact compatibility between this and first two routines may not be provided but hazardous regions can be fairly represented. The middle part and coastal zones seem again to be exposed to rainfall and/or earthquake – induced hazard but the differences, which mostly reveal itself at left and right sides of Tekirdağ City Center, may be resulted from the fact that all geological structure is considered as governing parameter

for soil in Mora and Vahrson (1994) in contrast to previous methods, which focus on only the first layer in soil stratification.

Taking everything into consideration, recommended algorithm acceptably makes through the rainfall – induced slope stability hazard under some assumptions and limitations but may be exhaustive due to parameter selections and time requirements in step – by – step calculations with respect to another two methodologies. The results attained from Montgomery and Dietrich (1994) and Mora and Vahrson (1994) may be identical to that of developed one but time – dependent factor of safety calculations concordantly conducted with those of pore pressures are attractive side of proposed algorithm and offer broader insight into the rainfall – related slope stability concept.

REFERENCES

Abramson, L. W. and T. S. Lee, S. Sharma, G. M. Boyce, 2002, *Slope Stability and Stabilization Methods*, 2_{nd} Edition.

Ansal, A., G. Tönük and Y. Bayraklı, 2005, *Microzonation for Site Conditions for Tekirdağ Municipality*, Boğaziçi University, Kandilli Observatory and Earthquake Research Institute, Earthquake Engineering Department.

Bear, J., 1972, *Dynamics of Fluids in Porous Media*, Elsevier Science, New York.

Beven, K. J. and M. J. Kirby, 1979, "A Physically Based, Variable Contributing Area Model of Basin Hydrology/Un Modèle à Base Physique de Zone d'appel Variable de L'hydrologie du Bassin Versant", *Hydrolog. Sci. Bull.*, 24, 43–69.

Bowles, J. E., 1996, *Foundation Analysis and Design*, 5_{th} Edition, The McGraw-Hill Companies, Inc.

Brutsaert, W., 2005, *Hydrology: An Introduction*, Cambridge University Press.

Carrier, W. D., 2003, "Goodbye, Hazen; Hello, Kozeny-Carman", *Journal of Geotechnical and Geoenvironmental Engineering, ASCE*, Vol. 129, No. 11.

Carrier, W. D. and J. F. Beckman, 1984, "Correlations Between Index Tests and the Properties of Remoulded Clays", *Geochnique* 34, No. 2, 211-228.

Dewoolkar, M. M. and R. J. Huzjak, 2009, "Drained Residual Shear Strength of Some Claystones from Front Range Colorado", *Journal of Geotechnical and Geoenvironmental Engineering*, GT-03-23577, 2005.

Eagleson, P. S., 1970, *Dynamic Hydrology*, 462 pp., McGraw-Hill, New York.

Fredlund, D. G., H. Rahardjo and M. D. Fredlund, 2012, *Unsaturated Soil Mechanics in Engineering Practice*, John Wiley & Sons.

Garcia – Gama, A. and A. Gomez – Bernal, 2008, "Relationships between Instrumental Ground Motion Parameters, and Modified Mercalli Intensity in Guerrero, Mexico", *The 14_{th} World Conference on Earthquake Engineering*, October 12 – 17, 2008, Beijing, China.

Ghiassian, H., S. Ghareh, 2008, "Stability of Sandy Slopes under Seepage Conditions", *Landslides* 5:397 – 406.

Ghanbarian – Alavijeh, B., A. Liaghat, H. Guan – Hua, and M. T. V. Genuchten, 2010, "Estimation of the Van Genuchten Soil Water Retention Properties from Soil Textural Data", *Soil Science Society of China*, 456–465, 2010.

Gurdal, T. and C. H. Benson, 2003, H*ydrologic Properties of Final Cover Soils from the Alternative Cover Assessment Program*, Geo Engineering Program, University of Wisconsin – Madison, Madison, Wisconsin 53706 USA.

Holtz, R. D. and W. D. Kovac, 1981, *An Introduction to Geotechnical Engineering*, Prentice Hall.

Iverson, R., 1990, "Groundwater Flow Fields in Infinite Slopes", *Geotechnique*, 40, 139-143.

Iverson, R., 2000, "Landslide Triggering by Rain Infiltration", *Water Resour. Res.*, 36, 1897 1910.

Iverson R. and J. J. Major, 1986, "Groundwater Seepage Vectors and the Potential for Hillslope Failure and Debris Flow Mobilization", *Water Resources Research*, Vol. 22, No.11 Pages 1543 - 1548, October.

İlhan, O., G. Tönük and A. Ansal, 2014, "Sızan Yağmur Suyunun Yamaç Stabilitesine Etkisi Üzerine Bir Yaklaşım", *Zemin Mekaniği ve Temel Mühendisliği Onbeşinci Ulusal Kongresi*, 16 – 17 Ekim 2014, Orta Doğu Teknik Üniversitesi, Ankara.

Lecture notes on flow nets and dupuit assumption, https://eng.ucmerced.edu/people/jfisher.

Malamud, B. D., D. L. Turcotte, F. Guzzetti and P. Reichenbach, 2004, "Landslide Inventories and Their Statistical Properties", *Earth Surface Processess and Landforms*, 687 – 711.

Miller, J. E., 1984, "Basic Concepts of Kinematic – Wave Models", *U. S. Geological Survey Professional Paper* 1302, United States Government Printing Office, Washington.

Montgomery, D. R., and W. E. Dietrich, 1994, "A Physically Based Model for the Topographic Control on Shallow Landsliding", *Water Resour. Res.*, 30, 1153–1171.

Mora, S. C. and W. G. Vahrson, 1994, "Microzonation Methodology for Landslide Hazard Determination", *Bulletin of the Association of Engineering Geologists*, Vol. XXXI, No. 1, pp. 49 – 58.

O' Loughlin, E. M., 1986, "Prediction of Surface Saturation Zones in Natural Catchments by Topographic Analysis", *Water Resources Research*, Vol. 22, No. 5, 794 – 804 p.

O' Loughlin, E. M., 1981, "Saturation Regions in Catchments and their Relations to Soil and Topographic Properties", *Journal of Hydrology* 229 – 246 p.

Richards, L. A., 1931, "Capillary Conduction of Liquids in Porous Mediums", *Physics*, 1, 318–333.

Skempton, A. W., 1964, *Long – Term Stability of Clay Slopes*, 4th Rankine Lecture.

Steiakakis, E., C. Gamvroudis and G. Alevizos, 2012, "Kozeny-Carman Equation and Hydraulic Conductivity of Compacted Clayey Soils", *Geomaterials*, 2, 37-41.

Technical Committee for Earthquake Geotechnical Engineering, 1994, *Manual for Zonation on Seismic Geotechnical Hazards (Revised Version)*, TC4, ISSMGE.

Zaslavsky, D. and A. S. Rogowski, 1969, "Hydrologic and Morphologic Implications of Anisotropy and Infiltration in Soil Profile Development", *Soil Sci. Soc. Am. Proc.*, 33: 594 - 599 p.

APPENDIX A: DERIVATION OF DARCY' S LAW COMPATIBLE RAIN WATER FLUX

Slope stability analysis, 2 – D Darcian parameters are usually adopted as isotropic and homogeneous such that permeability defined parallel to the groundwater flow is sufficient for calculation of pore pressure generation. This presumption is generally applicable for saturated soil but the truth of matter is different in the case of unsaturated soil since there exists matric suction disparity in soil matrix. Therefore, it is obligatory to consider the anisotropy of permeability in slope stability analysis to perform more elaborative analysis.

In terminology of anisotropy, the largest coefficient of permeability is called as *major coefficient of permeability*. The smallest one is in a direction perpendicular to largest permeability and is named as *minor coefficient of permeability*. Various cases for anisotopic heterogenous soil conditions are presented as;

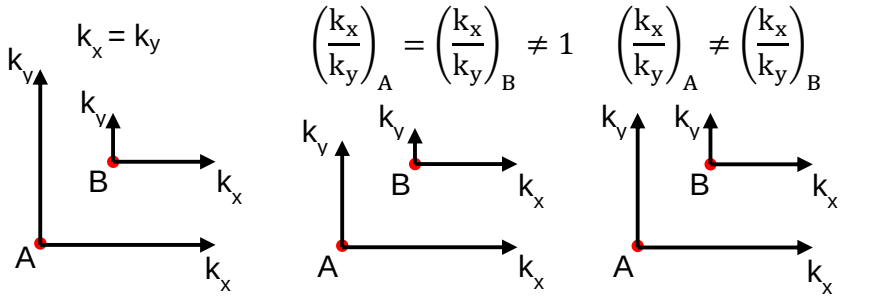

Heterogeneous, Isotropic steady – state seepage (This is due to matric suction)

Heterogeneous, Anisotropic steady – state seepage (*Different directions do not require different SWCC equations*)

(*Different directions require different SWCC equations*)

Figure A.1. Principal coefficient – of – permeability in unsaturated condition.

If Seepage through earth dams which is one of the most recognized instances of 2 – D seepage is adopted, it is customary to extract a cross – section from the whole body as in Figure A.2 and governing equation for continuity of flow can be expressed as follows;

$$\left(v_{wx} + \frac{\partial v_{wx}}{\partial x} dx - v_{wx}\right) dydz - \left(v_{wy} + \frac{\partial v_{wy}}{\partial y} dy\right) dxdz = 0 \quad (A.1)$$

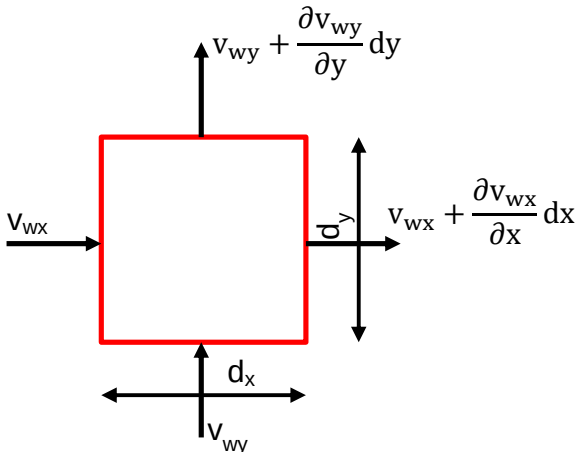

Figure A.2. Two – dimensional flow through an unsaturated soil element.

This Eq. (A.1) represents the condition corresponding to 2_{nd} on in Figure A.1 with the assumption that;

$$\left(\frac{k_{wx}}{k_{wy}}\right)_A = \left(\frac{k_{wx}}{k_{wy}}\right)_B \quad (A.2)$$

Then, solving the Eq. (A.1) yields;

$$\left(\frac{\partial v_{wx}}{\partial x} dx - v_{wx}\right) dydz - \left(v_{wy} + \frac{\partial v_{wy}}{\partial y} dy\right) dxdz = 0 \quad (A.3)$$

Once Darcy's Law is substituted into the Eq. (A.3);

$$\frac{\partial}{\partial x}\left\{k_{wx}(u_a - u_w)\frac{\partial h_w}{\partial x}\right\} + \frac{\partial}{\partial y}\left\{k_{wy}(u_a - u_w)\frac{\partial h_w}{\partial y}\right\} \quad (A.4)$$

where,

$k_{wx}(u_a - u_w)$, is the water coefficients of permeability as a function of matric suction, the permeability is able to vary with location in the x – direction.

$\partial h_w/\partial x$, is the hydraulic head in the x – direction.

Rearrange the Eq. (A.4) as;

$$k_{wx}\frac{\partial^2 h_w}{\partial x^2}+k_{wy}\frac{\partial^2 h_w}{\partial y^2}+\frac{\partial k_{wx}}{\partial x}\frac{\partial h_w}{\partial x}+\frac{\partial k_{wy}}{\partial y}\frac{\partial h_w}{\partial y} \quad (A.5)$$

If $k_{wx}=k_{wy}=k_w$,

$$k_w\frac{\partial^2 h_w}{\partial x^2}+k_w\frac{\partial^2 h_w}{\partial y^2}+\frac{\partial k_w}{\partial x}\frac{\partial h_w}{\partial x}+\frac{\partial k_w}{\partial y}\frac{\partial h_w}{\partial y} \quad (A.6)$$

The case mentined above is set forth as presumed that the major and minor permeability coefficients accounting for x and y – directions, respectively. What we encounter is if these coefficient have different directions;

$$v_{w1}=-k_{w1}\frac{\partial h_w}{\partial s_1} \quad (A.7)$$

$$v_{w2}=-k_{w2}\frac{\partial h_w}{\partial s_2} \quad (A.8)$$

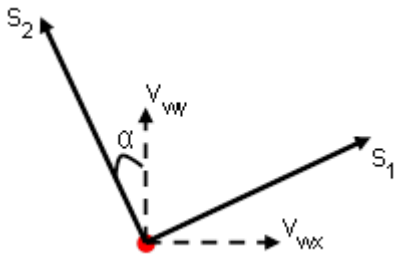

Figure A.3. Consideration of the orientation of the principal coefficients of permeability in heterogeneous and an isotropic unsaturated soil.

where s1 is the direction of major coefficient of permeability, s2 is the direction of minor coefficient of permeability, $\partial h_w/\partial s_1$ is the hydraulic head gradient in the s1 – direction, $\partial h_w/\partial s_2$ is the hydraulic head gradient in the s2 – direction.

The chain rule may be employed to express the hydraulic gradients in the s_1 and s_2 directions in terms of the gradients in the x – and y – directions

$$\frac{\partial h_w}{\partial s_1} = \frac{\partial h_w}{\partial x}\frac{\partial x}{\partial s_1} + \frac{\partial h_w}{\partial y}\frac{\partial y}{\partial s_1} \tag{A.9}$$

$$\frac{\partial h_w}{\partial s_2} = \frac{\partial h_w}{\partial x}\frac{\partial x}{\partial s_2} + \frac{\partial h_w}{\partial y}\frac{\partial y}{\partial s_2} \tag{A.10}$$

From using trigonometric relationships, it yields;

$$\frac{d_x}{ds_1} = \cos\alpha, \frac{d_y}{ds_1} = \sin\alpha, \frac{d_x}{ds_2} = -\sin\alpha, \frac{d_y}{ds_2} = \cos\alpha \tag{A.11}$$

If the Eqs. from (A.9) to (A.11) are substituted into (A.7), it gives;

$$v_{w1} = -k_{w1}\left(\cos\alpha\frac{\partial h_w}{\partial x} + \sin\alpha\frac{\partial h_w}{\partial y}\right) \tag{A.12}$$

$$v_{w2} = -k_{w2}\left(-\sin\alpha\frac{\partial h_w}{\partial x} + \cos\alpha\frac{\partial h_w}{\partial y}\right) \tag{A.13}$$

The water flow in the x – and y – directions can be rewritten by projecting the flow rates in the major and minor directions to the x - and y – directions

$$v_{wx} = v_{w1}\cos\alpha - v_{w2}\sin\alpha \tag{A.14}$$

$$v_{wy} = v_{w1}\sin\alpha + v_{w2}\cos\alpha \tag{A.15}$$

Then,

$$v_{wx} = -k_{w1}\cos^2\alpha\frac{\partial h_w}{\partial x} - k_{w1}\sin\alpha\cos\alpha\frac{\partial h_w}{\partial y} - k_{w2}\sin^2\alpha\frac{\partial h_w}{\partial x} + k_{w2}\sin\alpha\cos\alpha\frac{\partial h_w}{\partial y} \tag{A.16}$$

$$v_{wy} = -k_{w1}\sin\alpha\cos\alpha\frac{\partial h_w}{\partial x} - k_{w1}\sin^2\alpha\frac{\partial h_w}{\partial y} - k_{w2}\sin\alpha\cos\alpha\frac{\partial h_w}{\partial x} + k_{w2}\cos^2\alpha\frac{\partial h_w}{\partial y} \quad (A.17)$$

After the full simplification;

$$v_{wx} = -\left(k_{wxx}\frac{\partial h_w}{\partial x} + k_{wxy}\frac{\partial h_w}{\partial y}\right) \quad (A.18)$$

$$v_{wy} = -\left(k_{wyx}\frac{\partial h_w}{\partial x} + k_{wyy}\frac{\partial h_w}{\partial y}\right) \quad (A.19)$$

Where,

$$k_{xx} = k_{w1}\cos^2\alpha + k_{w2}\sin^2\alpha \quad (A.20)$$

$$k_{xy} = (k_{w1} - k_{w2})\sin\alpha\cos\alpha \quad (A.21)$$

$$k_{yx} = (k_{w1} - k_{w2})\sin\alpha\cos\alpha \quad (A.22)$$

$$k_{yy} = k_{w1}\sin^2\alpha + k_{w2}\cos^2\alpha \quad (A.23)$$

The Eq. (A.18) and Eq. (A.19) are modulated in the need of displaying steady, two – dimensional Darcian groundwater flow in the x – y plane of a saturated, heterogeneous, anisotropic medium;

$$\frac{\partial}{\partial x}\left(K_{xx}\frac{\partial h}{\partial x} + K_{yx}\frac{\partial h}{\partial y}\right) + \frac{\partial}{\partial y}\left(K_{yy}\frac{\partial h}{\partial y} + K_{xy}\frac{\partial h}{\partial x}\right) \quad (A.24)$$

In infinite slope – stability analysis, it is assumed that hydraulical forces only vary with respect to the slope – normal component corresponding to the y – direction in Figure A.4 in that the first term in the Eq. (A.24) set to be zero.

$$\frac{d}{dy}\left(K_{yy}\frac{\partial h}{\partial y} + K_{xy}\frac{\partial h}{\partial x}\right) = 0 \quad (A.25)$$

which represents the general equation for steady – state flow in isotropic, heterogeneous, infinite slope.

Integrating the Eq. (A.25) with respect to y finds out the well – known Darcy's Law for the y component of the ground water specific discharge, q_y;

$$K_{yy}(y)\frac{\partial h}{\partial y} + K_{xy}(y)\frac{\partial h}{\partial x} = -q_y \tag{A.26}$$

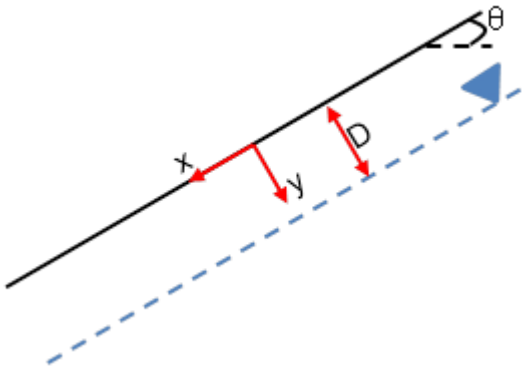

Figure A.4. Infinite – slope model.

$$K_{yy}(y)\frac{\partial h}{\partial y} + K_{xy}(y)\frac{\partial h}{\partial x} = -q_y \tag{A.27}$$

This Eq. (A.27) releases a fundamental constraint on steady groundwater flow in infinite slopes: the water flux normal to the slope must be constant at all points. Also, it can be employed to compute and delineate the distribution of hydraulic head in infinite slopes in that methods of characteristics frequently deployed to produce solution of linear partial differential equations. In our situation, the first step is to introduce a transformation of the Eq. (A.27) into new spatial coordinates, η(x, y) and ξ(x, y), which is achieved as;

$$K_{yy}\left(\frac{\partial h}{\partial \xi}\frac{\partial \xi}{\partial y} + \frac{\partial h}{\partial \eta}\frac{\partial \eta}{\partial y}\right) + K_{xy}\left(\frac{\partial h}{\partial \xi}\frac{\partial \xi}{\partial x} + \frac{\partial h}{\partial \eta}\frac{\partial \eta}{\partial x}\right) = -q_y \tag{A.28}$$

Rearranging the terms in the Eq. (A.28) yields;

$$\frac{\partial h}{\partial \xi}\left(K_{yy}\frac{\partial \xi}{\partial y} + K_{xy}\frac{\partial \xi}{\partial x}\right) + \frac{\partial h}{\partial \eta}\left(K_{yy}\frac{\partial \eta}{\partial y} + K_{xy}\frac{\partial \eta}{\partial x}\right) = -q_y \tag{A.29}$$

The methods of characteristics rests upon the fact that the Eq. (A.27) can be set forth as directional derivative as;

$$\left(K_{xy},\ K_{yy}\right) * \left(\frac{\partial h}{\partial x}, \frac{\partial h}{\partial y}\right) \text{ or } \left(K_{xy},\ K_{yy}\right) * \nabla h \tag{A.30}$$

Which means that the partial derivation equation does not change along or equation the –qy in that the solution should be constant in the direction of vector, $\left(K_{xy},\ K_{yy}\right)$.

The lines parallel to the vector have the equation,

$$K_{xy} i + K_{yy} j = \vec{v} \tag{A.31}$$

After this step, the η(x, y) is selected as constant lines to be rewritten as;

$$K_{yy} x - K_{xy} y = \eta \tag{A.32}$$

Then, the other spatial coordinate, ξ(x, y), perpendicular to the, η(x, y), can be calculated as;

$$K_{xy} x + K_{y} y = \xi \tag{A.33}$$

Which enables one to modulate the Eq. (A.29) as;

$$K_{yy}^2 \frac{\partial h}{\partial \xi} - K_{xy} K_{yy} \frac{\partial h}{\partial n} + K_{xy}^2 \frac{\partial h}{\partial \xi} + K_{xy} K_{yy} \frac{\partial h}{\partial \eta} = -q_y \tag{A.34}$$

After the full simplification of Eq. (A.34);

$$\left(K_{xy}^2 + K_{yy}^2\right)\frac{\partial h}{\partial \xi} = -q_y \tag{A.35}$$

This statement reveals that the water flux only varies with respect to the ξ(x, y) such that the coefficient of the second term in the left – hand side of (A.29) becomes zero;

$$K_{yy}\frac{\partial \eta}{\partial y} + K_{xy}\frac{\partial \eta}{\partial x} = 0 \tag{A.36}$$

Also, along the lines of constant η, the toal differential of η is zero;

$$d\eta = \frac{\partial \eta}{\partial x}dx + \frac{\partial \eta}{\partial y}dy = 0 \tag{A.37}$$

The Eq. (A.36) and Eq. (A.37) are linear partial differential equations in that if the matrix representation is appealed;

$$A = \begin{bmatrix} K_{xy} & K_{yy} \\ dx & dy \end{bmatrix} \tag{A.38}$$

$$x = \begin{Bmatrix} \partial\eta/\partial x \\ \partial\eta/\partial y \end{Bmatrix} \tag{A.39}$$

$$B = \begin{Bmatrix} 0 \\ 0 \end{Bmatrix} \tag{A.40}$$

Cramer's Rule states that the solution of $Ax = B$ can be found;

$$x_i = \frac{\det(A_i)}{\det(A)} \tag{A.41}$$

Then,

$$\partial\eta/\partial x = \frac{\begin{bmatrix} 0 & K_{yy} \\ 0 & dy \end{bmatrix}}{\begin{bmatrix} K_{xy} & K_{yy} \\ dx & dy \end{bmatrix}} \tag{A.42}$$

$$\partial\eta/\partial y = \frac{\begin{bmatrix} K_{xy} & 0 \\ dy & 0 \end{bmatrix}}{\begin{bmatrix} K_{xy} & K_{yy} \\ dx & dy \end{bmatrix}} \tag{A.43}$$

It can be seen that the Eq. (A.42) and Eq. (A.43) yield the trivial solution that $\partial\eta/\partial x$ and $\partial\eta/\partial y$ are computed as zero. However, Cramer's Rule proposes that the Eq. (A.36) and Eq. (A.37) have a nontrivial solution if and only if the determinant of their coefficient matrix is zero. Setting this determinant to zero yields;

$$\begin{bmatrix} K_{xy} & K_{yy} \\ dx & dy \end{bmatrix} = 0 \tag{A.44}$$

$$dyK_{xy} - dxK_{yy} = 0 \tag{A.45}$$

This is an exact differential equation of function;

$$\eta = x - \frac{K_{xy}}{K_{yy}}y + c \tag{A.46}$$

Actually, these characteristics are the quantification of streamlines through which water flows in response to variation of hydraulic gradient with only a y component. This again proves the statement above , thus equating ξ to y and employing Eq. (A.36) to reduce the Eq. (A.29) to;

$$K_{yy}\left(\frac{\partial h}{\partial \eta}\right)_{\eta \text{ constant}} = -q_y \tag{A.47}$$

Which is a specialized form of Darcy's Law.

APPENDIX B: DERIVATION OF THE WETNESS PARAMETER

In Montgomery and Dietrich's Methodology, the subsurface flux is devised to consist of both groundwater flux and that fed by rain water infiltration in that wetness state of interested area represents the groundwater effect and steady – state local flux on slope stability. To specify the wetness state as compatible with this logic, W, it is possible to consider a landshape given in Figure B.1, where control volume for quantifying the variation in water flux is bounded by red dashed lines. The assumption is made on the fact that total of vertical seepage and corresponding subsurface flux is conserved such as;

$$\rho V a dt + \rho I_z b dt dx - \rho \left(V + \frac{\partial V}{\partial x} dx\right)\left(a + \frac{\partial a}{\partial x} dx\right) dt = \rho \frac{\partial a}{\partial t} dt dx \tag{B.1}$$

Where V is the seepage velocity, a is the cross – section area, b is the width of the control volume, A is the projection of irregular surface area, h is the GWL, z is the soil depth.

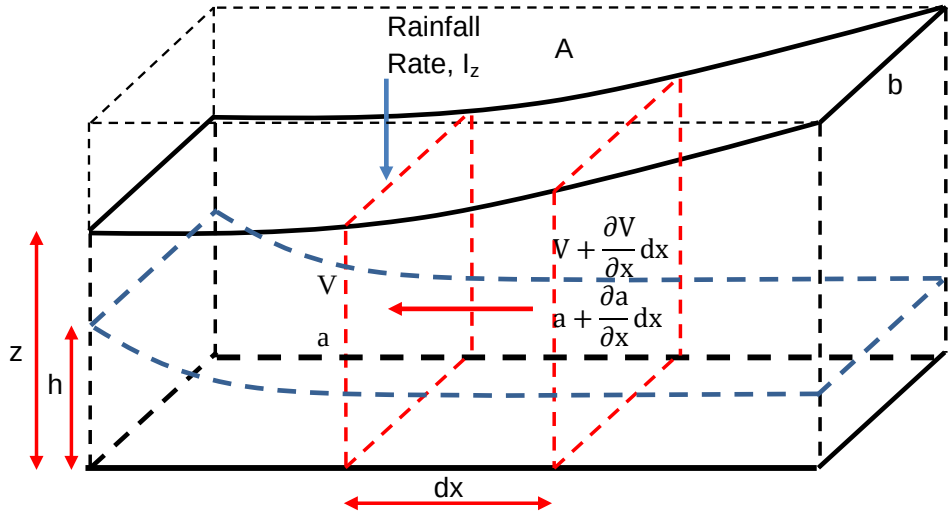

Figure B.1. Definition sketch for the wetness state calculation.

Should higher – order terms be neglected, it produces,

$$\frac{\partial a}{\partial t} + V\frac{\partial a}{\partial x} + a\frac{\partial V}{\partial x} = I_z b \tag{B.2}$$

Then, it is known that, $Q_x = V_x A$,

$$\frac{\partial Q_x}{\partial x} + \frac{\partial A}{\partial t} = I_z b \tag{B.3}$$

By dividing b (remembering that $A = b * x$) , (well – known Continuity Equation)

$$\frac{\partial Q_x}{\partial A} + \frac{\partial h}{\partial t} = I_z \tag{B.4}$$

At that point, hydrological response of soil mass is presumed to be governed by steady – state condition, where time parameter goes to the infinity, thus resulting in that the 2_{nd} term at RHS of Eq. (B.4) becomes zero. Also, Figure 5.6 reveals that rain water is thought to reduce into a steady – state discharge equation such as;

$$Q_x = I_z A \tag{B.5}$$

Suppose again Figure 5.6 that volumetric water discharge can be arranged into more recognizable form;

$$Q_x = bhK_x \sin\theta \tag{B.6}$$

Should Eq. (B.5) and Eq. (B.6) be combined to conclude the verification process,

$$h = \frac{I_z A}{bK_x \sin\theta} \tag{B.7}$$

APPENDIX C: ASSIGNED PARAMETERS IN TEKIRDAĞ CASE STUDY

Table C.1. Assigned parameters in Tekirdağ case study.

Cells	Z (m)	γ_{sat} (kN/m^3)	K_{sat} (cm/sec)	φ^0	USCS Type	USDA Type	D_0 (m^2/sec)	d_Z (m)
F16	1	18.2	1.00E-04	18.1	CL	Clay	1.07E-04	1
G16	1	18.2	1.00E-04	18.1	CL	Clay	1.07E-04	1
G17	1	18.2	1.00E-04	18.1	CL	Clay	1.07E-04	1
H16	1	18.2	1.00E-04	18.1	CL	Clay	1.07E-04	1
F17	1	18.2	1.00E-04	18.1	CL	Clay	1.07E-04	1
E16	1.1	18.1	1.00E-04	21.6	CL	Clay	1.23E-04	1.1
F15	1	18.1	7.94E-04	15.7	CH	Clay	8.22E-04	1
F14	1	18.1	7.94E-04	15.7	CH	Clay	8.22E-04	1
E12	1	18.1	1.00E-04	18.8	CL	Clay	1.06E-04	1
F12	1	18.1	1.00E-04	18.8	CL	Clay	1.06E-04	1
F11	1	17.7	1.00E-04	18.3	CL	Clay	1.04E-04	1
F10	1	17.7	1.00E-04	18.3	CL	Clay	1.04E-04	1
F9	1	17.7	1.00E-04	20.4	CL	Clay	1.36E-04	1
F20	1.25	18.4	8.08E-04	22.0	CL	Clay	1.38E-03	1.25
G19	1.25	18.4	8.08E-04	22.0	CL	Clay	1.38E-03	1.25
F19	1.25	18.4	8.08E-04	22.0	CL	Clay	1.38E-03	1.25
E8	1	18.1	1.00E-04	20.1	CL	Clay	1.07E-04	1
S10	3	18.1	3.16E-02	19.6	ML	Silt	4.22E-02	2.5
U9	1	18.2	1.00E-04	18.6	CL	Clay	1.15E-04	1
V9	1	18.2	1.00E-04	18.6	CL	Clay	1.15E-04	1
AB8	1	18.6	2.17E-02	18.8	ML	Silt	1.96E-02	1
AN3	2.75	18.4	3.16E-02	28.0	SM	Loamy Sand	4.61E-03	2.75
AM4	1	18.5	3.16E-02	28.0	SM	Loamy Sand	3.38E-03	1
AN4	1	18.5	3.16E-02	28.0	SM	Loamy Sand	3.38E-03	1
AN5	1	18.5	3.16E-02	28.0	SM	Loamy Sand	3.38E-03	1
AO5	1	18.5	3.16E-02	28.0	SM	Loamy Sand	3.38E-03	1
AM5	1	18.5	3.16E-02	28.0	SM	Loamy Sand	3.38E-03	1
AB7	1	20.1	1.00E-04	15.9	CH	Clay	9.43E-05	1
U8	1	18.2	1.00E-04	18.6	CL	Clay	1.03E-04	1
U7	1.5	18.2	1.00E-04	18.6	CL	Clay	1.03E-04	1.5
T6	1.5	19.8	1.00E-04	18.6	CL	Clay	1.15E-04	1.5
F8	1.5	19.6	7.24E-04	16.9	CL	Clay	8.80E-04	1.5
D12	1	20.5	5.57E-04	16.8	CL	Clay	7.31E-04	1
E11	1	18.1	9.21E-04	16.3	CL	Clay	9.74E-04	1

Table C.1. Assigned parameters in Tekirdağ case study (Cont' d).

Cells	Z (m)	γ_{sat} (kN/m^3)	K_{sat} (cm/sec)	φ^0	USCS Type	USDA Type	D_0 (m^2/sec)	d_Z (m)
G18	1	20.2	1.00E-04	22.0	CL	Clay	1.40E-04	1
E13	1.7	20.6	3.71E-04	15.7	CH	Clay	4.57E-04	1.7
F13	1.7	20.6	3.71E-04	15.7	CH	Clay	4.57E-04	1.7
H10	1	18.3	1.00E-04	16.8	CL	Clay	1.08E-04	1
I9	1	18.4	1.00E-04	17.5	CL	Clay	1.14E-04	1
T9	3	18.1	3.16E-02	19.6	ML	Silt	4.22E-02	2.5
W6	1	17.9	1.00E-04	21.2	CL	Clay	1.14E-04	1
G14	1.5	18.1	1.00E-04	22.0	CL	Clay	1.09E-04	1.5
H14	1.5	18.1	1.00E-04	22.0	CL	Clay	1.09E-04	1.5
G15	1.5	18.1	1.00E-04	22.0	CL	Clay	1.09E-04	1.5
H15	1.5	18.1	1.00E-04	22.0	CL	Clay	1.09E-04	1.5
I15	1.5	18.1	1.00E-04	22.0	CL	Clay	1.09E-04	1.5
E15	1.1	18.1	1.00E-04	21.6	CL	Clay	1.23E-04	1.1
E14	1	18.1	7.94E-04	15.7	CH	Clay	8.22E-04	1
I14	1	18.1	1.00E-04	18.8	CL	Clay	1.05E-04	1
J13	1	18.1	1.00E-04	18.8	CL	Clay	1.05E-04	1
I13	1	18.1	1.00E-04	18.8	CL	Clay	1.05E-04	1
G12	1	18.1	1.00E-04	18.6	CL	Clay	1.04E-04	1
H13	1	18.1	1.00E-04	18.6	CL	Clay	1.04E-04	1
H12	1	18.1	1.00E-04	18.6	CL	Clay	1.04E-04	1
K11	1.4	17.9	1.00E-04	21.0	CL	Clay	1.07E-04	1.4
I11	1	18.2	1.00E-04	19.8	CL	Clay	1.16E-04	1
J10	1	18.2	1.00E-04	19.8	CL	Clay	1.16E-04	1
H11	1	18.3	1.00E-04	16.8	CL	Clay	1.08E-04	1
G11	1	17.7	1.00E-04	18.3	CL	Clay	1.04E-04	1
E7	1	18.1	1.00E-04	20.1	CL	Clay	1.07E-04	1
G13	1	17.9	1.00E-04	16.8	CL	Clay	1.06E-04	1
I10	1	18.4	1.00E-04	17.5	CL	Clay	1.14E-04	1
J8	1	18.2	1.00E-04	19.8	CL	Clay	1.16E-04	1
J9	1	18.2	1.00E-04	19.8	CL	Clay	1.16E-04	1
L11	1	18.3	3.16E-05	28.0	Sandstone	Sandstone	3.93E-06	1
M10	1	18.3	3.16E-05	28.0	Sandstone	Sandstone	3.93E-06	1
M11	1	18.3	3.16E-05	28.0	Sandstone	Sandstone	3.93E-06	1
L10	1	18.3	3.16E-05	28.0	Sandstone	Sandstone	3.93E-06	1
L9	1	18.3	3.16E-02	30.0	SM	Loamy sand	3.93E-03	1
L8	1	17.9	1.00E-04	21.3	CL	Clay	1.17E-04	1
K9	1	17.9	1.00E-04	21.3	CL	Clay	1.17E-04	1
K8	1	18.1	1.00E-04	18.3	CL	Clay	1.11E-04	1

Table C.1. Assigned parameters in Tekirdağ case study (Cont' d).

Cells	Z (m)	γ_{sat} (kN/m^3)	K_{sat} (cm/sec)	φ^0	USCS Type	USDA Type	D_0 (m^2/sec)	d_Z (m)
K7	1	18.1	1.00E-04	18.3	CL	Clay	1.11E-04	1
M8	1	17.9	1.00E-04	21.3	CL	Clay	1.17E-04	1
L7	1	17.9	1.00E-04	21.3	CL	Clay	1.17E-04	1
P11	3	18.4	3.16E-02	28.0	SM	Loamy Sand	3.77E-03	3
T10	3	18.1	3.16E-02	19.6	ML	Silt	4.22E-02	2.5
S9	1	18.1	1.00E-04	21.0	CL	Clay	1.18E-04	1
R8	1	18.1	1.00E-04	21.0	CL	Clay	1.18E-04	1
P10	1	18.3	1.00E-04	21.0	CL	Clay	1.16E-04	1
T7	1.35	18.4	3.16E-02	28.0	SM	Loamy Sand	4.65E-03	1.35
U10	1	18.2	1.00E-04	18.6	CL	Clay	1.15E-04	1
X8	1.3	17.7	5.26E-04	15.6	CH	Clay	5.81E-04	1.3
X9	1.3	17.7	5.26E-04	15.6	CH	Clay	5.81E-04	1.3
Y9	1.3	17.7	5.26E-04	15.6	CH	Clay	5.81E-04	1.3
Z9	1.3	17.7	5.26E-04	15.6	CH	Clay	5.81E-04	1.3
Y8	1.3	17.7	5.26E-04	15.6	CH	Clay	5.81E-04	1.3
AA8	1	18.6	2.17E-02	18.8	ML	Silt	1.96E-02	1
AA9	1	18.6	2.17E-02	18.8	ML	Silt	1.96E-02	1
AC8	1	18.6	2.17E-02	18.8	ML	Silt	1.96E-02	1
AD8	1	18.6	2.17E-02	18.8	ML	Silt	1.96E-02	1
AK6	1	17.9	1.00E-04	21.0	CL	Clay	1.44E-04	1
AJ6	1	17.9	1.00E-04	21.0	CL	Clay	1.44E-04	1
AE7	1	17.9	1.00E-04	21.0	CL	Clay	1.06E-04	1
AF7	1	17.9	1.00E-04	21.0	CL	Clay	1.06E-04	1
AG7	1	17.9	1.00E-04	21.0	CL	Clay	1.06E-04	1
AF6	1	17.9	1.00E-04	21.0	CL	Clay	1.06E-04	1
AO3	2.75	18.4	3.16E-02	28.0	SM	Loamy Sand	4.61E-03	2.75
AP3	2.75	18.4	3.16E-02	28.0	SM	Loamy Sand	4.61E-03	2.75
AQ3	2.75	18.4	3.16E-02	28.0	SM	Loamy Sand	4.61E-03	2.75
AM3	2.75	18.4	3.16E-02	28.0	SM	Loamy Sand	4.61E-03	2.75
AH6	1	17.9	1.00E-04	21.0	CL	Clay	1.06E-04	1
AI6	1	17.9	1.00E-04	21.0	CL	Clay	1.06E-04	1
K10	1.4	18.3	3.16E-02	28.0	SM	Loamy Sand	3.93E-03	1.4
I12	1	18.0	1.00E-04	20.1	CL	Clay	1.03E-04	1
J12	1	18.0	1.00E-04	20.1	CL	Clay	1.03E-04	1
E19	1.65	18.4	3.16E-02	28.0	SM	Loamy Sand	3.77E-03	1.65
W9	3	18.4	3.16E-02	28.0	SM	Loamy Sand	4.65E-03	3
AO4	1	18.5	3.16E-02	28.0	SM	Loamy Sand	3.38E-03	1
AP4	1	18.5	3.16E-02	28.0	SM	Loamy Sand	3.38E-03	1

Table C.1. Assigned parameters in Tekirdağ case study (Cont' d).

Cells	Z (m)	γ_{sat} (kN/m^3)	K_{sat} (cm/sec)	φ^0	USCS Type	USDA Type	D_0 (m^2/sec)	d_Z (m)
AP5	1	18.5	3.16E-02	28.0	SM	Loamy Sand	3.38E-03	1
AQ4	1	18.5	3.16E-02	28.0	SM	Loamy Sand	3.38E-03	1
AL5	1	17.7	3.16E-02	28.0	ML	Silt	4.49E-02	1
AL4	1	17.7	3.16E-02	28.0	ML	Silt	4.49E-02	1
AK5	1	17.9	1.00E-04	21.0	CL	Clay	1.06E-04	1
AJ5	1	17.9	1.00E-04	21.0	CL	Clay	1.06E-04	1
AI5	1	19.1	3.16E-02	28.0	SM	Loamy Sand	4.95E-03	1
AG5	1	18.3	1.00E-04	16.2	CH	Clay	1.07E-04	1
AG6	1	17.9	1.00E-04	21.0	CL	Clay	1.06E-04	1
AD7	1	17.9	1.00E-04	19.1	CL	Clay	1.06E-04	1
AC7	1	17.9	1.00E-04	19.1	CL	Clay	1.06E-04	1
AE6	1	17.9	1.00E-04	19.3	CL	Clay	1.06E-04	1
Z8	1	17.7	5.26E-04	15.6	CH	Clay	5.81E-04	1
Y7	1	17.9	1.00E-04	21.2	CL	Clay	1.14E-04	1
W8	1	18.2	1.00E-04	18.6	CL	Clay	1.03E-04	1
V8	1	18.2	1.00E-04	18.6	CL	Clay	1.03E-04	1
W7	1	17.9	1.00E-04	21.2	CL	Clay	1.14E-04	1
V7	1	17.7	3.16E-02	28.0	ML	Silt	4.49E-02	1
V6	1	17.7	3.16E-02	28.0	ML	Silt	4.49E-02	1
N9	1	18.3	8.23E-04	21.0	CL	Clay	1.29E-03	1
Q9	1	19.6	3.16E-02	28.0	SM	Loamy Sand	5.18E-03	1
M9	1.8	19.6	1.00E-04	21.0	CL	Clay	1.29E-04	1.8
T8	1	19.9	1.00E-04	21.0	CL	Clay	1.20E-04	1
K6	1	17.9	1.00E-04	22.0	CL	Clay	1.14E-04	1
F6	3	20.4	1.00E-04	28.0	CL	Clay	1.40E-04	1.5
G7	1	20.0	1.00E-04	20.1	CL	Clay	1.24E-04	1
F7	1	20.0	1.00E-04	20.1	CL	Clay	1.24E-04	1
G8	1.5	19.6	7.24E-04	16.9	CL	Clay	8.80E-04	1.5
D4	3	19.8	3.16E-02	28.0	ML	Silt	5.37E-02	3
E3	3	19.8	3.16E-02	28.0	ML	Silt	5.37E-02	3
E4	3	19.8	3.16E-02	28.0	ML	Silt	5.37E-02	3
D3	3	19.8	3.16E-02	28.0	ML	Silt	5.37E-02	3
E6	1	18.1	1.00E-04	20.1	CL	Clay	1.07E-04	1
E5	1	18.1	1.00E-04	20.1	CL	Clay	1.07E-04	1
E17	1	20.2	1.00E-04	22.0	CL	Clay	1.40E-04	1
F18	1	20.2	1.00E-04	22.0	CL	Clay	1.40E-04	1
E18	1	20.2	1.00E-04	22.0	CL	Clay	1.40E-04	1
G10	1	21.0	1.00E-04	22.0	CL	Clay	1.54E-04	1

Table C.1. Assigned parameters in Tekirdağ case study (Cont' d).

Cells	Z (m)	γ_{sat} (kN/m^3)	K_{sat} (cm/sec)	φ^0	USCS Type	USDA Type	D_0 (m^2/sec)	d_Z (m)
R10	1	18.3	1.00E-04	17.2	CL	Clay	1.05E-04	1
O11	1	18.3	3.88E-04	17.4	CL	Clay	5.53E-04	1
R11	1	18.3	2.53E-03	21.5	CL-ML	Silty Clay l.	3.59E-04	1
Q11	1	18.3	2.53E-03	21.5	CL-ML	Silty Clay loam	3.59E-04	1
N10	1	18.3	1.00E-04	18.5	CL	Clay	1.21E-04	1
Q10	1	18.3	1.00E-04	17.2	CL	Clay	1.05E-04	1
R9	1	18.3	1.00E-04	17.2	CL	Clay	1.05E-04	1
O10	1	18.3	3.88E-04	17.4	CL	Clay	5.53E-04	1
K5	1	17.9	1.00E-04	22.0	CL	Clay	1.14E-04	1
X7	1	17.9	1.00E-04	21.2	CL	Clay	1.14E-04	1
U6	1.5	18.2	1.00E-04	18.6	CL	Clay	1.03E-04	1.5
P9	1	19.6	3.16E-02	28.0	SM	Loamy Sand	5.18E-03	1
S7	1	20.1	1.00E-04	21.0	CL	Clay	1.22E-04	1
J6	1	17.9	1.00E-04	22.0	CL	Clay	1.14E-04	1
Q8	1.6	19.0	3.16E-02	28.0	SM	Loamy Sand	4.84E-03	1.6
S8	1	19.9	1.00E-04	21.0	CL	Clay	1.20E-04	1
J7	1	17.9	1.00E-04	22.0	CL	Clay	1.14E-04	1
J5	1	21.1	1.00E-04	22.0	CL	Clay	1.55E-04	1
I8	1	18.6	1.00E-04	22.0	CL	Clay	1.22E-04	1
I7	1	18.6	1.00E-04	22.0	CL	Clay	1.22E-04	1
H9	1	17.9	1.00E-04	22.0	CL	Clay	1.14E-04	1
G9	1	21.0	1.00E-04	22.0	CL	Clay	1.54E-04	1

APPENDIX D: ASSIGNED PARAMETERS IN MORA AND VAHRSON METHODOLOGY (1994)

Table D.1. Assigned parameters in Mora and Vahrson Methodology (1994).

Cells	Converted RR	S_r	S_h	S_l	T_p	T_s	H_i	I	PGA (g)	Lithology	MMI
D3	0.199999	2	1	3	1	7	48	III	0.473243	DFC	9
D4	0.199999	2	1	3	1	7	48	III	0.473243	DFC	9
D12	0.057654	0	1	5	1	7	0	I	0.600987	QA	9
E3	0.199999	2	1	3	1	7	48	III	0.473243	DFC	9
E4	0.199999	2	1	3	1	7	48	III	0.473243	DFC	9
E5	0.064084	0	1	3	1	7	0	I	0.52138	DFC	9
E6	0.057464	0	1	3	1	7	0	I	0.534153	DFC	9
E7	0.109363	1	1	3	1	8	27	II	0.649203	DFC	10
E8	0.061423	0	1	5	1	8	0	I	0.664177	QA	10
E11	0.056581	0	1	5	1	7	0	I	0.581957	QA	9
E12	0.032816	0	1	5	1	8	0	I	0.68986	QA	10
E13	0.103022	1	1	5	1	7	40	III	0.569927	QA	9
E14	0.083124	1	1	3	1	7	24	II	0.302537	DFC	9
E15	0.095098	1	1	3	1	8	27	II	0.697903	DFC	10
E16	0.049402	0	1	5	1	8	0	I	0.71597	QA	10
E17	0.100029	1	1	3	1	8	27	II	0.74348	DFC	10
E18	0.107458	1	1	3	1	8	27	II	0.758167	DFC	10
E19	0.199999	2	1	3	1	7	48	III	0.642953	DFC	9
F6	0.085209	1	1	3	1	7	24	II	0.535957	DFC	9
F7	0.074419	0	1	3	1	7	0	I	0.567017	DFC	9
F8	0.055538	0	1	5	1	7	0	I	0.53303	QA	9
F9	0.051294	0	1	5	1	7	0	I	0.58623	QA	9
F10	0.062776	0	1	5	1	8	0	I	0.65235	QA	10
F11	0.044137	0	1	5	1	8	0	I	0.667533	QA	10
F12	0.040515	0	1	5	1	8	0	I	0.70476	QA	10
F13	0.052294	0	1	5	1	7	0	I	0.568313	QA	9
F14	0.026138	0	1	5	1	7	0	I	0.302537	QA	9
F15	0.016099	0	1	5	1	7	0	I	0.303897	QA	9
F16	0.020385	0	1	5	1	7	0	I	0.457297	QA	9
F17	0.074543	0	1	5	1	7	0	I	0.461067	QA	9
F18	0.105941	1	1	3	1	8	27	II	0.758167	DFC	10
F19	0.105608	1	1	5	1	7	40	III	0.582887	QA	9
F20	0.15	1	1	5	1	7	40	III	0.5933	QA	9
G7	0.090225	1	1	3	1	7	24	II	0.5806	DFC	9
G8	0.067433	0	1	3	1	7	0	I	0.53303	DFC	9

Table D.1. Assigned parameters in Mora and Vahrson Methodology (1994) (Cont' d).

Cells	Converted RR	S_r	S_h	S_l	T_p	T_s	H_i	I	PGA (g)	Lithology	MMI
G9	0.062417	0	1	3	1	7	0	I	0.575833	DFS	9
G10	0.07355	0	1	3	1	7	0	I	0.58916	DFC	9
G11	0.073884	0	1	3	1	8	0	I	0.667533	DFC	10
G12	0.082685	1	1	3	1	8	27	II	0.756167	DFC	10
G13	0.075243	0	1	3	1	8	0	I	0.655543	DFC	10
G14	0.057315	0	1	3	1	7	0	I	0.538407	DFC	9
G15	0.045361	0	1	3	1	7	0	I	0.547283	DFC	9
G16	0.055504	0	1	5	1	7	0	I	0.457297	QA	9
G17	0.05	0	1	5	1	7	0	I	0.461067	QA	9
G18	0.044894	0	1	5	1	8	0	I	0.758167	QA	10
G19	0.080771	1	1	5	1	8	45	III	0.65882	QA	10
H9	0.094879	1	1	3	1	7	24	II	0.594183	DFS	9
H10	0.05631	0	1	3	1	7	0	I	0.602513	MMF	9
H11	0.064445	0	1	3	1	7	0	I	0.61516	DFC	9
H12	0.073595	0	1	3	1	8	0	I	0.77283	DFC	10
H13	0.088902	1	1	3	1	8	27	II	0.77283	DFC	10
H14	0.08876	1	1	3	1	7	24	II	0.547283	DFC	9
H15	0.08717	1	1	3	1	7	24	II	0.547283	DFC	9
H16	0.091271	1	1	5	1	7	40	III	0.457297	QA	9
I7	0.068668	0	1	3	1	7	0	I	0.5806	DFS	9
I8	0.068796	0	1	3	1	7	0	I	0.594183	DFS	9
I9	0.071238	0	1	3	1	7	0	I	0.55995	MMF	9
I10	0.080987	1	1	3	1	7	24	II	0.56863	DFC	9
I11	0.076012	1	1	3	1	7	24	II	0.63889	DFC	9
I12	0.069865	0	1	3	1	7	0	I	0.617777	DFC	9
I13	0.083977	1	1	3	1	7	24	II	0.607393	DFC	9
I14	0.078732	1	1	3	1	7	24	II	0.61839	DFC	9
I15	0	0	1	3	1	7	0	I	0.555377	DFC	9
J5	0.091504	1	1	3	1	8	27	II	0.68214	DFS	10
J6	0.054172	0	1	4	1	7	0	I	0.603253	EF	9
J7	0.061338	0	1	3	1	7	0	I	0.618093	DFS	9
J8	0.060548	0	1	3	1	7	0	I	0.598623	DFC	9
J9	0.065316	0	1	3	1	7	0	I	0.61149	DFC	9
J10	0.103284	1	1	3	1	7	24	II	0.623607	DFC	9
J11	0.160348	1	1	0	1	7	0	I	0.59179		9
J12	0.120411	1	1	3	1	7	24	II	0.617777	DFC	9
J13	0.087669	1	1	3	1	7	24	II	0.607393	DFC	9
K5	0.070118	0	1	4	1	7	0	I	0.611007	EF	9
K6	0.104422	1	1	3	1	7	24	II	0.603253	DFC	9

Table D.1. Assigned parameters in Mora and Vahrson Methodology (1994) (Cont' d).

Cells	Converted RR	S_r	S_h	S_l	T_p	T_s	H_i	I	PGA (g)	Lithology	MMI
K7	0.104813	1	1	3	1	7	24	II	0.541027	DFC	9
K8	0.114927	1	1	3	1	7	24	II	0.55169	DFC	9
K9	0.118749	1	1	3	1	7	24	II	0.598367	DFC	9
K10	0.107857	1	1	3	1	7	24	II	0.6106	DFC	9
K11	0.101237	1	1	3	1	8	27	II	0.701153	DFC	10
L7	0.123356	1	1	3	1	8	27	II	0.688053	DFC	10
L8	0.092316	1	1	3	1	7	24	II	0.598367	DFC	9
L9	0.081966	1	1	3	1	8	27	II	0.785323	DFC	10
L10	0.068028	0	1	3	1	8	0	I	0.906687	DFC	10
L11	0.054858	0	1	3	1	8	0	I	0.924347	DFC	10
M8	0.079533	1	1	3	1	8	27	II	0.702767	DFC	10
M9	0.0897	1	1	3	1	7	24	II	0.60128	DFC	9
M10	0.128823	1	1	3	1	8	27	II	0.906687	DFC	10
M11	0	0	1	3	1	8	0	I	0.924347	DFC	10
N9	0.128119	1	1	3	1	7	24	II	0.63059	DFC	9
N10	0.249999	2	1	3	1	7	48	III	0.540427	DFC	9
O10	0.293527	2	1	3	1	7	48	III	0.622363	DFC	9
O11	0.1	1	1	3	1	7	24	II	0.616037	DFC	9
P9	0.077137	1	1	4	1	8	36	III	0.6508	EF	10
P10	0.167527	1	1	3	1	7	24	II	0.598113	DFC	9
P11	0.299999	2	1	3	1	7	48	III	0.582487	DFC	9
Q8	0.113238	1	1	3	1	7	24	II	0.63229	DFS	9
Q9	0.088946	1	1	3	1	7	24	II	0.541357	DFC	9
Q10	0.08954	1	1	3	1	7	24	II	0.5638	DFC	9
Q11	0.299999	2	1	3	1	8	54	III	0.73745	DFC	10
R8	0.077536	1	1	3	1	8	27	II	0.801457	DFC	10
R9	0.080705	1	1	3	1	8	27	II	0.81714	DFC	10
R10	0.104671	1	1	3	1	8	27	II	0.677653	DFC	10
R11	0.1	1	1	3	1	8	27	II	0.669283	DFC	10
S7	0.137329	1	1	4	1	7	32	III	0.57279	EF	9
S8	0.095006	1	1	3	1	8	27	II	0.686867	DFS	10
S9	0.075041	0	1	3	1	8	0	I	0.81714	DFC	10
S10	0.206968	2	1	5	1	7	80	III	0.640783	QA	9
T6	0.108943	1	1	5	1	7	40	III	0.49838	QA	9
T7	0.098682	1	1	3	1	8	27	II	0.70707	DFC	10
T8	0.123301	1	1	3	1	8	27	II	0.686867	DFC	10
T9	0.076875	1	1	3	1	7	24	II	0.627817	MMF	9
T10	0.199999	2	1	3	1	7	48	III	0.640783	DFC	9
U6	0.046771	0	1	4	1	7	0	I	0.556997	EF	9

Table D.1. Assigned parameters in Mora and Vahrson Methodology (1994) (Cont' d).

Cells	Converted RR	S_r	S_h	S_l	T_p	T_s	H_i	I	PGA (g)	Lithology	MMI
U7	0.032923	0	1	5	1	7	0	I	0.569387	QA	9
U8	0.11528	1	1	5	1	7	40	III	0.466287	QA	9
U9	0.146547	1	1	5	1	8	45	III	0.65099	QA	10
U10	0.249999	2	1	3	1	8	54	III	0.663443	DFC	10
V6	0.072722	0	1	3	1	8	0	I	0.668957	DFC	10
V7	0.055049	0	1	3	1	8	0	I	0.68458	DFC	10
V8	0.036508	0	1	3	1	7	0	I	0.466287	DFC	9
V9	0.057681	0	1	5	1	8	0	I	0.65099	QA	10
W6	0.070166	0	1	4	1	8	0	I	0.67301	TF	10
W7	0.067324	0	1	3	1	8	0	I	0.68818	DFC	10
W8	0.074091	0	1	3	1	7	0	I	0.466287	DFC	9
W9	0.168258	1	1	3	1	8	27	II	0.65182	DFC	10
X7	0.05459	0	1	4	1	8	0	I	0.646827	EF	10
X8	0.073817	0	1	3	1	8	0	I	0.661163	DFC	10
X9	0.22654	2	1	3	1	8	54	III	0.676023	DFC	10
Y7	0.06545	0	1	3	1	8	0	I	0.646827	DFC	10
Y8	0.10339	1	1	3	1	8	27	II	0.661163	DFC	10
Y9	0.183645	2	1	3	1	8	54	III	0.676023	DFC	10
Z8	0.061916	0	1	3	1	7	0	I	0.580927	DFC	9
Z9	0.249999	2	1	3	1	8	54	III	0.676023	DFC	10
AA8	0.081358	1	1	3	1	7	24	II	0.335417	DFC	9
AA9	0	0	1	3	1	7	0	I	0.338357	DFC	9
AB7	0.029936	0	1	5	1	7	0	I	0.635023	QA	9
AB8	0.1	1	1	5	1	7	40	III	0.335417	QA	9
AC7	0.1	1	1	3	1	7	24	II	0.57723	DFC	9
AC8	0	0	1	3	1	7	0	I	0.335417	DFC	9
AD7	0.11513	1	1	3	1	7	24	II	0.57723	DFC	9
AD8	0	0	1	3	1	7	0	I	0.335417	DFC	9
AE6	0.07764	1	1	3	1	7	24	II	0.630817	DFC	9
AE7	0.093012	1	1	3	1	7	24	II	0.61373	DFC	9
AF6	0.052164	0	1	3	1	7	0	I	0.600923	DFC	9
AF7	0.1	1	1	3	1	7	24	II	0.61373	DFC	9
AG5	0.066649	0	1	3	1	8	0	I	0.7011	DFC	10
AG6	0.05	0	1	3	1	7	0	I	0.62385	DFC	9
AG7	0	0	1	3	1	7	0	I	0.61373	DFC	9
AH6	0.1	1	1	3	1	7	24	II	0.531023	DFC	9
AI5	0.060188	0	1	3	1	8	0	I	0.671163	DFC	10
AI6	0.1	1	1	3	1	7	24	II	0.531023	DFC	9
AJ5	0.041098	0	1	3	1	7	0	I	0.522223	DFC	9

Table D.1. Assigned parameters in Mora and Vahrson Methodology (1994) (Cont' d).

Cells	Converted RR	S_r	S_h	S_l	T_p	T_s	H_i	I	PGA (g)	Lithology	MMI
AJ6	0.1	1	1	3	1	7	24	II	0.562727	DFC	9
AK5	0.08627	1	1	3	1	7	24	II	0.522223	DFC	9
AK6	0	0	1	3	1	7	0	I	0.562727	DFC	9
AL4	0.089089	1	1	3	1	7	24	II	0.533933	DFC	9
AL5	0.078005	1	1	3	1	7	24	II	0.60941	DFC	9
AM3	0.111248	1	1	3	1	7	24	II	0.605383	DFC	9
AM4	0.045253	0	1	5	1	7	0	I	0.499333	QA	9
AM5	0	0	1	5	1	7	0	I	0.514263	QA	9
AN3	0.042384	0	1	5	1	7	0	I	0.591043	QA	9
AN4	0.054786	0	1	5	1	7	0	I	0.499333	QA	9
AN5	0.1	1	1	5	1	7	40	III	0.514263	QA	9
AO3	0.059734	0	1	3	1	7	0	I	0.591043	DFC	9
AO4	0.074272	0	1	3	1	7	0	I	0.499333	DFC	9
AO5	0.1	1	1	5	1	7	40	III	0.514263	QA	9
AP3	0.060113	0	1	3	1	7	0	I	0.591043	DFC	9
AP4	0.139873	1	1	3	1	7	24	II	0.499333	DFC	9
AP5	0.15	1	1	3	1	7	24	II	0.514263	DFC	9
AQ3	0.15	1	1	3	1	7	24	II	0.591043	DFC	9
AQ4	0.15	1	1	3	1	7	24	II	0.499333	DFC	9